



UNIVERSITY OF
LIVERPOOL

**The Role of Nrf2 in Pancreatic Cancer
and the Evaluation of Brusatol as a
Chemotherapeutic Agent**

Thesis submitted in accordance with the
requirements of the University of Liverpool for the
degree of Doctor in Philosophy by

Dylan Williams

January 2020

Abstract

Pancreatic ductal adenocarcinoma (PDAC) is one of the leading causes of cancer-related deaths. PDAC is an intractable disease and exhibits considerable chemoresistance. Identifying the mechanisms underlying PDAC chemoresistance may therefore provide a basis for developing methods to improve the efficacy of chemotherapy and improve patient prognosis. The transcription factor Nrf2 has been reported to contribute to the chemoresistance of PDAC and other cancers through its modulation of the antioxidant system. The *Brucea javanica* extract brusatol is commonly used as an Nrf2 inhibitor and as an anti-tumour agent. The aim of this study was to investigate the effects of brusatol upon Nrf2 in the context of PDAC, to explore the mechanism of action of brusatol and to determine whether brusatol is a potentially useful form of chemotherapy for the treatment of PDAC.

The effects of chemotherapy upon Nrf2 protein abundance and activity, and upon Nrf2 downstream targets (NQO1, AKR1C1/2), were investigated in cultured PDAC cells and in two distinct mouse models. Nrf2-inducible luciferase reporters, in cultured cells and in a mouse model, were utilised to determine how treatment with gemcitabine and 5-FU affected Nrf2 expression. The mechanism of action of brusatol and the involvement of Nrf2 in the anti-cancer effects of brusatol treatment were investigated in cultured cells using viability assays and protein synthesis analyses. A three-armed experiment compared the efficacy of brusatol monotherapy to that of gemcitabine monotherapy and vehicle control against PDAC tumours *in vivo*. This was performed using the KPC (LSL-KRas^{G121D/+}; LSL-p53^{R172H/+}; PDX1-Cre) genetically engineered mouse model of PDAC.

Nrf2, NQO1 and AKR1C1/2 were depleted from cultured cells in response to gemcitabine and 5-FU. Additionally, gemcitabine and 5-FU appeared to result in the downregulation of NQO1 in healthy mouse tissue, but did not noticeably affect Nrf2 activity as measured by the *in vivo* luciferase reporter. However, both gemcitabine and 5-FU increased Nrf2 activity in cultured cells, as measured by a luciferase reporter.

Brusatol exerted multiple anti-cancer mechanisms such as an inhibition of PDAC cell viability, motility and colony forming capability. The effect of brusatol upon viability did not appear to be dependent upon its inhibition of Nrf2. Although brusatol did not directly synergise with gemcitabine or 5-FU during PDAC cell co-treatments, it did sensitise PDAC cells to subsequent gemcitabine and 5-FU treatment. Nevertheless, brusatol monotherapy did not statistically improve KPC outcome compared to either gemcitabine monotherapy or vehicle treated control.

In conclusion, Nrf2 and NQO1 does not contribute to acquired chemoresistance of PDAC following chemotherapy exposure, and the anti-cancer effects of brusatol cannot be attributed to the inhibition of Nrf2. Although brusatol monotherapy did not improve the prognosis of KPC mice, the range of anti-cancer mechanisms it displayed upon pancreatic cancer cells suggests that further research may identify a useful treatment regimen incorporating brusatol.

Acknowledgements

I would like to thank my supervisors Prof Eithne Costello, Dr Pedro Perez-Mancera and Prof Bill Greenhalf for their help and support during the course of my PhD research. Their guidance has been invaluable

I would also like to thank the pancreatic cancer research group, our collaborators, and friends for their support. In particular, Dr Anthony Evans and Dr Lawrence Barrera for their help with various techniques and analyses.

I am grateful for the support of the Pancreatic Cancer Research Fund (PCRF) who funded my PhD and the majority of work described in this thesis, and I hope these findings help promote our aims of improving pancreatic cancer prognosis. I am also grateful for the financial support awarded by the University of Liverpool Technology Directorate.

I would like to thank patients for taking part in clinical trials, such as those used during the course of this work.

I would also like to thank Iona, Evelyn, and Isla for their loving support and kindness.

List of Abbreviations

AKR1C1/2	Aldo-Keto Reductase Family 1 Member C1/2
ARE	Antioxidant Response Element
BCA	Bicinchoninic Acid
CHX	Cycloheximide
Cre	Causes recombination
CDDO-Me	2-Cyano-3,12-dioxooleana-1,9(11)-dien-28-oic acid methyl ester
dFdC	Difluorodeoxycytidine
dFdCDP	Difluorodeoxycytidine Diphosphate
dFdCMP	Difluorodeoxycytidine Monophosphate
dFdCTP	Difluorodeoxycytidine Triphosphate
DMSO	Dimethyl Sulphoxide
DTT	Dithiothreitol
ECL	Enhanced Chemiluminescence
EMT	Epithelial-Mesenchymal Transition
ESPAC	European Study Group for Pancreatic Cancer
FBS	Foetal Bovine Serum
FdUMP	Fluorodeoxyuridine monophosphate
FdUTP	Fluorodeoxyuridine triphosphate
FOLFIRINOX	Folinic Acid, fluorouracil, irinotecan, oxaliplatin
FUDR	Floxuridine
GCL	Glutamate Cysteine Ligase
GCLC	Glutamate Cysteine Ligase Catalytic Subunit
GCLM	Glutamate Cysteine Ligase Modifier Subunit
GemCap	Gemcitabine, Capecitabine
GEMM	Genetically Engineered Mouse Model
GSH	Glutathione (Reduced)
GSR	Glutathione reductase
GSS	Glutathione synthetase

GSSG	Glutathione (Oxidised)
hENT1	Human equilibrative nucleoside transporter 1
HRP	Horseradish Peroxidase
ICC	Immunocytochemistry
IHC	Immunohistochemistry
IPMN	Intraductal papillary mucinous neoplasm
Keap1	Kelch-like ECH-associated protein 1
KPC	LSL-KRas ^{G121D/+} ; LSL-p53 ^{R172H/+} ; PDX1-Cre
LSL	Lox-Stop-Lox
MCN	Mucinous cystic neoplasm
NADPH	Nicotinamide adenine dinucleotide phosphate
NFE2L2	Nuclear Factor Erythroid 2 Like 2
NQO1	NAD(P)H Quinone Dehydrogenase 1
NRF2	Nuclear factor erythroid 2 Related Factor 2
PAGE	Polyacrylamide Gel Electrophoresis
PanIN	Pancreatic Intraepithelial Neoplasia
PBS	Phosphate Buffered Saline
PCR	Polymerase Chain Reaction
PDAC	Pancreatic Ductal Adenocarcinoma
PDX1	pancreatic and duodenal homeobox 1
ROS	Reactive Oxygen Species
SDS	Sodium dodecyl sulphate
siRNA	Short interfering RNA
SQSTM1	Sequestosome 1
TeloVac	Telomerase Vaccine
TP53	Tumour Protein 53
VIP	Vandetanib in Pancreatic Cancer

Table of Contents

1 – General Introduction	17
1.1 The History of Cancer	18
1.2 The Biology of Cancer	18
1.2.1 <i>The Mortality of Cancer</i>	19
1.2.2 <i>The Hallmarks of Cancer</i>	20
1.2.3 <i>The Treatment of Cancer</i>	22
1.3 Biology of the Pancreas.....	23
1.3.1 <i>The Exocrine Pancreas</i>	23
1.3.2 <i>The Endocrine Pancreas</i>	23
1.4 Pancreatic Cancer Background	24
1.4.1 <i>The Development of Pancreatic Ductal Adenocarcinoma</i>	24
1.4.2 <i>Treatment of Pancreatic Cancer</i>	26
1.4.3 <i>Biomarkers of Pancreatic Cancer</i>	30
1.5 The Biology of PDAC Models.....	31
1.5.1 <i>In Vitro Models</i>	31
1.5.2 <i>In Vivo Transplantation Models</i>	31
1.5.3 <i>In Vivo Genetically Engineered Mouse Models</i>	32
1.6 The Antioxidant System in Pancreatic Cancer	34
1.6.1 <i>Redox Reactions</i>	34
1.6.2 <i>Chemical Stressors in Cancer</i>	35
1.6.3 <i>The Nrf2-Mediated Antioxidant System</i>	36
1.6.4 <i>Nrf2 in Pancreatic Cancer</i>	39
1.7 Brusatol	41
1.7.1 <i>Brusatol as Chemotherapy</i>	41
1.7.2 <i>The Mechanism of Action of Brusatol</i>	42
1.8 Purpose and Hypotheses	44
1.9 Aims and Objectives	45
2 - Materials and Methods	46
2.1 Cell Culture.....	47
2.2 Drug Treatments	47
2.3 Protein isolation, Separation and Western Blotting	47
2.4 Protein Synthesis Analysis.....	49
2.5 Knockdown.....	50
2.6 Nrf2 Luciferase Assay	51

2.7 Viability Assays.....	52
2.8 Colony Formation.....	53
2.9 Migration Assay.....	54
2.10 SNP Analysis	55
2.11 Methylation Analysis.....	55
2.12 <i>In Vivo</i> analysis	57
2.12.1 <i>In Vivo – Nrf2 Luciferase</i>	57
2.12.2 <i>In Vivo – KPC Mouse Model</i>	58
2.13 Immunohistochemistry and Haematoxylin Counterstain.....	59
2.14 Statistical Analysis.....	61
3 - Nrf2 in Pancreatic Cancer and Chemotherapy Response	62
3.1 Introduction	63
3.2 Results.....	65
3.2.1 <i>Validation of Nrf2 antibody and the identification of multiple Nrf2 bands</i>	65
3.2.2 <i>Nrf2, NQO1 and AKR1C1/2 Responded to the Nrf2 Activator CDDO-Me</i>	66
3.2.3 <i>Identification of bands corresponding to newly-synthesised and stable Nrf2</i>	69
3.2.4 <i>Nrf2, NQO1 and AKR1C1/2 Proteins were Depleted Following Treatment with Gemcitabine</i>	71
3.2.5 <i>Nrf2, NQO1 and AKR1C1/2 proteins were depleted following treatment with 5-FU</i>	73
3.2.6 <i>Cells Remain Capable of Accumulating Nrf2 whilst in the Presence of Gemcitabine and 5-FU</i>	76
3.2.7 <i>Validation of a luminescent reporter for the detection of Nrf2 activity in cultured cells</i>	77
3.2.8 <i>Gemcitabine and 5-FU induced Nrf2 activity in cultured cells</i>	80
3.2.9 <i>Validation of the Bioluminescent OKD48-mediated Nrf2 Reporter Mouse Model</i> 81	
3.2.10 <i>Gemcitabine and 5-FU did not consistently affect Nrf2 activity in vivo</i>	85
3.2.10 <i>Gemcitabine and 5-FU did not affect NQO1 abundance in vivo</i>	90
3.2.12 <i>KEAP1 gene promoter was not found to be methylated in PDAC tumour patient Samples</i>	91
3.2.13 <i>NQO1 SNP rs1800566 status did not correlate with the probability of developing resectable PDAC, or with prognosis in response to treatment</i>	94
3.3 Discussion.....	101
3.3.1 <i>Nrf2 and downstream targets were not consistently affected by chemotherapy</i>	101
3.3.2 <i>NQO1 SNP was not associated with patient prognosis</i>	101
3.3.3 <i>Future Work</i>	102
4 – The Mechanism of Action of Brusatol	105

4.1 Introduction	106
4.2 Results	107
4.2.1 <i>Brusatol treatment inhibited protein synthesis and resulted in depletion of Nrf2</i>	107
4.2.2 <i>CDDO-Me-mediated accumulation of Nrf2 did not mitigate the effects of brusatol upon protein synthesis</i>	109
4.2.3 <i>CDDO-Me-mediated accumulation of Nrf2 did not mitigate the effects of brusatol upon cell viability</i>	110
4.2.4 <i>ML385 did not inhibit Nrf2 activity below baseline activity</i>	114
4.3 Discussion.....	116
5 – Analysis of Brusatol as a Form of Chemotherapy	119
5.1 Introduction	120
5.1.1 <i>Models of drug synergy</i>	121
5.1.2 <i>Licensing for in vivo work</i>	123
5.2 Results.....	125
5.2.1 <i>Brusatol inhibited cell viability</i>	125
5.2.2 <i>Brusatol and gemcitabine act predominantly additively or antagonistically during co-treatment</i>	126
5.2.3 <i>Brusatol and 5-FU act predominantly additively or antagonistically during co-treatment</i>	129
5.2.4 <i>Brusatol pretreatment sensitises PDAC cell lines to chemotherapy</i>	132
5.2.5 <i>Brusatol, gemcitabine and 5-FU each inhibited the colony forming capabilities of pancreatic cancer cells under certain conditions</i>	136
5.2.6 <i>Brusatol, but not gemcitabine or 5-FU alone, inhibits the motility of pancreatic cancer cells</i>	140
5.2.7 <i>Continuous brusatol treatment from an early timepoint in KPC GEMM tumour development did not improve prognosis</i>	142
5.2.8 <i>Long term treatment of brusatol or gemcitabine did not appear to affect NQO1 abundance in KPC tumours</i>	144
5.3 Discussion.....	145
5.3.1 <i>Synergy analysis identified brusatol as a chemosensitiser in pancreatic cancer</i>	145
5.3.2 <i>Brusatol inhibited colony formation efficiency of pancreatic cancer cell lines</i> ...	146
5.3.3 <i>Brusatol inhibited motility of pancreatic cancer cell lines</i>	147
5.3.4 <i>Early intervention brusatol monotherapy did not improve prognosis in KPC GEMM of PDAC</i>	147
5.3.5 <i>Brusatol did not appear to affect NQO1 abundance in KPC tumours</i>	149
5.3.6 <i>Future work</i>	149
6 – Discussion	151

6.1 Overview	152
6.2 Nrf2 in Pancreatic Cancer	153
6.2.1 NQO1 in Pancreatic Cancer	154
6.3 Brusatol	155
6.3.1 Mechanism of Action and Nrf2	155
6.3.2 Efficacy of brusatol as chemotherapy.....	156
6.4 Future Research	161
6.5 Overall Conclusions.....	162

List of Tables

Table 2.1: The solvents/dilutants and suppliers of chemicals frequently used <i>in vitro</i> in this work.	47
Table 2.2: 4x Laemmli buffer components.	48
Table 2.3: Antigens detected via western blotting, the primary antibodies used to do so, and the concentrations of primary and secondary antibodies.	49
Table 2.4: The volumes of reagents used in each solution prior to combining 1:1 for a knockdown. siRNA volume varied depending upon the concentration to be used (shown italicised in parentheses).	51
Table 2.5: The quantities of reagents used in each solution prior to combining 1:1 for transient transfection of an Nrf2-inducible reporter. Volumes are shown as $\mu\text{L}/\text{well}$ except DNA, which is shown as mass (ng) as volume varied depending upon the stock concentration.	52
Table 2.6: The volumes of each reagent used in the detection of NQO1 SNP rs1800566.	55
Table 2.7: Paraffin infiltration of tissue for IHC analysis. Tissue was prepared using a series of ethanol dehydrations, xylene treatments and paraffin infiltration	60
Table 3.1: Methylation status of patient-matched PDAC tumour and healthy acinar tissue.	93
Table 3.2: Hardy-Weinberg equilibrium was measured using χ^2 test comparing observed germline allele distribution of resectable cancer (ESPAC) and advanced cancer (TeloVac/VIP) to expected distribution based upon allele frequency. Allele distribution was also compared to a European cohort (gnomAD v2.1.1 (controls))	98

List of Figures

Figure 1-1: Coloured bars show the increase in 5-year survival rates of different forms of cancer between the 5-year survival rate of 1975-1977 (grey) and the 5-year survival rate of 2006-2012 (grey plus coloured). Graph was created using published data from Jemal A. et al.	20
Figure 1-2: The glutathione synthesis and restoration pathway. Nrf2 transcriptional targets are shown in blue. GCLM, GCLC and GSS contribute to the initial production of GSH molecules. GSR utilises NADPH to reduce GSSG (two oxidised GSH molecules) back into two GSH molecules. Abbreviations: GCLM, Glutamate-Cysteine Ligase Modifier Subunit; GCLC, Glutamate-Cysteine Ligase Catalytic Subunit; GSS, Glutathione Synthetase; GSH, Glutathione (reduced); GSR, Glutathione-Disulfide Reductase; NADPH, Nicotinamide adenine dinucleotide phosphate; GSSG, Glutathione disulphide (oxidised).	38
Figure 3-1: Western blot of SUIT-2 cell lysate following 24h knockdown of Nrf2 and exposure to 100nM CDDO-Me. The protein ladder is shown to the leftmost lane. β -Actin levels were obtained as a control for loading. Abbreviations: OT, Off Target siRNA.	65
Figure 3-2: SUIT-2 cell lysate, following 24h exposure to CDDO-Me, probed for Nrf2 and downstream targets AKR1C1 and NQO1. Nrf2, β -Actin levels were ascertained as a control for loading. Representative image shown from three independent experiments.....	67
Figure 3-3: Densitometric analysis of Nrf2 bands (103kDa, 108kDa, and 115kDa) from Fig. 3-2. Band intensities were normalised to β -Actin loading control and expressed as fold change relative to vehicle only (0nM CDDO-Me) control.	68
Figure 3-4: Alternative representation of densitometric analysis of Nrf2 bands (103kDa, 108kDa, and 115kDa) from Fig. 3-2, shown on a log ₁₀ scale alongside densitometric analysis of AKR1C1/2 and NQO1, also from Fig. 3-2. Band intensities were normalised to β -Actin loading control and expressed as fold change relative to vehicle only (0nM CDDO-Me) control.	69

Figure 3-5: Nrf2 western blot following treatment with brusatol, cycloheximide and/or MG132. Different exposure times (50 sec and 10 min) are shown to account for the large differences in Nrf2 abundance between treatments. Red highlighted areas are overexposed and are not used for comparison at that exposure time. β -Actin levels were ascertained as a control for loading. Representative image shown from 3 independent experiments. Abbreviations: Bru, Brusatol. CHX, Cycloheximide.....	71
Figure 3-6: Western Blot of Nrf2 and downstream proteins from SUIT-2 and MIA PaCa-2 cells following treatment with gemcitabine. Representative images shown from three independent experiments.....	73
Figure 3-7: Western Blot of Nrf2 and downstream proteins from SUIT-2 and MIA PaCa-2 cells following treatment with 5-FU. Representative images shown from three independent experiments.	75
Figure 3-8: Western blot of SUIT-2 cells either drug/vehicle treated for 24h or cultured in FBS-free medium ('serum-starved') for 24h prior to harvest. Representative image shown from three independent experiments.....	77
Figure 3-9: Assay specificity analysis. HEK293 cells were transiently transfected with <i>Renilla</i> Luciferase only and Firefly 8xARE (Nrf2Luc) Luciferase only. Dual-glo assay was performed in full on each to measure the extent of background and residual luciferase activity. +/- SEM. Abbreviations: AU, Arbitrary Units.....	78
Figure 3-10 (A) Treatment of HEK-293 with brusatol, CDDO-ME and vehicle control (DMSO) following transient transfection of Nrf2 luciferase, N=1 (B) Treatment of HEK-293 with gemcitabine and 5-FU following transient transfection of Nrf2 luciferase, N=1. CDDO-ME and brusatol served as positive and negative controls of luciferase activity respectively. Error bars +/- SEM of technical replicates.....	80
Figure 3-11 Luminescence readings of MIA PaCa-2, PANC-1 and SUIT-2 cells treated with gemcitabine (Gem) and 5-FU following transient transfection of Nrf2 luciferase. Work contributed to by MRes students Lewis Wignall and Chris Brown under my direct supervision. Data represent the mean of three individual experiments, each performed in triplicate. Error bars +/- SEM. Statistical analysis was performed using two-tailed <i>t</i> -test between each condition and vehicle control.....	81

Figure 3-12: Graphical representation of the dual mechanisms utilised by the luciferase OKD48 3xARE Nrf2 activity reporter. OKD48 expression was activated by Nrf2 activity upon the release of Nrf2 from Keap1. The accumulation of OKD48 protein was inhibited under the same circumstances under which Nrf2 would be inhibited (Keap1-mediated under non-stressed conditions due to OKD48 comprising Neh2, the Keap1 binding region of Nrf2). Degradation of OKD48 under circumstances in which Nrf2 would also be degraded reduced the effects of aberrant expression of OKD48, and ensured that any OKD48 protein synthesised in response to Nrf2 activity would not continue to be present following cessation of that activity. OKD48 is therefore a sensitive reporter of Nrf2 and its abundance at any specific time is a reliable indicator of Nrf2 activity at that time.....82

Figure 3-13: A: Representative image of a single OKD48^{+/-} mouse prior to treatment with CDDO-Me and at 4h, 24h and 1 week (1w) post-treatment. The location of intensity of radiance, as a marker of Nrf2 activity, is represented by coloured overlay. B: Mean of the average luminescence readings from CDDO-Me treated mice at 4h, 24h and 1 week (1w) normalised to pretreatment readings. Errors bars +/- SEM.....84

Figure 3-14: Representative images of mice treated with vehicle (DPBS) only, gemcitabine (100mg/kg), or 5-FU (50mg/kg). Small areas of localised Nrf2 activation were detected irregularly in all treatment arms as seen at 24h, however these were not to the extent or spread of activation following treatment with CDDO-Me.....85

Figure 3-15: The fold change between the average pretreatment reading and the average reading at 4h, 24h and 1w post-treatment of 5-FU (A) or gemcitabine (B). The same DPBS controls are shown in both A and B for comparison purposes.....89

Figure 3-16: MIA PaCa-2 cells were treated with off-target (A, Control) or Nrf2 (B) siRNA on cover slips and subsequently stained via ICC for Nrf2 (brown). Figure adapted from Dr Thompson Gana's PhD thesis. Abbreviations: ICC, Immunocytochemistry.....90

Figure 3-17: IHC sections of organs taken from Nrf2Luc mice 48h post drug-treatment. 100x magnification.....91

Figure 3-18: qPCR results to determine genomic NQO1 SNP status in MIA PaCa-2, PANC-1 and SUIT-2 cell lines under various conditions. Endpoint signals of fluorescence indicating C allele (A) and T allele (B) amplification were combined (C) to separate the two groups and colour coded (red – CT; green – TT). Positive results for each cell line are labelled. Negative results, including negative control, are shown in grey and labelled separately.....96

Figure 3-19: Representative images of qPCR results to determine genomic NQO1 SNP status in ESPAC patient samples. Endpoint signals of fluorescence indicating C allele (A) and T allele (B) amplification were combined (C) to separate the three groups and colour coded (blue – CC; red – CT; green – TT). Negative control is shown in grey.....97

Figure 3-20: Kaplan-Meier plots of overall survival of patients according to NQO1 SNP (A), survival in response to gemcitabine treatment (B), and survival in response to GemCap treatment (C). TT genotype was excluded from individual arm analysis due to small numbers of patients.....99

Figure 3-21: Median survival time (months) of patients of each germline NQO1 genotype of any intervention (A), when treated with gemcitabine (B), or when treated with GemCap (C). Error bars +/- SEM.100

Figure 4-1: Two alternative proposed mechanisms of action of brusatol investigated during this course of work. Left, brusatol as a direct Nrf2 inhibitor with downstream effects upon protein translation. Right, brusatol as a direct inhibitor of translation resulting in the depletion of proteins such as Nrf2.....107

Figure 4-2: Brusatol inhibited nascent protein synthesis (cycloheximide treatment shown as a positive control) within SUIT-2 cells. The maximal effect was observed at 80nM. Abbreviation: CHX: Cycloheximide.....108

Figure 4-3: The effect of CHX (10µg/mL) and brusatol (100nM) on protein synthesis following 4 hour CDDO-Me pretreatment. Newly synthesised protein shown as a visualisation of the degree of protein synthesis. Total protein loaded shown as loading control. Abbreviations: Bru: brusatol. CHX: cycloheximide.....110

Figure 4-4: Relative viability of MIA PaCa-2 (A), PANC-1 (B) and SUIT-2 (C) cells with CHX, Bru or H₂O₂ for various periods of time either with (solid colour) or without (patterned colour) 4h CDDO-Me pretreatment. Viability was normalised to a vehicle control with the same 4h CDDO-Me pretreatment (with/without). Statistical analysis was performed using *t*-test between pretreated and non-pretreated for each drug and timepoint, with Bonferroni correction to account for multiple comparisons. * p-value below 0.0033. Each bar is the mean of three experiments each performed in triplicate. Error bars +/- SEM. Abbreviations: CHX: cycloheximide. Bru: Brusatol. CDDO: CDDO-Me.....113

Figure 4-5: Treatment of MIA PaCa-2 (A), PANC-1 (B) and SUIT-2 (C) cells with CDDO-Me and ML385 following transient transfection of Nrf2 luciferase. Data are the mean of three experiments, each performed in triplicate. Work contributed to by MRes student Lewis Wignall with my direct supervision and input. Error bars +/- SEM.....114

Figure 4-6: Treatment of MIA PaCa-2 (A), PANC-1 (B) and SUIT-2 (C) cells with CDDO-Me, ML385 and combination following transient transfection of Nrf2 luciferase. Data are the mean of three experiments, each performed in triplicate. Work contributed to by MRes student Chris Brown with my direct supervision and input. Error bars +/- SEM.....115

Figure 5-1: MTT analysis of MIA PaCa-2, PANC-1, and SUIT-2 cells treated with brusatol, gemcitabine or 5-FU for 48h prior to MTT assay. Representative image of three independent experiments, mean IC₅₀ shown in italics.....125

Figure 5-2: Synergy analysis of MIA PaCa-2 (A), PANC-1 (B) and SUIT-2 (C) cells treated with gemcitabine and brusatol, visualised using Bliss, HSA, Loewe and ZIP models of synergy. Images represent one preliminary experiment. Abbreviations: HSA, Highest Single Agent. ZIP, Zero Interaction Potency.....128

Figure 5-3: Synergy analysis of MIA PaCa-2 (A), PANC-1 (B) and SUIT-2 (C) cells treated with 5-FU and brusatol, visualised using Bliss, HSA, Loewe and ZIP models of synergy. Images represent one preliminary experiment. Abbreviations: HSA, Highest Single Agent. ZIP, Zero Interaction Potency.....131

Figure 5-4: Synergy analysis of MIA PaCa-2 (A), PANC-1 (B) and SUI-2 (C) cells treated with gemcitabine following 24h brusatol pretreatment, visualised using Bliss, HSA, Loewe and ZIP models of synergy. Representative images of three independent experiments. Abbreviations: HSA, Highest Single Agent. ZIP, Zero Interaction Potency.....133

Figure 5-5: Synergy analysis of MIA PaCa-2 (A), PANC-1 (B) and SUI-2 (C) cells treated with 5-FU following 24h brusatol pretreatment, visualised using Bliss, HSA, Loewe and ZIP models of synergy. Representative images of three (MIA PaCa-2, SUI-2)/two (PANC-1) independent experiments. Abbreviations: HSA, Highest Single Agent. ZIP, Zero Interaction Potency.....135

Figure 5-6: Clonogenic assay of MIA PaCa-2, PANC-1 and SUI-2 cells treated with brusatol, 5-FU, gemcitabine or vehicle (H₂O). A: Cells were treated for 24h prior to replating for clonogenic seeding. B: Cells were treated following clonogenic seeding until analysis. Representative images from three independent experiments, each performed in triplicate.137

Figure 5-7: Quantification of clonogenic assay of MIA PaCa-2, PANC-1 and SUI-2 cells treated with brusatol, 5-FU, gemcitabine or vehicle (DMSO, H₂O). Cells were treated for 24h prior to replating for clonogenic seeding. Data represents the mean of 3 experiments each performed in triplicate, +/- SEM. Statistical analysis was performed using Dunnett's multiple comparisons test of a one-way ANOVA for each analysis. *= $p < 0.05$; **= $p = 0.01$; ***= $p < 0.001$; ****= $p < 0.0001$ relative to vehicle control. Abbreviations: Veh, vehicle; Bru, brusatol; Gem, gemcitabine.....139

Figure 5-8. Wound healing assay of MIA PaCa-2, PANC-1 and SUI-2 cells treated with combinations of gemcitabine, 5-FU and brusatol. A: Representative images of monolayer wounds of three independent experiment at the time of treatment (0h) and 48h following treatment for each cell line and drug combination. B: Quantification of mean cell migration of three independent experiments at 24h and 48h, normalised to 0h (100% wound size). Abbreviations: Veh, Vehicle (H₂O). Gem, Gemcitabine. Bru, Brusatol.....141

Figure 5-9: Kaplan-Meier analysis of the absolute survival time of brusatol, vehicle and gemcitabine treated KPC mice. No individual arm reached statistical significance (gemcitabine v vehicle $p = 0.057$, brusatol v vehicle $p=0.63$).....143

Figure 5-10: IHC of NQO1 in dissected tumours of KPC mice treated with vehicle (DPBS, 4% DMSO v/v), brusatol or gemcitabine. Images of tumours from three separate mice per treatment arm are shown.....144

1 – General Introduction

1.1 The History of Cancer

Humanity has known of cancer for thousands of years. Cancer has been found in ancient Egyptian mummies and the disease has been referenced in ancient texts (1-3). The term 'cancer' is derived from the ancient Greek "Καρκινος" (Karkinos) meaning crab, named by Hippocrates due to the crab-like appearance of the surface tumours he described. Hippocrates is commonly referred to as the "Father of Medicine" as he popularised the idea that diseases had natural causes, rather than spiritual, so could have natural treatments. Hippocrates believed that many diseases, such as cancer, were the result of imbalances in the four 'humours' – blood, phlegm, black bile and yellow bile. Curing disease often took the form of attempting to address this imbalance, resulting in remedies such as bloodletting. The four humours model and related treatments were widely accepted for two thousand years until the Renaissance, at which point the rapid advancement of scientific understanding gave rise to more evidence-based ideas (4). However, it was not until the 20th century that the causes and nature of cancer were beginning to be well understood. In particular, the discovery of DNA structure and mutations shed light on the processes underlying carcinogenesis (5-7). In regards to treatment, although efforts to resect tumours had been undertaken since ancient times, it was not until the 19th-20th century that surgery became a viable option for many cancers (and other afflictions) (8). Chemotherapy was also developed for cancer treatment in the early 20th century (9, 10). Although cancer therapy has advanced further still over the past century, cancer is still commonly lethal and particular types, such as pancreatic, continue to have a dismal prognosis (11).

1.2 The Biology of Cancer

Cancer is often defined as the uncontrolled proliferation and spread of abnormal cells, which comprises a broad range of distinct diseases (12). Further to this, tumour cells utilise complex

interactions to direct their own maintenance and proliferation, as well as establish tumours comprised of multiple cell types (13, 14).

1.2.1 The Mortality of Cancer

Cancer is a leading cause of death due to its high incidence, despite the fact that the majority of cancer sufferers now survive the disease (although mortality rates vary between different types of cancers (Fig. 1-1)) (11). Although in general cancer survivability has improved over time, prognosis of some cancers have seen little improvement (15). The 5-year survival rate of pancreatic cancer in particular has remained low (now at 9%) (11, 16).

Cancer is the second most common cause of death (after heart disease) overall in the USA and the leading cause of death in England (11, 17). In 2016, cancer accounted for 30.3% of deaths in females and 25.6% of deaths in males, considerably more than the second leading causes which were dementia and Alzheimer's disease (which accounted for 15.8% of deaths of females) and heart disease (which accounted for 13.6% of deaths of males) (17). Cancer is also the most common cause of death in the USA for individuals between the ages of 60 and 79, as well as the most common natural cause for individuals between the ages of 1 and 19 (11).

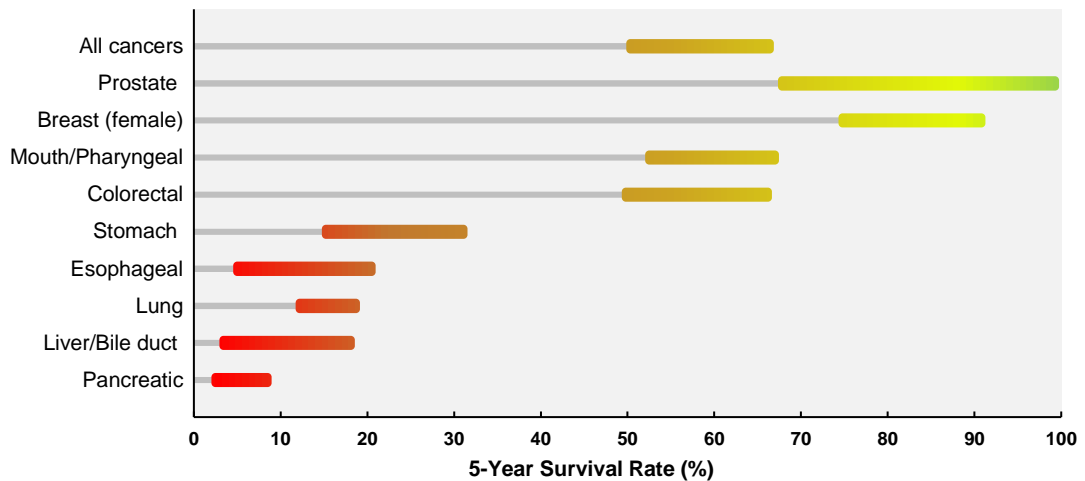


Figure 1-1: Coloured bars show the increase in 5-year survival rates of different forms of cancer between the 5-year survival rate of 1975-1977 (grey) and the 5-year survival rate of 2006-2012 (grey plus coloured). Graph was created using published data from Jemal A. et al. (15).

1.2.2 The Hallmarks of Cancer

A number of defining hallmarks of cancer cells have been proposed (13, 14). These hallmarks promote the survival and replication of cancer cells under conditions which would be restrictive to healthy cells (13, 14). In 2000, six hallmarks (Resisting cell death; Inducing angiogenesis; Enabling replicative immortality; Activating invasion and metastasis; Evading growth suppressors; and Sustaining proliferative signalling) were described by Hanahan and Weinberg which became a foundation for understanding the characteristics of cancer (13). These hallmarks were expanded upon in 2011 with an additional publication which detailed eight hallmarks, comprised of the original six plus two additional hallmarks (Deregulating cellular energetics; and Avoiding immune destruction), as well as two enabling characteristics (Genome instability and mutation; and Tumour-promoting Inflammation) (14).

The purpose of these hallmarks is to support the processes of development, maintenance, and proliferation of cancerous cells. Healthy cells are prevented from developing cancerous characteristics by various anti-cancer mechanisms and the innate limitations cells must face,

such as only being able to divide a finite number of times (13, 14). As such, the development of characteristics to avoid anti-cancer mechanisms are ubiquitous characteristics of cancers and can therefore be used as hallmarks of the disease. For instance, there are multiple obstacles which would normally prevent a healthy cell from proliferating to the extent of a cancer cell. Cells can typically only replicate a limited number of times, so cancer cells must develop replicative immortality. As well as this, healthy cells often rely upon external signals to determine their rate of growth (either positively or negatively), so a cancer cell must sustain proliferative signalling and evade growth suppression from other sources. Cellular structures also need an adequate blood supply for maintenance, so in order to continue growing cancer cells must induce angiogenesis to recruit blood vessels to meet the increased demand.

Cells are subjected to internal and external anti-tumour processes that lead to the death of a cell developing cancerous properties. A cancerous cell must evade the immune system and resist its own pro-apoptotic signalling. Other hallmarks such as the induction of tumour-promoting inflammation, deregulation of cellular energetics, and exhibiting genetic instability allow the cancer to develop by creating a suitable environment for cancerous growth and giving the cells the ability to rapidly adapt. Finally, a defining feature of cancer is its ability to invade other tissues. This can be either locally or, in advanced cases, distant to the point of tumour origin (metastasis). A tumour which does not spread is considered benign rather than cancerous. Benign tumours are often removed due to the risk of them developing into malignant cancerous tumours, however many benign tumours do not justify surgical resection, either because they can only be removed by invasive procedures (for internal benign tumours) or are such a low risk and/or can be observed for any development (for superficial benign tumours).

Carcinogenesis is a multistep process so the acquisition of these hallmarks will occur at different points and across different timespans depending upon cancer type (13, 14). Cancerous growths adversely affect health due to a number of reasons, such as developing into a physical obstacle to normal systems and depriving healthy tissue of resources due to the higher demands of the rapidly proliferating tumour cells.

1.2.3 The Treatment of Cancer

A variety of therapies exist for the treatment of cancer. The particular course of therapy used to treat each case depends upon multiple factors such as the specific cancer type and the stage of the disease. Tumours are surgically resected where possible. This can be a curative treatment if all tumour tissue is successfully removed, however it is not always possible to do so. Once tumours have begun to spread and metastasise it may not be possible to find the individual cancer cells or small tumours throughout the body due to their microscopic nature. If they are present then subsequent surgeries may remove them once they have grown into larger detectable tumours (18-20), however in many cases and types of cancer this may not yield much effect (21).

Chemotherapy is a common form of treatment which is used individually or in combination with other treatments such as surgery (22-24). Neoadjuvant chemotherapy may be used prior to surgery, whereas adjuvant chemotherapy may be used post-surgery to treat remaining tumour cells that cannot be detected for surgical removal (23, 25).

In regards to pancreatic cancer, the focus of this thesis, only 15-20% of patients present with a tumour suitable for surgical resection at the time of diagnosis (23, 25, 26). The remainder with advanced pancreatic cancer may be treated with chemotherapy alone (27, 28). Treatment of pancreatic cancer specifically is discussed further in Chapter 1.4.2.

1.3 Biology of the Pancreas

The pancreas is a vital organ located in the abdomen. The pancreas is comprised of both exocrine and endocrine components. The exocrine pancreas is responsible for the production of digestive enzymes, such as amylase and lipase, to be secreted into the gastro-intestinal tract. The endocrine pancreas produces and releases hormones, such as insulin and glucagon, into the bloodstream.

1.3.1 The Exocrine Pancreas

The pancreas is a predominantly exocrine organ, by mass and volume, which is responsible for producing and delivering digestive enzymes into the duodenum of the small intestine. Enzymes are produced by, and secreted from acinar cells, which drain into ductules which combine to form larger ducts. These in turn combine and feed into the pancreatic duct, which exits the pancreas through the ampulla of Vater (also known as the hepatopancreatic ampulla). The ampulla of Vater is formed by the union of the pancreatic duct and the common bile duct (the common bile duct itself is formed by the union of the cystic duct and the common hepatic duct draining the gall bladder and the liver, respectively). At this point the sphincter of Oddi controls the flow of liquid into the duodenum, forming a protuberance named the major duodenal papilla.

1.3.2 The Endocrine Pancreas

One to two percent of the pancreas consists of the pancreatic islets (islets of Langerhans) of the endocrine system. The islets are clusters of cells amongst the exocrine pancreas and are involved in the production of hormones. Two such hormones are glucagon and insulin which are produced by the alpha (α) and beta (β) cells, respectively. Glucagon and insulin modulate blood glucose regulation (29, 30). High levels of blood glucose promote the release of insulin from beta cells which in turn promotes cellular uptake of glucose. Conversely, low levels of

insulin prompt the release of glucagon, which causes the liver to convert glucose stores (glycogen) into glucose and release it into the bloodstream. Delta (δ) cells, which produce somatostatin, can also be found within the pancreatic islets (as well as in other areas of the body).

1.4 Pancreatic Cancer Background

Pancreatic cancer, of which Pancreatic Ductal Adenocarcinoma (PDAC) accounts for ~90% of cases (31), is the fourth leading cause of cancer-related death (32). This is continuing to rise and by 2030 it is expected that PDAC will become the second leading cause of cancer-related death, largely due to an increase in incidences of PDAC and the continued improvements seen in the treatment of other forms of cancers (32, 33). Although patient survivability of most common cancers has increased over time, the 5-year survival rate of pancreatic cancer patients has changed little since the 1970s (Fig. 1) (32). The dismal prognosis is due in part to the poor response to chemotherapy, and the fact that diagnosis typically occurs at advanced stages of the disease (28, 32).

1.4.1 The Development of Pancreatic Ductal Adenocarcinoma

The understanding of how PDAC develops from precursor lesions can shed light on how the disease functions and how appropriate models of PDAC may be used. There are multiple precursor lesions known to give rise to PDAC development. These lesions include Pancreatic Intraepithelial Neoplasia (PanIN), Intraductal Papillary Mucinous neoplasms (IPMN) and Mucinous Cystic Neoplasms (MCN). MCNs are typically asymptomatic with a low risk of malignancy and characterised by an ovarian-like stroma (34-36). MCNs are predominantly found in women and over the age of 40 (34, 35). IPMNs typically occur in individuals over the age of 60 and are characterised by intraductal papillary growths and dilation of the main and/or branch pancreatic ducts (37, 38). PanINs are the most common precursor to PDAC and are considered to be the most important in regards to cancer development and, as such,

are the most well understood (36, 39). PanINs can be further divided into PanIN-1A, PanIN-1B, PanIN-2 and PanIN-3.

Normal pancreatic ducts consist of cuboidal epithelial cells forming a lumen. As PanINs develop a variety of abnormal characteristics are identifiable as they progress, several of which are used to divide them based on their severity. PanIN-1A and PanIN-1B are defined by the epithelium comprising tall columnar cells, although with mostly normal appearing nuclei. PanIN-1A and PanIN-1B are distinguished from one another by exhibiting either flat (PanIN-1A) or papillary (PanIN-1B) epithelial architecture. PanIN-2 refers to such lesions exhibiting abnormal nuclei, such as crowding, loss of polarity, or being oversized. PanIN-3, a form of carcinoma *in situ*, is used to describe a lesion exhibiting the budding of affected cells into the lumen. Although PanINs will not necessarily progress into more severe classifications or develop into PDAC, they are the predominant source of pancreatic cancer cases. Earlier detection of PanINs and other pancreatic lesions is an attractive target for earlier diagnosis as it would make it possible to remove precancerous tissue before it can develop into a malignant tumour. However, there is currently no reliable method to detect these lesions and they are typically asymptomatic. Even once PDAC has developed, the cancer is usually asymptomatic in its earlier stages and so will typically be detected in a more advanced state.

1.4.1.1 Mutations in PDAC development

Multiple mutations are known to be commonly associated with PDAC development. In particular the genes *KRAS*, *TP53*, and *SMAD4* are frequently mutated in instances of PDAC.

Ras proteins are GTPases which stimulate proliferation through their functions as signalling molecules (40). Dysregulation of this system can lead to inappropriate proliferation and therefore promote a cancerous phenotype, and as such *RAS* genes are among the most common oncogenic mutations in cancer. Of the 3 *RAS* genes (*KRAS*, *HRAS*, and *NRAS*), *KRAS* mutations are the most common and are an early mutation in PDAC and precursor lesion

development (41, 42). The G12D mutation is the most common form of *KRAS* mutation in PDAC (41). *KRAS*G12D promotes tumorigenesis through multiple mechanisms, including the upregulation of Nrf2 (43).

Mutation of Tumour Protein 53 (*TP53*, encoding p53) is one of the most common events in the development of cancers. Wild type p53 contributes to the prevention of carcinogenesis and so the loss of this function is an integral part of cancer development. However, missense mutations such as p53 R172H can cause a dominant gain of function with oncogenic potential (44, 45). Such mutations therefore not only result in the loss of a tumour suppressor mechanism but also the gain of an oncogenic mechanism. In PDAC specifically, oncogenic gain of function *TP53* mutations are common and are known to be important for metastasis to occur (45). The effect of p53 mutation in p53^{R172H/+} mice (R172H is the murine homologue of human R157H) upon aggressiveness of tumours, including pancreatic, has been shown to be greater than in p53^{-/-} mice, indicating that the mechanism of action is not limited to the loss of wild type p53 and is instead an oncogenic gain of function (44, 45).

SMAD4 is a tumour suppressor gene commonly deactivated in PDAC (46-51). It was originally termed “homozygously deleted in pancreatic carcinoma, locus 4” (*DPC4*), as it was identified due to its role in pancreatic cancer. However, not all mutations of *SMAD4* are homozygous deletions. Other mutations, commonly missense, can result in reduced levels of *SMAD4* protein and contribute to PDAC progression (46, 49, 51).

1.4.2 Treatment of Pancreatic Cancer

The effectiveness of PDAC treatment has improved only slightly since the introduction of gemcitabine as a chemotherapeutic agent. The only potentially curative option is surgical resection of the tumour, however only <20% of pancreatic cancer patients present with resectable disease at the time of diagnosis (23, 25, 26). Chemotherapy treatment is commonly used in both resectable and advanced cancer, predominantly featuring

gemcitabine and 5-FU (either individually or as part of combination therapies) (27, 28, 52-56).

1.4.2.1 Surgical Therapy

Depending upon the location of the pancreatic tumour, one of two main forms of surgery may be used. If the tumour is located within the head of the pancreas, a pancreaticoduodenectomy (also known as a Whipple Procedure) may be performed. A conventional pancreaticoduodenectomy involves the removal of the head of the pancreas, the duodenum, the gall bladder, and parts of the stomach and jejunum (57). Multiple variants of this procedure exist, such as the pylorus-preserving pancreaticoduodenectomy which can leave the stomach and proximal duodenum unresected if the cancer has not spread to these areas (57, 58). Although surgical resection is the only potentially curative option for PDAC, pancreaticoduodenectomy is a high-risk procedure. Half of patients experience post-operative morbidity, and the procedure has a mortality rate of <4%.

If the tumour is in the body or tail of the pancreas, a distal pancreatectomy may be performed (59, 60). Although distal pancreatectomy procedures have a mortality rate as low as 0.8% so are typically much safer than a pancreaticoduodenectomy, only 20-25% of resectable PDAC cases involve a tumour arising from the body or tail (59, 60).

1.4.2.2 Gemcitabine Chemotherapy

Gemcitabine is a commonly used form of chemotherapy for the treatment of pancreatic cancer. Gemcitabine, also known as dFdC, is eventually triphosphorylated to dFdCTP (triphosphate) once inside cells (61). Gemcitabine must first be transported inside the cells by human equilibrative nucleoside transporter 1 (hENT1) (62). It has been seen that high hENT1 correlates with improved prognosis of PDAC patients, likely due to the ready uptake of gemcitabine by tumour cells (62). Once inside the cell, dFdC is first phosphorylated to dFdCMP (monophosphate) (61, 63), which in turn is further phosphorylated to dFdCDP

(diphosphate) by UMP-CMP kinase (61, 63) before being converted to dFdCTP (61). dFdCTP is a nucleoside analogue which can be incorporated into the genome, at which point it prevents elongation of the newly synthesised DNA strand and therefore results in cell death (61, 64). As an inhibitor of replication, the effects of gemcitabine are selective to replicating cells and therefore tumours.

Gemcitabine monotherapy has commonly been used as a mainline therapy for the treatment of PDAC, however gemcitabine-incorporating combination therapies have been developed showing increased efficacy (27, 28, 52). The combination of gemcitabine and capecitabine (“GemCap”) has been shown during clinical trials to improve prognosis of patients either with advanced disease or following pancreatic tumour resection, relative to gemcitabine alone (27, 52). Capecitabine is a prodrug of 5-FU (discussed further in Section 1.4.2.3), which is first metabolised in the liver to produce 5’DFUR before finally to 5-FU by thymidine phosphorylase (TP) within other cells, such as in tumours (65, 66). Treatment with GemCap was found to increase median survival time of patients with advanced disease from 6.2 months (when treated with gemcitabine alone) to 7.1 months. Similarly, the ESPAC 4 trial of resectable pancreatic cancer demonstrated a median survival time of 25.5 months in patients treated with gemcitabine alone, increasing to 28 months in patients treated with the GemCap combination (52). Although these were promising findings and the introduction of GemCap represented one of the few advancements in the efficacy of pancreatic cancer therapy, GemCap still only increased the survival time of pancreatic cancer patients by a modest amount.

Nab-paclitaxel, a form of albumin-bound paclitaxel, is used in combination with gemcitabine to treat metastatic and borderline resectable PDAC (67-69). Nab-paclitaxel has been seen to enhance the uptake of gemcitabine by cells, and the combination of Nab-paclitaxel and gemcitabine has been seen to result in an improved prognosis relative to gemcitabine

monotherapy (67). However, nab-paclitaxel treatment has also been found to have increased toxicity compared to gemcitabine alone which has limited its clinical usefulness (69).

1.4.2.3 5-FU Chemotherapy

5-FU is one of the oldest chemotherapeutic agents for the treatment of PDAC still in use (56). Once it is inside the cell, 5-FU is converted to multiple metabolites which inhibit replication through various mechanisms (65). 5-FU is converted to FUDR by thymidine phosphorylase, and FUDR is converted to FdUMP by thymidine kinase (TK). FdUMP inhibits thymidylate synthase, resulting in deregulated DNA synthesis (65). FdUMP is also further metabolised to FdUTP, which causes DNA damage directly through misincorporation into the genome (65).

5-FU is commonly used as part of combination treatments. One such example is FOLFIRINOX, which includes 5-fluorouracil (5-FU), folinic acid (leucovorin), irinotecan and oxaliplatin, which is predominantly used in non- or borderline-resectable cases (55, 70). Despite FOLFIRINOX increasing the survival time of pancreatic cancer patients relative to those treated with single-agent gemcitabine therapy, FOLFIRINOX also exhibits increased toxicity and is only tolerated in high performance status patients (54, 69). The intractable side effects of FOLFIRINOX has therefore limited its clinical usefulness (69).

The FOLFIRINOX regimen is derived from a simpler treatment, 5-FU and folinic acid. Although 5-FU and folinic acid is less toxic than FOLFIRINOX, it is also less effective. 5-FU and folinic acid has been trialled in cases of surgically resectable PDAC as an alternative to single-agent gemcitabine, which demonstrated that the two forms of treatment were highly similar in terms of patient outlook and toxicity (71).

Because of the dismal prognosis of pancreatic cancer and there being only modest efficacy of currently available therapies, the development of new therapies to treat pancreatic cancer is critically important. Identifying more effective treatment regimens could overcome the chemoresistance exhibited by PDAC and improve patient survivability. Even in the absence

of curative treatment options, improving quality of life and/or delaying disease progression may be of benefit to patients.

1.4.3 Biomarkers of Pancreatic Cancer

One of the major avenues of pancreatic cancer research is the investigation of biomarkers for earlier diagnosis or assessing prognosis. PDAC is typically detected in an advanced state at the time of diagnosis, with only 10-20% of patients eligible for surgical resection (69). This late diagnosis comes from the absence of specific symptoms for PDAC. The symptoms of pancreatic cancer are often generic, and do not immediately suggest PDAC specifically. If it were possible to diagnose PDAC earlier, patient outlook could be improved by treating the disease at a less advanced state.

The only potentially curative option available for PDAC patients is surgical resection. Only 10-20% of individuals are diagnosed early enough for surgical resection to be an option, and 75% of patients who have undergone surgical resection develop metastatic recurrence (72). Development of methods for earlier detection of PDAC may therefore be of benefit in reducing the mortality associated with pancreatic cancer. The ability to detect PDAC earlier would greatly improve the accessibility and efficacy of potentially curative surgical resection. Additionally, the improved ability to detect precancerous lesions could make it possible to prevent the development of PDAC before it became a threat to the patient. This could be done either through resection of the tissue or targeting the dysfunction using another form of therapy to prevent carcinogenesis occurring (such as chemoprevention).

1.5 The Biology of PDAC Models

1.5.1 *In Vitro* Models

Cancers, including PDAC, can be investigated using cultured tumour cells. The use of cultured cells allows a broad range of analyses and is relatively inexpensive, quick, and simple compared to *in vivo* and clinical research. This form of research is also less likely to be affected by ethical and legal factors. Despite these advantages, there are also various limitations. Cell culture commonly involves a single cell type grown in a monolayer. Cells *in vivo* are influenced by their interactions with surrounding cells, chemical messengers, and the functioning of bodily systems. Any results may therefore be affected by the absence of these features a cancer would normally be exposed to. Additionally, cultured cells often exhibit substantial differences to their parent cell types *in vivo* so cannot perfectly recapitulate the internal and self-regulated functions of the cells (73-75).

The use of 3D cell culture, such as spheroids and organoids, can at least partially offset these limitations (74-77). Tumour spheroids are aggregates of tumour cells which allow increased cell-cell interaction, and can use multiple cell types to better mimic cancer *in vivo* (78, 79). Organoids are grown in an artificial matrix which allows them to spontaneously develop tumour-like and organ-like structures (80). Although organoids can recapitulate structures that a tumour may form *in vivo*, they are not subject to the effects of the wider organism such as the immune system, changes in hormonal signalling, and anatomical influences that a tumour would be.

1.5.2 *In Vivo* Transplantation Models

Transplantation of cancerous tissue into mice is another method of researching cancer. Transplantation approaches enable the involvement of biological systems and anatomical influences in tumour development and response to treatment. Pancreatic cancer tissue may

be transplanted orthotopically to the pancreas or heterotrophically to other sites (such as subcutaneous or intramuscular) (81). Orthotopic xenografts may mitigate potential anatomical issues relating to the location of the transplant, however superficial heterotrophic xenografts allow easier monitoring of tumour development (82). The implanted tissue is usually either murine-derived allografts or human-derived xenografts. As murine-derived allografts can be implanted into immunocompetent syngeneic mice, this approach can be used to investigate the involvement of the immune system in cancer treatment and development. Human-derived xenografts, which typically require implantation into immunocompromised mice, allow the analysis of the human cell lines and tissue which may be more applicable to human PDAC (83).

The use of human-derived cancer tissue often involves transplantation of cultured cell lines. However, the use of xenografts of tissue derived from patient tissue, rather than cultured cell lines, is also possible (84). The use of patient derived tissue mitigates some limitations associated with the use of cultured cells (as described in section 1.5.1).

Although transplantation of cancerous tissue is a useful tool to study pancreatic cancer, it has various limitations. In addition to the limitations of the specific approaches already discussed, the direct implantation of cancerous tissue does not recapitulate initial tumour development (83). Transplantation approaches therefore preclude the analysis of early tumour development and progression, as well as bypasses any effects of early tumour development upon the body and its responses to the cancer.

1.5.3 *In Vivo* Genetically Engineered Mouse Models

The use of Genetically Engineered Mouse Models (GEMMs) of pancreatic cancer enable the study of pancreatic tumours *in vivo*, including the development of healthy tissues into cancerous tumours and any associated processes. The KPC GEMM (Genetically Engineered

Mouse Model) is a well-established preclinical model of PDAC. KPC mice possess three particular genetic modifications to mimic human pancreatic cancer (most commonly *LSL-KRas^{G12D/+}; LSLp53^{R172H/+}; Pdx1Cre*, which were used during the course of this research) (83). In most tissues of KPC animals, the KRas and p53 mutants are prevented from being expressed due to a preceding LSL (lox-stop-lox) site, comprised of a stop codon flanked by lox sites. The Cre-recombinase system allows the expression of these alleles by binding to the lox sites and excising the LSL, therefore removing the stop codon. In the KPC model Cre-recombinase is expressed under a Pdx1 (pancreatic and duodenal homeobox 1) promoter so is only active in cells expressing Pdx1. As Pdx1 largely contributes to pancreatic development, its effects are selective to the developing pancreas (85, 86). All tissue derived from these affected cells also do not possess the LSL and therefore express the mutant genes due to the irreversible genetic alteration caused by Cre activity.

The KPC model is widely used as the standard genetically-engineered mouse model of PDAC due to it faithfully recapitulating the development and presentation of the human form of PDAC (83). By 8 weeks of age KPC mice typically exhibit early PanINs, precursors to PDAC, with most animals having developed PDAC by 16 weeks (83). The predictable and rapid development of the disease in KPC mice enables pre-clinical and basic experimentation before undertaking clinical trials involving human patients.

As the most widely used and well characterised model of pancreatic cancer, KPC mice possessing *LSL-KRas^{G12D/+}; LSLp53^{R172H/+}; Pdx1Cre* alterations were used during the course of this work. However, other forms of the KPC GEMM also exist. Although the original KPC mouse model was developed in mice of a mixed background (129Sv and C57BL/6), strains of KPC mice of a C57BL/6J background (through dilution of other strains over multiple generations) has also been used (83).

The specific genetic alterations used in KPC mice can also vary, potentially having an effect on phenotype of the disease and therefore must be carefully noted. Alternative promoters have been used to regulate Cre expression, such as p48 (83, 87). P48, like Pdx1, is expressed in the developing pancreas. Use of a p48 promoter appears to reduce the likelihood of other tumours, such as papilloma, due to the expression of Pdx1 in other tissues (83). However, despite these apparent advantages this form of the model is not as widely used or as well validated, so may exhibit disadvantages that are yet to be observed or reported.

The original KPC model expresses an oncogenic form of p53 (44, 88, 89). This results in both the loss of a wild-type tumour-suppressor p53 allele and the gain of its pro-tumour function. However, a deactivating mutation ($p53^{flox/+}$) has also been used in KPC GEMMs to trial potential PDAC therapies and investigate PDAC biology (87, 90).

The KPC model was preceded by models featuring either mutation (p53 or KRas) targeted to the pancreas (44, 88, 91). The KRas variant, termed KC, is still a commonly used model of pancreatic cancer. This can either be individually or alongside parallel KPC studies. Due to the longer period of time required for KC mice to develop tumours, the KC model is particularly useful to research PanIN progression and initial PDAC development (92-95).

A variant of the KPC model termed KPPC features homozygous alterations to p53 (45, 87, 90). These can be either $p53^{R172H/R172H}$ or $p53^{flox/flox}$. KPPC mice exhibit decreased survival time and more aggressive tumourigenesis relative to KPC mice (45, 87, 90).

1.6 The Antioxidant System in Pancreatic Cancer

1.6.1 Redox Reactions

The term 'oxidation' originally referred to a substance accepting an oxygen atom and was named for this process. However, the term was broadened to cover any reaction involving a loss of electrons. Similarly, reduction, named for its reduction of oxygen content, now

typically refers to the gain of electrons. Reduction is the necessary partner to oxidation; a redox reaction comprises electron transfer from one component to another, with reduction and oxidation being relative to the specific agents being described.

Most intracellular oxidants are oxygen-containing molecules produced by the mitochondria, termed Reactive Oxygen Species (ROS). ROS play an important role in healthy cells as second messengers, particularly in the inflammatory response, however high levels of ROS can cause damage to cells. ROS comprise many different chemicals that can cause different forms and extent of damage to cells. Most severe is the hydroxyl radical, a free radical which can cause severe disruption to DNA. As DNA damage can result in cell death or carcinogenesis, ROS activity is relevant to cancer as causes of, and potentially limiting factors of, tumours.

1.6.2 Chemical Stressors in Cancer

Intracellular ROS levels are tightly controlled in both healthy and cancerous tissue. However, tumour cells exhibit higher levels of ROS than healthy tissue (43, 96-99). Although ROS may contribute to initial carcinogenesis, and cell signalling related to increased oxidation is an important part of tumour cell function (96, 99, 100), increased abundance of ROS is harmful to cells (43, 96, 97, 99, 101, 102). Tumour cells therefore also exhibit increased expression of antioxidant genes, as discussed further in 1.6.3.

1.6.2.1 Glycolysis and the Warburg Effect

An increase in intracellular ROS contributes to the initiation of the Warburg effect, a near ubiquitous feature of cancers (97). The Warburg effect refers to the shift in glycolytic respiration from aerobic to anaerobic, even in the presence of oxygen.

Glycolysis is a series of respiratory reactions by which ATP is produced from ADP, using energy released from the conversion of glucose to pyruvate. This process is also associated with the reduction of NAD⁺ to NADH. In healthy cells with sufficient oxygen supply, pyruvate

can be further metabolised aerobically to produce additional ATP. In conditions where oxygen levels are not sufficient for aerobic respiration, pyruvate is instead fermented to lactate. This process results in the oxidation of NADH to NAD⁺, which can be used during glycolysis so therefore increases the potential for anaerobic respiration.

In cancer cells, however, the fermentation of pyruvate to lactate happens even in the presence of sufficient oxygen. This results in the accumulation of lactate, which is pumped into the extracellular space. The subsequent decrease in extracellular pH may also contribute to metastasis of the tumour due to degradation of the extracellular matrix (103).

1.6.3 The Nrf2-Mediated Antioxidant System

Nuclear factor erythroid 2 Related Factor 2 (Nrf2) is a transcription factor encoded by the gene *NFE2L2* (Nuclear Factor Erythroid 2 Like 2) (104). As the master regulator of the antioxidant system, it activates the transcription of over 200 genes by binding to the Antioxidant Response Element (ARE) of their promoter regions (105). It has been investigated as both a tumour suppressor and an oncogene due to its function to protect cells against cytotoxic stress (43, 106-111). Although its ability to defend cells against chemical and oxidative stresses may prevent carcinogenesis occurring, once cancer has developed, tumour cells use Nrf2 and its downstream targets to promote their own survival (43, 106, 109, 112-117). Various well-described oncogenes such as KRas exert their effects partly through the induction of Nrf2 (43).

Many downstream targets of Nrf2 act either as antioxidants or as a support for the antioxidant system, so therefore rely upon electron donors, typically glutathione (GSH) and/or NADPH (previously known as TPNH₂). To facilitate this need Nrf2 upregulates genes of the pentose phosphate pathway, which produces NADPH at various points of a multistep process (118). NADPH is either involved directly in reduction reactions catalysed by Nrf2

downstream genes, resulting in its oxidation to NADP⁺, or the restoration of antioxidants such as GSH which acts as the electron donor in such reactions.

The production of GSH, a tripeptide, is catalysed by multiple proteins upregulated by Nrf2 (Fig. 1-2). GCLC and GCLM, also known as GCS(h) and GCS(l) respectively, are Nrf2-downstream genes responsible for the synthesis of γ -glutamyl cysteine synthetase (GCL) (119-122). GCL produces γ -glutamyl cysteine from the amino acids cysteine and glutamate. Glutathione synthetase (GSS), also upregulated by Nrf2, then condenses γ -glutamyl cysteine and the amino acid glycine to form GSH (122-125). GSH is then available to act as a reducing agent to respond to oxidative stressors, and the action of GSH is one of the main mechanisms by which Nrf2 exerts its antioxidative influence. Due to its action as an electron donor, GSH itself becomes oxidised when utilised in redox reactions to form glutathione disulphide (GSSG) with another oxidised GSH molecule. To revert GSSG to two active GSH molecules, the Nrf2-downstream enzyme glutathione reductase (GSR) reduces GSSG using NADPH as an electron donor (126, 127).

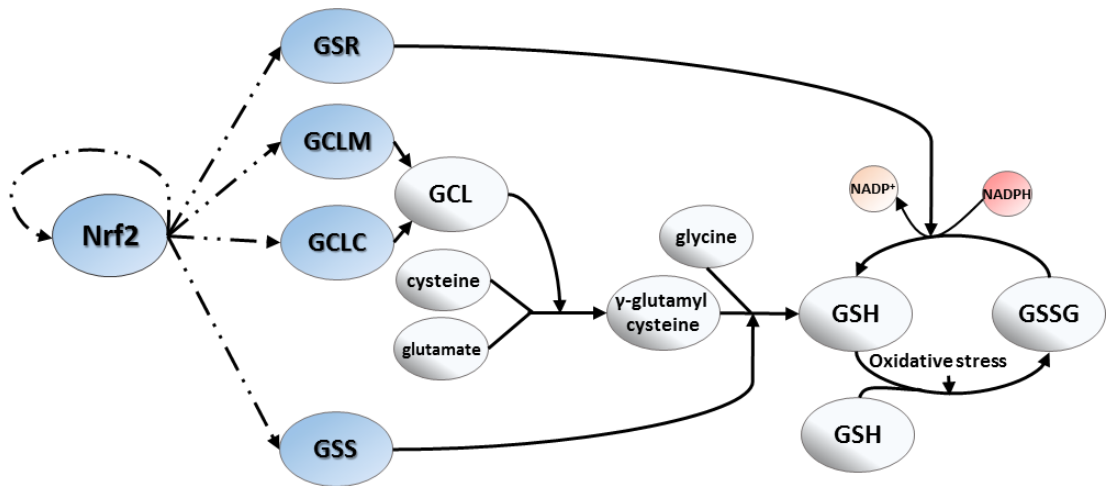


Figure 1-2: The glutathione synthesis and restoration pathway. Nrf2 transcriptional targets are shown in blue. GCLM, GCLC and GSS contribute to the initial production of GSH molecules. GSR utilises NADPH to reduce GSSG (two oxidised GSH molecules) back into two GSH molecules. Abbreviations: GCLM, Glutamate-Cysteine Ligase Modifier Subunit; GCLC, Glutamate-Cysteine Ligase Catalytic Subunit; GSS, Glutathione Synthetase; GSH, Glutathione (reduced); GSR, Glutathione-Disulfide Reductase; NADPH, Nicotinamide adenine dinucleotide phosphate; GSSG, Glutathione disulphide (oxidised).

Under basal conditions Nrf2 is inhibited in healthy cells by Keap1 (Kelch-like ECH-Associated Protein 1), also known as INrf2. Keap1 forms a homodimer and binds both Nrf2 and actin filaments, tethering Nrf2 in the cytoplasm and therefore preventing its translocation to the nucleus and the subsequent transcription of its downstream targets. Keap1-bound Nrf2 is also ubiquitinated by the Cullin-RING box E3 ligase Cul3-RBX1 to mark it for proteasomal degradation (128). Under basal conditions, the Keap1-mediated degradation system is active and Nrf2 has a half-life of approximately 20 minutes (129). The half-life of Nrf2 is greatly extended in response to oxidative stress. Oxidation causes deformation of Keap1 and therefore the release of Nrf2, preventing its ubiquitination and allowing it to translocate to the nucleus. Nrf2 is therefore activated by the conditions it is equipped to counteract. Once in the nucleus it binds to the ARE regions of the gene promoters of its targets to upregulate

their expression. A positive feedback loop then reinforces Nrf2 activity as multiple Nrf2-activating proteins (such as P62/SQSTM1) and Nrf2 itself are encoded by genes activated by Nrf2.

1.6.4 Nrf2 in Pancreatic Cancer

Nrf2 has been identified as a tumour promoting protein due to its ability to protect cancer cells from their own metabolic stress and treatments such as chemotherapy. Nrf2 has been shown to be upregulated in multiple forms of cancer, including PDAC (99, 109, 113, 116, 117, 130). Additionally, nuclear translocation of Nrf2 has been demonstrated to correlate with poorer patient prognosis (115). Although cancer cells are known to be rendered chemoresistant by Nrf2 activity (99, 109, 130-133), the response of Nrf2 to chemotherapy is not clear. It has previously been shown that treatment with gemcitabine activates the Nrf2 pathway in pancreatic cancer cells, however a reduction in Nrf2 activity has also been observed via a luciferase-based assay following treatment with gemcitabine (134, 135).

The increased Nrf2 activity under basal conditions in tumours appears to have multiple causes and varies depending upon cancer type (113, 136). Although loss of Nrf2 inhibition through *KEAP1* methylation has been shown in multiple forms of cancer, it has only been demonstrated in PDAC *in vitro* rather than in clinical samples (136-140).

1.6.4.1 – NQO1 in Pancreatic Cancer

NQO1 (NAD(P)H Quinone Dehydrogenase 1), a downstream target of Nrf2 which functions to reduce quinones, has commonly been used as a marker of Nrf2 activity. This is partly due to difficulty detecting Nrf2 directly, as there has been controversy regarding how to interpret antibody-mediated detection of Nrf2 (such as by western blot) (141). Additionally, the abundance of Nrf2 protein would not necessarily correspond to Nrf2 activity as closely as the abundance of its downstream targets would, as their accumulation is a result of that Nrf2 activity.

Previous unpublished work within this research group has found that high levels of NQO1 correlate with better patient prognosis (142). Retrospective analysis of ESPAC-1 and ESPAC-3 samples of resected pancreatic tumour found that tumours exhibiting high levels of cytoplasmic NQO1 correlated with increased patient survival time in response to gemcitabine treatment (142). Hypothetically, this may be due to high levels of NQO1 correlating with high levels of intracellular stress, and therefore tumours exhibiting a large amount of NQO1 protein would already be compromised by that intracellular so therefore potentially more vulnerable to chemotherapy. Although it does not appear to directly support the hypothesis that NQO1 would defend cancer cells from chemotherapy, it may be that only additional NQO1 would be expected to achieve this rather than NQO1 already present and responding to already present threats. Pretreatment levels of NQO1 may not be a direct reliable marker of how much NQO1 is available to respond to subsequent stressors.

Multiple polymorphisms of NQO1 have been described (143). One such polymorphism is the C609T (Pro187Ser) SNP, rs1800566 (143-147). This substitution almost entirely removes the antioxidant effect of the resultant protein by causing rapid degradation of the mutant NQO1. The effect of the inactivating rs1800566 SNP of NQO1 upon the development of cancer appears to vary between different types of cancer (144-147). Although rs1800566 has been seen to be associated with probability of developing colorectal and digestive tract cancers (145, 146), investigations into others cancers have either not found an association (as in bladder cancer (144)) or have found that the SNP is protective against cancer (such as oesophageal (147)). A significant effect of rs1800566 has not been demonstrated for pancreatic cancer (148). However, once cancer has developed it could be expected to defend cancerous cells from their own metabolic stressors and chemotherapy. As such, in the context of cancer treatment NQO1 loss-of-function may be hypothesised to render the tumour cells more sensitive to treatment.

1.7 Brusatol

Brusatol, a small molecule extracted from the plant *Brucea javanica*, is widely used as an Nrf2 inhibitor (101, 112, 149-155). Brusatol has traditionally been proposed to have multiple potential medical uses due to displaying anti-tumour and anti-malarial properties (101, 151, 156).

1.7.1 Brusatol as Chemotherapy

The anti-tumour effect of brusatol in particular has been focused upon in recent years. Previous studies have shown that brusatol exhibits anti-cancer properties both *in vitro* and *in vivo* (101, 151, 157-159). In addition to its own cytotoxic effects, brusatol appears to synergise with and sensitise cells to other forms of chemotherapy, as well as different avenues of therapy such as radiation treatment (101, 151).

Brusatol inhibited the colony forming ability of A549 cells *in vitro* and limited A549 xenograft tumour growth *in vivo*, particularly in combination with cisplatin (151). Although brusatol did not appear to cause DNA damage when analysed by comet assay, it was reported to enhance the DNA-damage effect of 6 Gy γ -irradiation and so appears to act as a radiosensitiser. *Brucea javanica* extract has also been seen to cause cell cycle arrest, prevent proliferation, induce apoptosis and increase ROS content in a number of cells lines, specifically A549 and H446 (158). However, it is not certain to what extent, if any, brusatol was responsible for these effects as the exact contents of the extract were not investigated.

In regards to pancreatic cancer, brusatol has been shown to inhibit the growth of orthotopic xenografts of cell lines in mice both individually and in combination with chemotherapy (gemcitabine and 5-FU) (157). However, to our knowledge there is no prior published research investigating the effects of brusatol in a genetic model of PDAC.

1.7.2 The Mechanism of Action of Brusatol

Although inhibition of Nrf2 is an attractive concept for cancer therapy, efforts to identify a pharmacological inhibitor have been met with limited success. Brusatol is currently widely used as an Nrf2 inhibitor (133, 153-155, 160-162), however it has also been demonstrated that brusatol is a protein synthesis inhibitor and that brusatol may not act specifically upon Nrf2 (159, 163, 164).

1.7.2.1 Brusatol as a Protein Synthesis Inhibitor

The mechanism of action of brusatol is not well known. Although it is known to inhibit protein synthesis and the protein Nrf2 (among others), the method by which it does so has not been definitively identified (151, 159, 164). The related compound bruceantin, an extract of *Brucea antidysenterica*, has been shown to inhibit the formation of peptide bonds and therefore protein synthesis through binding to the ribosome (164, 165). The combination of their related structure and similar effects may suggest that brusatol functions through a mechanism similar to that of bruceantin. Although the effects of brusatol to inhibit protein synthesis has been known for several decades (164), this was at large concentrations (up to 50 μ M). 500nM brusatol appeared to have little to no effect upon protein synthesis (164), whereas 40nM was seen to result in depletion of Nrf2 in separate studies (151). The large discrepancy may have suggested these were unrelated separate effects, however subsequent work demonstrated protein synthesis inhibition occurring at similar concentrations (100nM) (159, 163). It therefore seems that protein synthesis previously only being seen following treatment with high concentrations of brusatol was a result of the cell line used (rabbit reticulocytes) rather than it being a separate mechanism to the depletion of Nrf2.

It has been suggested that the seemingly selective inhibitory effect of brusatol upon Nrf2 abundance may be due to the short half-life of the protein. If brusatol were to globally inhibit

translation, the abundance of proteins would decrease at a rate dependent upon their rate of degradation. Nrf2, which has a half-life of 20 minutes under basal conditions, would be depleted more quickly than longer lived proteins. An effect upon protein synthesis may therefore appear to be specific to Nrf2 and other proteins with a short half-life. In this case the specific cause(s) of tumour inhibition is not directly clear. Although protein synthesis would likely be directly required for tumour progression, cell death and reduction in viability as a result of brief loss of synthesis may suggest the rapid depletion of specific proteins results in failure of tumour maintenance. Effects upon Nrf2 in particular are a reasonable possibility due to being one of few proteins observed to noticeably deplete following brusatol treatment, the loss of Nrf2-mediated pro-survival function, and the observation of toxic events (such as the accumulation of ROS) consistent with Nrf2 depletion following brusatol treatment (101). The combination of depleting Nrf2 to prevent the transcription of pro-survival genes and directly preventing their translation may be responsible for the toxic and anti-tumour effects observed following brusatol treatment.

1.7.2.2 Brusatol as an Nrf2 Inhibitor

Since the discovery that similar concentrations of brusatol inhibit protein synthesis and reduce Nrf2 abundance, it has been demonstrated that Nrf2 inhibition would result in the inhibition of protein translation (116). Depletion of Nrf2 and subsequent accumulation of ROS has previously been shown to inhibit protein synthesis due to the large number of cysteine residues, which are vulnerable to oxidative stress, in translational machinery (116). As such, it is possible that the effect of brusatol upon protein synthesis is secondary to a selective effect upon Nrf2. The observation that both effects occur simultaneously does not necessarily suggest which, if either, the primary effect is as either could result from the other. Another possibility is that brusatol causes both effects independently of each other through multiple mechanisms of action. However, the presence of protein synthesis inhibition and

Nrf2 inhibition have since been demonstrated to occur following treatment with similar concentrations of brusatol, and neither effect has been seen without the other, rendering an explanation involving two independent mechanisms, unlikely.

1.7.2.3 Mechanisms of action of Brusatol and the alternative Nrf2 inhibitor, ML385

Understanding the mechanism of action of brusatol will be beneficial to evaluating its viability as a potential chemotherapeutic agent. As such, the mechanism of action of brusatol and through what method it inhibits tumour viability was investigated during the course of this project. A more recently identified inhibitor of Nrf2 is ML385 (166). ML385 demonstrates inhibition of Nrf2 by binding to its DNA-binding domain (Neh1), with effects consistent with previously observed consequences of Nrf2 inhibition such as an increase in chemosensitivity (109, 166). The efficacy of ML385 as an inhibitor of Nrf2 was also investigated during the course of this work (Chapter 4).

1.8 Purpose and Hypotheses

PDAC has a dismal prognosis, which is in large part due to it being resistant to chemotherapy. The aim of this research was to evaluate the mechanism of action of brusatol, particularly in relation to its function as an Nrf2 inhibitor, and explore its potential usefulness as a chemotherapeutic agent. The purpose of this research was to identify ways of rendering PDAC more chemosensitive and to determine if brusatol in particular could enhance the chemosensitivity or act as a useful form of chemotherapy.

I hypothesised that Nrf2 and select downstream targets contribute to acquired chemoresistance of pancreatic cancer, and that the use of brusatol can contribute to treatment for pancreatic cancer.

1.9 Aims and Objectives

The aim of this research was to investigate the involvement of the Nrf2 pathway, including downstream targets such as NQO1, in patient response to chemotherapy and explore if brusatol is a viable form of chemotherapy (either through modulation of Nrf2 or as a result of other mechanisms of action).

The objectives of this research were as follows:

1. Analyse the role of the Nrf2-mediated antioxidant system in PDAC.
 - a. Identify how chemotherapy treatment affects Nrf2 abundance and activity both *in vitro* and *in vivo*.
 - b. Identify the effect of modulating Nrf2 upon cancer cell viability and chemotherapy efficacy.
 - c. Investigate protein abundance and genetic/epigenetic alterations in Nrf2-related genes such as *KEAP1* and *NQO1* in patient samples, and how they correlate with response to treatment.
2. Explore the mechanism of action of the Nrf2-inhibitor brusatol.
 - a. Explore if, and how, protein synthesis inhibition and Nrf2 depletion are causally related.
 - b. Determine to what extent Nrf2 depletion accounts for the anti-tumour effects of brusatol.
3. Determine the efficacy of brusatol as a potential chemotherapeutic agent.
 - a. Determine the viability of brusatol *in vitro* as either a combination or monotherapy.
 - b. Determine if brusatol treatment can improve survival time in a GEMM of PDAC (KPC), and determine its effectiveness and toxicity relative to current mainline therapy (gemcitabine).

2 - Materials and Methods

2.1 Cell Culture

MIA PaCa-2, PANC-1, SUIT-2 and HEK-293 cells were maintained and passaged regularly in T75 flasks (10364131, Fisher Scientific) in 10% FBS (cos10270106, Invitrogen) Dulbecco's Modified Eagle's Medium (D6429, Sigma), in a humidified incubator at 37°C with 5% CO₂. Unless otherwise stated, numbers of cells seeded in 6-well plates were 1x10⁵ (MIA PaCa-2, SUIT-2) or 2.5x10⁵ (PANC-1) per well. The number of cells seeded in 96-well plates were 2x10³ (MIA PaCa-2, SUIT-2) or 4x10³ (PANC-1) per well.

2.2 Drug Treatments

Except where otherwise stated, chemicals used for treatment during *in vitro* assays were dissolved in 10% FBS Dulbecco's Modified Eagle's Medium. Experiments were performed alongside a vehicle control (of the solvent/dilutant) to an equivalent volume added during drug treatment.

Table 2.1: The solvents/dilutants and suppliers of chemicals frequently used *in vitro* in this work.

Chemical	Solvent/Dilutant	Supplier, Cat. No.
Gemcitabine hydrochloride	H ₂ O	Sigma-Aldrich, G6423
5-FU	H ₂ O	Sigma-Aldrich, F6627
Brusatol	DMSO	Carbosynth, FB30016
CDDO-Me	DMSO	Sigma-Aldrich, SMB00376
ML385	DMSO	Sigma-Aldrich
MG-132	DMSO	Sigma-Aldrich
Hydrogen Peroxide (H ₂ O ₂), 30%	H ₂ O	Sigma-Aldrich

2.3 Protein isolation, Separation and Western Blotting

Cells to be analysed by western blot were harvested in RIPA buffer (89900, Thermo Scientific, UK) containing a final concentration of 1% protease inhibitor (186281, Thermo Scientific, UK) and 0.1% of proteasome inhibitor MG-132. The protein concentration of the cell lysate was determined using a bicinchoninic acid (BCA) assay (23225, Thermo Scientific, UK) according

to manufacturer's instructions. 4x reducing sample buffer (RSB) was prepared at the time of use from Laemmli buffer (Table 2.2) and DTT (final concentration 0.1M). The volume of RSB added was one third that of the protein lysate volume per sample to produce 1xRSB/lysate combination. Equal masses (20µg) of protein were incubated at 95°C for ten minutes in RSB. Samples were then dispensed into wells of a precast BioRad Miniprep SDS-PAGE gel. The gels used were 7.5% concentration (456-1026) when Nrf2 was to be detected, otherwise Any KD (456-9033) was used. For the detection of Nrf2, proteins were separated using electrophoresis at low voltage (60V) at 4°C for 30 min. Voltage was then increased to 90V for the maximum length of time possible whilst retaining all proteins of interest. If Nrf2 was not to be detected, electrophoresis was performed at 300V at RT (RT). Proteins were then transferred to PVDF membranes (1704156, BioRad) and analysed using western blotting.

Table 2.2: 4x Laemmli buffer components

<u>Component</u>	<u>Final Concentration in dH₂O (4x Laemmli Buffer)</u>
Glycerol	40% v/v
TrisHCl (1M, pH 8.8)	24% v/v
SDS	8% w/v
Bromophenol Blue	0.04% w/v

Membranes were blocked in 5% milk 0.1% PBST (Phosphate Buffered Saline; 0.1% Tris-20 v/v) w/v for ≥2 h. Incubation with primary antibody (Table 2.3) was performed for ≥2 hours.

Table 2.3: Antigens detected via western blotting, the primary antibodies used to do so, and the concentrations of primary and secondary antibodies.

Antigen	Primary Antibody Concentration	Secondary Antibody Concentration	Primary Antibody Supplier, Cat. No.
Nrf2	1:1000	1:1000	Abcam, ab62352
NQO1	1:2000	1:2000	Invitrogen, MA1-16672
AKR1C1/2	1:2000	1:2000	Abcam, ab96087
GCLC	1:1000	1:1000	Abcam, ab190685
β -Actin	1:20,000	1:4000	Sigma-Aldrich, A2228

Following multiple washes with 0.1% PBST, membranes were transferred to secondary antibody (Anti-rabbit – P0448, Dako; Anti-mouse – P0447, Dako) and incubated for ≥ 2 h. Clarity Western ECL Substrate (1705061, BioRad) was added to membranes for 5 min following an additional wash sequence. All washes and incubations were performed under gentle agitation at RT, or at 4°C for ≥ 15 h. The resulting chemiluminescence measured using a BioRad Chemidoc Touch.

2.4 Protein Synthesis Analysis

Cells were seeded at 1×10^6 (Suit2, MIA PaCa-2) and 2.5×10^6 (Panc1) cells per well of a 6 well plate. Where CDDO-Me pretreatment was to be performed, cells were treated with CDDO-Me four hours in advance and returned to the incubator. At 80% confluence cells were treated with brusatol, cycloheximide (CHX) or DMSO vehicle control for 15 min. Medium was removed and wells were then washed twice with PBS. The chemical treatments (brusatol/CHX/DMSO) were prepared in methionine-free medium (A14517-01, Gibco), then were added and allowed to incubate for 30 min. The methionine analogue L-azidohomoalanine (C10102, Invitrogen) was then added to a final concentration of 50 μ M and allowed to incubate for an hour. Plates were washed twice with PBS and harvested in 1% SDS pH 7.4 tris buffer containing proteinase inhibitors (1861281, Thermo Scientific) and 0.1% MG-

132. Lysis was achieved using three freeze-thaw cycles separated by 10-second mixing via vortex. The Click reaction with Biotin Alkyne (B10185, Invitrogen) was performed according to manufacturer's instructions (C10276, ThermoFisher), followed by protein precipitation and resuspension in 1xRSB. Up to 10 μ g of protein was loaded onto a premade SDS-PAGE gel (456-9033, BioRad) and separated using electrophoresis, then transferred to a PVDF membrane (1704156, BioRad). The membrane was blocked in 5% milk 0.1% PBST for 1 h followed by 16-hour incubation at 4°C with streptavidin-HRP (N50, Thermo - 1:1000 dilution in 5% milk 0.1% PBST). Following multiple 0.1% PBST washes, the membrane was incubated with ECL (170-5061, BioRad) at RT for five minutes and chemiluminescence detected using a BioRad Chemidoc Touch.

2.5 Knockdown

Transfection of siRNA was performed using lipofection. Lipofectamine (Lipofectamine™ 2000 – 11668500, Invitrogen) and siRNA (Nrf2 SMARTpool: L-003755-00-0005, Dharmacon; Non-Targeting: D-001220-01-05, Dharmacon) were each separately diluted in Opti-MEM™ I Reduced Serum Medium (11058021, Gibco) and incubated for 5 min (Table 2.4), then combined and incubated at RT for 20 min. Cells in 6-well plates were washed with PBS and fresh medium added, then the combined siRNA-containing solutions were added dropwise to a final volume of 3mL. Cells were incubated for 24h before harvest for western blot.

Table 2.4: The volumes of reagents used in each solution prior to combining 1:1 for a knockdown. siRNA volume varied depending upon the concentration to be used (shown italicised in parentheses).

Reagent	Volume ($\mu\text{L}/\text{well}$)	
	Solution A	Solution B
Opti-MEM	200	200
Lipofectamine	4	-
siRNA (20 μM)	-	3 (20nM)/ 6 (40nM)

2.6 Nrf2 Luciferase Assay

A luciferase-based assay was utilised to measure Nrf2 activity. An Nrf2-inducible PGL4.11 vector containing 8 Nrf2-responsive ARE sequences was transiently transfected into MIA PaCa-2, PANC-1, SUIT-2 or HEK-293 cell lines. The HEK-293 cell line, a human embryonic kidney cell line commonly used in transfection studies for their reliably high rate of transfection, was utilised for the purposes of optimisation. A solution comprising 200ng Nrf2-Luciferase plasmid, 20ng *Renilla* control plasmid (E6921, ProMega) and 25 μL Opti-MEM was added per well of a white based 96-well plate (655083, Greiner Bio-One). A second solution containing 0.8 μL Lipofectamine 2000 and 25 μL Opti-MEM per well was prepared and incubated at RT for 5 min before combining with the DNA solution (Table 2.5).

Table 2.5: The quantities of reagents used in each solution prior to combining 1:1 for transient transfection of an Nrf2-inducible reporter. Volumes are shown as $\mu\text{L}/\text{well}$ except DNA, which is shown as mass (ng) as volume varied depending upon the stock concentration.

Reagent	Volume ($\mu\text{L}/\text{well}$)	
	Solution A	Solution B
Opti-MEM	25	25
Lipofectamine	0.8	-
DNA	-	20ng (<i>Renilla</i>)/ 200ng (<i>8xARE</i>)

Once the two solutions were combined with each other, the combined solution was incubated for a further 30 min before adding dropwise to cells in a 96-well plate. Luciferase activity was detected using Dual-Glo[®] Luciferase Assay System (E2920, ProMega) according to manufacturer's instructions. Luminescence was measured using an integration time of 1 second. Firefly luciferase activity was normalised to activity of the ubiquitously expressed *Renilla* luciferase.

2.7 Viability Assays

Viability assays were performed to determine the effect of chemical treatments upon the total viability of a population (one well of a 96-well plate) of cells. This was performed by MTT assay, or by EZ4U – Cell Proliferation Assay (BI-5000, Biomedica Medizinprodukte) for synergy analyses (Section 2.9). Cells were treated with drug of interest in 96-well plates in sextuplicate. Forty-eight hours post-treatment, cell vitality was analysed using an MTT assay. MTT solution was added to a final concentration of $500\mu\text{g}/\text{mL}$ and incubated at 37°C for 3-4 h. Medium was then aspirated and $50\mu\text{L}$ DMSO applied to solubilise formazan. Absorbance was read using a microplate reader with a filter of 570nm. Cell viability was normalised to the mean result of vehicle-treated cells.

Drug synergy/antagonism analyses were performed via EZ4U – Cell Proliferation Assay. The EZ4U – Cell Proliferation Assay is a viability assay which produces a water-soluble product and therefore does not require the removal of medium and the addition of a solvent, as in an MTT assay. This reduced the possibility of variation in results being introduced by the loss of solid formazan during the process of replacing medium with solvent. The EZ4U – Cell Proliferation Assay was used for synergy analyses due to the larger number of unique conditions to compare in synergy assays than in other viability assays during the course of this work, as well as the reduced possibility for replicates during each experiment. Cells were seeded as described above for the MTT assay and exposed to various concentrations of brusatol and either gemcitabine or 5-FU and incubated for 48 h before viability assay. For the purposes of testing the effects of adding drugs sequentially, the concentration range of brusatol was added first and the cells returned to incubate for 24h before addition of the gemcitabine/5-FU range, then incubated for a further 48 h before viability analysis as described. The viability of cells treated with each combination were then compared using multiple models of synergy (Highest Single Agent (HSA), Loewe Additivity Model, Bliss Independence Model, and Zero Interaction Potency (ZIP)) to determine the effect of drug combinations upon various aspects of drug synergy. Synergy analyses were performed and figures obtained using R Package SynergyFinder in R Studio.

2.8 Colony Formation

Various numbers of cells (MIA PaCa-2, SUIT-2, PANC-1) were seeded per well of 6-well plates to determine optimum seeding density. Subsequent experiments involved seeding of 300 (MIA PaCa-2)/500 (SUIT-2 and Panc1) cells per well. Two separate forms of clonogenic assay were performed, defined by the application of treatment either prior to- or post-seeding.

Treatment prior to seeding was used to investigate the effect of gemcitabine, 5-FU and brusatol to prevent cells from forming colonies at a later point (A), whilst treatment following

seeding was used to investigate the effect of gemcitabine, 5-FU and brusatol on the colony forming process directly (B).

To assess the effect of drug treatment prior to clonogenic seeding (A), cells were seeded at a density of 100,000 cells/well of 6-well plates and allowed to adhere for 24 h. The medium was then replaced with drug/vehicle-treated medium for 24h. The treated cells were then suspended via trypsinisation, counted using a BioRad TC10, and 300 (MIA PaCa-2)/500 (Suit-2 and Panc1) cells of the suspension were seeded into wells of 6-well plates.

To assess the effect of drug treatment following clonogenic seeding (B), 300 (MIA PaCa-2)/500 (Suit-2 and Panc1) cells were first seeded in 6-well plates and allowed to adhere for 4h. The medium was then replaced with drug/vehicle-treated medium.

Colonies were allowed to develop for 10 days. At this point medium was removed and cells washed with PBS. A solution containing 6.0% glutaraldehyde/0.5% crystal violet in dH₂O was added to the wells and incubated at RT for 30 min. The solution was then removed and the residual solution washed away via immersion of plates in water. Plates were airdried for >12h and then imaged. The number and size of colonies was then measured using ImageJ and direct visual comparison.

2.9 Migration Assay

Cells were seeded (3×10^5 (MIA PaCa-2, SUIT-2)/ 5×10^5 (PANC-1)) per well of 6-well plates in medium supplemented with 10% FBS. Cells were left to adhere and form a confluent monolayer for 24h, then medium was replaced following a PBS wash with FBS-free medium and cells were serum starved for 16 h. A P200 pipette tip was used to create a scratch. Cellular debris was washed away with a PBS wash and then drug-treated medium supplemented with 1% FBS was added to the cells. The same area of each scratch was imaged at this point (0 h) and at 24h, 48h and 72h after. Analysis was performed by visual comparison and the MRI

Wound Healing Tool macro for ImageJ (167). The wound size at each timepoint was normalised to its 0 h (100%) starting point.

2.10 SNP Analysis

NQO1 polymorphism rs1800566 was analysed using NQO1 SNP Assay (4362691, Assay ID: C___2091255_30, Thermo Scientific). The primers were combined with sample of interest, nuclease-free water, and Roche LightCycler 480 Probe Master Mix (4707494001, Roche LifeScience) in a white 96-well reaction plate for amplification using a Roche LightCycler 480 (Table 2.6). Reagents were prepared according to Table 2.6 except where otherwise stated.

Table 2.6: The volumes of each reagent used in the detection of NQO1 SNP rs1800566.

Reagent	Volume per well (μL)
Nuclease-free water	4
ThermoFisher NQO1 SNP Assay	1
Roche LightCycler 480 Probe Master Mix	10
DNA Sample (10ng/ μL)	5

Hardy-Weinberg equilibrium of NQO1 polymorphism rs1800566 among the trial population was measured using χ^2 test comparing the observed allele distribution to the expected distribution based upon allele frequency. Allele distribution was also compared to that expected of a European cohort (gnomAD v2.1.1 (controls) (168)). A single European cohort was generated from a weighted mean of Finnish and non-Finnish European data. The NQO1 genotype was correlated with survival time.

2.11 Methylation Analysis

Five sets of pancreatic cancer patient matched tumour and acinar tissue were analysed. Tissues sections were mounted on Leica Frameslides, then haematoxylin and eosin

counterstained. Tumour and acinar cells were laser-capture microdissected from the tissue using a Leica LMD7000. Genomic DNA was extracted from the samples using QIAamp DNA FFPE Tissue Kit using an adapted version of the manufacturer's instructions. Samples were incubated with 180 μ L tissue lysis buffer ATL and 20 μ L proteinase K under gentle agitation at 56°C for 18 h. They were then incubated at 70°C before addition of lysis buffer AL (200 μ L) and proteinase K (20 μ L) and incubated for a further 4 h at 56°C under gentle agitation. Samples were mixed with 230 μ L absolute ethanol before being transferred to QIAamp MinElute columns. Samples were centrifuged at 2,000xg for 4 min and 700 μ L buffer AW1 was then added to the membrane. They were then centrifuged at 6,000xg for 1 minute. 700 μ L buffer AW2 was added and the samples centrifuged at 6,000xg for one minute, twice. To dry the membrane, columns were centrifuged at 17,200xg for 4 min. 30 μ L elution buffer ATE was added to the membrane and incubated at RT for 30 min. The eluted DNA was then centrifuged at 17,200xg for 3 min into a collection tube. The extracted genomic DNA then underwent bisulphite conversion using EZ DNA Methylation-Gold Kit according to manufacturer's instructions (D5006, Zymo Research).

Amplification of the bisulphite-treated genomic DNA was performed via PCR using Pyromark PCR Kit reagents (978703, QIAGEN). Two primer mixes (*KEAP1a* and *KEAP1b*) were prepared consisting of 3.75 μ L biotin-tagged primer, 7.5 μ L non-tagged primer and 88.75 μ L ddH₂O. 1.2 μ L of each primer mix was separately combined with 15 μ L Master Mix, 0.6 μ L MgCl₂, 3 μ L CoralLoad loading buffer, 4 μ L of bisulphite treated genomic DNA and 6.2 μ L ddH₂O. Samples were then placed into a thermocycler for initial PCR activation of 95°C for 15 min, followed by 40 cycles of 30 seconds 94°C, 30 seconds 51°C annealing temperature (established during previous optimisation), and 30 seconds 72°C, plus a final 72°C extension of 10 min following completion of all cycles. Amplification of *KEAP1a* and *KEAP1b* was confirmed by electrophoresis of a selection of samples on an agarose gel and UV imaging to detect the DNA.

Pyrosequencing was performed upon the amplified samples using a PyroMark Q96 ID and reagents (972812, QIAGEN) according to manufacturer's instructions.

2.12 *In Vivo* analysis

2.12.1 *In Vivo* – Nrf2 Luciferase

C57BL/6J B6(Cg)-*Tyr*^{c-2l}/J (B6-albino) mice expressing the OKD48 reporter of oxidative stress are described previously (169, 170) and were used here through collaboration with Dr Ian Copple, Prof BK Park and Prof Chris Goldring, Department of Pharmacology and Therapeutics, University of Liverpool, as part of a wider study. Previous research has shown that the Nrf2-reporter of this model does not influence Nrf2 or its downstream targets (169). The albino variant of the model was utilised as pigmentation of the fur and skin was previously identified to obscure the luminescence signal (169). Although this could be mitigated to some extent through shaving of the fur, pigmentation of the skin would result in unavoidable interference. The albino model, however, produced a clear signal without the need for shaving.

Mice were treated with luciferin (E1605, ProMega) via intra-peritoneal (IP) injection and imaged prior to treatment with Dulbecco's Phosphate Buffered Saline (DPBS; 14190-144, gibco), gemcitabine, 5-FU, or CDDO-Me. All volumes of luciferin, gemcitabine, 5-FU and DPBS were standardised and delivered via IP injection at 10ml/kg in DPBS. 10mg/kg CDDO-Me, delivered via IP injection, was used as a positive control of Nrf2 activity induction. CDDO-Me was dissolved and delivered in 100% DMSO (2ml/kg) rather than being diluted to 10ml/kg in DPBS as with other treatments, due to precipitation occurring when CDDO-Me/DMSO solution was diluted in DPBS.

IP injection of luminescent agent luciferin stimulated luminescence in the tissues expressing luciferase proportional to its abundance. The optimum time to image post-luciferin injection was decided following a kinetic analysis in which images were captured every 3 min for a

period of 18 min. During subsequent experiments, a range of images were taken over 15 min and the readings showing peak activity were used for further analysis. Luminescence was measured in radiance (p/sec/cm²/sr). The colouration of signal intensity was kept constant when images of animals from different sessions were to be compared.

Mice were imaged prior to drug treatment and at 4 h, 24 h, 48 h and 1 week post-treatment using an IVIS scanner to detect luminescence. In addition to the images gathered, the average intensity of luminescence across the whole body and also the greatest signal intensity detected from each animal were recorded. For analysis, post-treatment readings were normalised to pretreatment readings to generate fold change in response to treatment (post-treatment/pre-treatment). Tissues of interest were formalin fixed and stored in 70% ethanol for subsequent IHC analysis.

2.12.2 *In Vivo* – KPC Mouse Model

The effect of brusatol on the KPC mouse model of pancreatic cancer was measured relative to vehicle and gemcitabine. KPC (LSL-KRas^{G121D/+}; LSL-p53^{R172H/+};PDX1-Cre) mice were randomly allocated for treatment with brusatol (2mg/kg body mass), gemcitabine (100mg/kg) or vehicle (DPBS/4% DMSO v/v). Each treatment was delivered in 10 µL/g DPBS/4% DMSO solution. Each mouse was treated twice weekly until sacrifice at a humane endpoint. The length of survival was entered into a survival analysis for comparison between each treatment arm of the study.

Several mice developed benign papillomas, a common occurrence amongst KPC mice due to the expression of PDX1 and therefore PDX1-Cre in the skin. Mice with such growths were carefully monitored and humanely culled if a papilloma resulted in impairment of vital functions. All mice found to have papilloma were noted. Any mice culled due to papilloma or other non-pancreatic causes were censored on Kaplan-Meier analysis at the time of exit.

A post-mortem was performed on all mice. Tumours and internal organs were formalin fixed for 72 h and stored in 70% ethanol for subsequent IHC analysis.

2.13 Immunohistochemistry and Haematoxylin Counterstain

Formalin-fixed tissues were dehydrated in 70% ethanol and cut into 3mm sections for processing. Tissue dehydration and paraffin infiltration was performed using a Leico HistoCore PEARL programmed to follow a protocol outlined in Table 2.7.

Table 2.7: Paraffin infiltration of tissue for IHC analysis. Tissue was prepared using a series of ethanol dehydrations, xylene treatments and paraffin infiltration.

Reagent	Temperature (°C)	Time (h:mm)
Formalin	37	1:00
Water	RT	0:02
70% Ethanol	45	0:40
80% Ethanol	45	0:40
95% Ethanol	45	40
100% Ethanol	45	1:00
100% Ethanol	45	1:00
100% Ethanol	45	1:00
Xylene	45	1:00
Xylene	45	1:00
Xylene	45	1:00
Paraffin	65	1:00
Paraffin	65	1:00
Paraffin	65	1:30

Following paraffin infiltration, tissue was immediately embedded into solid paraffin blocks. 7µm sections were mounted on Superfrost Plus slides (J1800AMNZ, Thermo Scientific) and dried overnight prior to IHC and/or haematoxylin and eosin staining.

IHC staining was performed to detect NQO1. NQO1 in mouse-derived (Nrf2Luc and KPC) samples was detected using 1:500 Rb Anti-NQO1 (ab34173, Abcam). Unless otherwise stated, all IHC reagents were part of a detection kit (Anti-rabbit (K4011, Dako)). Sections were first subjected to antigen retrieval using Target Retrieval Solution pH 9.0 (K8004, Dako) in a PT Link (PT10126, Dako), after which sections were washed repeatedly with 0.1% TBST (Tris-Buffered Saline, 0.1% Tween-20 v/v). Residual TBST was removed and peroxidase block added for 10 min. This was then washed repeatedly with TBST, and then the primary antibody added for 1 h. Primary antibody was diluted in Antibody Diluent (S2022, Dako) to the

appropriate concentration. Following TBST wash, the appropriate labelled secondary antibody was applied for 1 h. This was then washed off and DAB substrate/chromagen solution was added for 10 min. Following a final TBST wash sequence, slides were rested in dH₂O for counter staining.

Following IHC, slides were placed in haematoxylin solution for 30 sec. Haematoxylin was then thoroughly rinsed from the slides using running tap water. They were then placed in acid water (0.25% HCl in dH₂O) for 5 sec, before being briefly placed in fresh tap water. They were then placed in Scott's Tap Water (0.2% KHCO₃ w/v, 2% MgSO₄ w/v) for 30 sec before being placed in fresh tap water. Slides were then serially dehydrated in 90% ethanol and two rounds of 100% ethanol for 1 min each. Once dehydrated, slides were placed in xylene twice for 1 min each. DPX mountant (06522, Sigma-Aldrich) was used to adhere cover slips to slides. After being allowed to dry at least overnight, slides were imaged under microscopy.

2.14 Statistical Analysis

Except where otherwise stated, statistical analysis was performed by me and with a *p*-value of <0.05 being considered statistically significant.

Two-tailed *t*-tests were used to investigate increases or decreases relative to vehicle control, such as *in vitro* luciferase assays (as in Chapter 3.2.8, Fig. 3-11). Dunnett's multiple comparisons test was used when various arms were compared to one another, rather than just to a single control arm (Chapter 5.2.5.3, Fig. 5-7).

Log-rank test was used to assess differences in survival trends between different arms of survival analyses (Chapter 3.2.13, Chapter 5.2.7). Because I was blinded to patient ID and survival time relating to each patient sample, the log-rank test of clinical trial data (Fig. 3-20, Chapter 3.2.13) was performed by Dr Eftychia-Eirini Psarelli.

**3 - Nrf2 in Pancreatic
Cancer and Chemotherapy
Response**

3.1 Introduction

The transcription factor Nrf2 (Nuclear factor erythroid 2-Related Factor 2), is the master regulator of the antioxidant system and is encoded by the gene *NFE2L2* (nuclear factor erythroid-derived 2-like 2) (104). Nrf2 has been investigated as a tumour-promoting protein for over a decade (106, 109). The function of Nrf2 is to activate the antioxidant system (110, 171), as described in Chapter 1.6. Although the induction of antioxidant genes may prevent carcinogenesis in healthy tissue (by protecting cells from toxins and carcinogens), the same response is cytoprotective for cancer cells, protecting them from the harmful effects of both intrinsic and extrinsic insults, including from chemotherapy (106, 109, 112). Nrf2 has been shown to be overexpressed in PDAC tissue, as well as promote PDAC cell line survival and chemoresistance (113). Modulation of Nrf2 to render pancreatic cancer more chemosensitive may, therefore, be a promising avenue of research.

Although its basal activity has been shown to contribute to the innate chemoresistance of cancers (including pancreatic) (102, 130, 132, 134, 172), Nrf2 is an inducible agent and it is not currently clear if chemotherapy induces additional Nrf2 activity in cancer or healthy tissue. If so, chemotherapy treatment may result in increased chemoresistance of cancers, including pancreatic cancer, through the induction of Nrf2. Chemotherapy is typically less effective after multiple rounds of treatment (173). Identifying the mechanisms by which chemoresistance is induced following initial chemotherapy treatments may make it possible to target those mechanisms to prevent, or reduce, the subsequent resistance to chemotherapy. In cancers with chemoresistance attributable to Nrf2 (such as PDAC) (102, 117, 130, 131, 134, 172), modulation of Nrf2 in combination with conventional chemotherapy may render cancerous tissue initially more chemosensitive. If inducible Nrf2 contributes to acquired chemoresistance in PDAC, as was investigated during the course of this work, Nrf2 inhibition may enhance the efficacy of subsequent rounds of treatment.

I hypothesised that inhibition of Nrf2 activity would increase chemosensitivity of pancreatic cancer cell lines, and that Nrf2 would be induced following exposure to chemotherapy which would subsequently contribute to acquired chemoresistance of pancreatic cancer. Multiple potential pharmaceutical agents have been shown to inhibit Nrf2 (166, 174, 175), including the *Brucea javanica* extract brusatol (151, 152). Although the exact mechanism(s) of action of brusatol are not well known, it has been shown to result in the rapid depletion of Nrf2 as well as the inhibition of global protein synthesis. The potential mechanisms of action of brusatol, and the relevance of its inhibition of Nrf2 to its anti-tumour properties (101, 151-154, 157, 159, 162, 176), are discussed further in Chapter 4 of this thesis.

The promoter region of *KEAP1* has been shown to be hypermethylated in multiple forms of cancerous tumours (138-140). *KEAP1* promoter methylation has also been demonstrated in PDAC cell lines and the Keap1 protein has been shown to be frequently absent in PDAC tissue (113, 137). Methylation of CpG sites of promoter regions has the potential to inhibit or reduce gene expression, depending upon their location (177, 178). Previous unpublished research within this laboratory developed a method to detect the methylation status of *KEAP1* in laser microdissected FFPE tissue. The *KEAP1* promoter methylation status of two patient matched samples of tumour and stroma were analysed for the purposes of method development, with all samples showing only low levels of methylation (142).

The optimal interpretation of western blots probed for Nrf2 has been the subject of controversy (141, 179). Based upon the open reading frame of Nrf2, a band of ~60kDa would be expected (141). Although many commercially available antibodies were described as targeting the 60kDa form of Nrf2, it now appears that the more relevant bands are detected in the region of ~100kDa (141). The cause of this discrepancy is not clear and the relevance of the 60kDa band, if any, and why multiple Nrf2 bands appear between 95-110kDa is not well understood. I hypothesise that the different relevant Nrf2 bands may correspond to

different states of Nrf2 based upon factors such as its location and phosphorylation/ubiquitination status. As such it may be possible to focus on specific bands, their locations, and relative quantities to develop a more sophisticated western blot analysis of Nrf2 to measure function rather than simply total protein abundance.

3.2 Results

3.2.1 Validation of Nrf2 antibody and the identification of multiple Nrf2 bands

Three bands were detected between 100kDa and 130kDa (Fig. 3-1). This was consistent with published literature (141) which described the region of biologically relevant Nrf2 bands as being ~95-110kDa. Experiments were conducted to determine the authenticity of these bands. siRNA-mediated knockdown of Nrf2 resulted in depletion of these bands relative to off-target control siRNA. The lower two bands were not detected following Nrf2 knockdown, whereas the highest band was still present but noticeably reduced. Incubation with Nrf2 activator CDDO-Me resulted in increased intensity of each band, with a particularly prominent increase in the lower of the three.

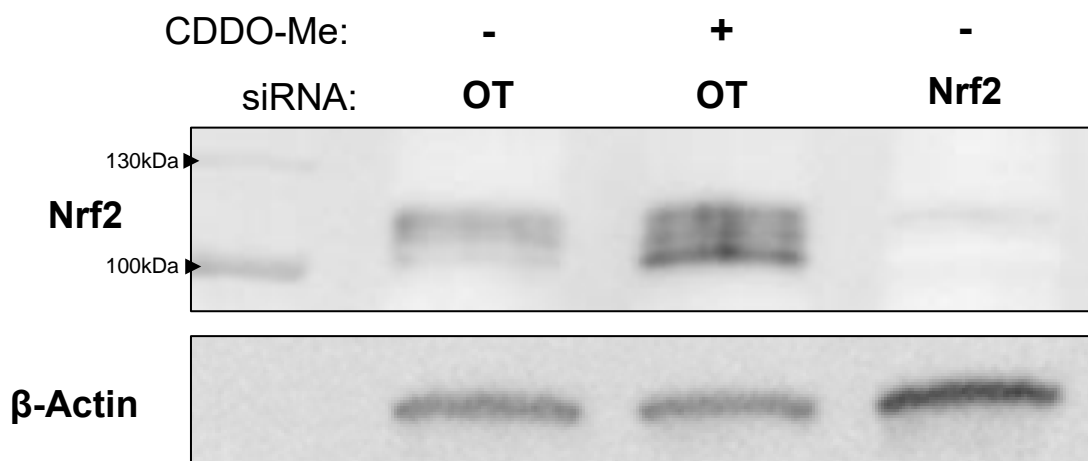


Figure 3-1: Western blot of SUIT-2 cell lysate following 24h knockdown of Nrf2 and exposure to 100nM CDDO-Me. The protein ladder is shown to the leftmost lane. β -Actin levels were obtained as a control for loading. Abbreviations: OT, Off Target siRNA.

3.2.2 Nrf2, NQO1 and AKR1C1/2 Responded to the Nrf2 Activator CDDO-Me

Further western blotting was performed using a heavily optimised protocol (Chapter 2, Section 2.3) to increase resolution and separation in the 100kDa region to visualise the multiple Nrf2 bands previously observed (Fig. 3-1 and Fig. 3-2). The three bands are hereafter referred to as 103kDa, 108kDa and 115kDa (from lowest to highest in position on the membrane), based upon their apparent molecular weights following improved separation (Fig. 3-2). Nrf2 protein abundance and select downstream targets following 24h incubation with CDDO-Me were analysed (Fig. 3-2). The intensity of Nrf2 bands, especially the 108kDa and 115kDa bands, were increased. The 103kDa band also increased in intensity, as confirmed by densitometry, although to a lesser extent than the others (Fig. 3-2, Fig. 3-3). AKR1C1/2 and NQO1 were noticeably upregulated following treatment with most concentrations of CDDO-Me, the extent of which varied between different CDDO-Me concentrations.

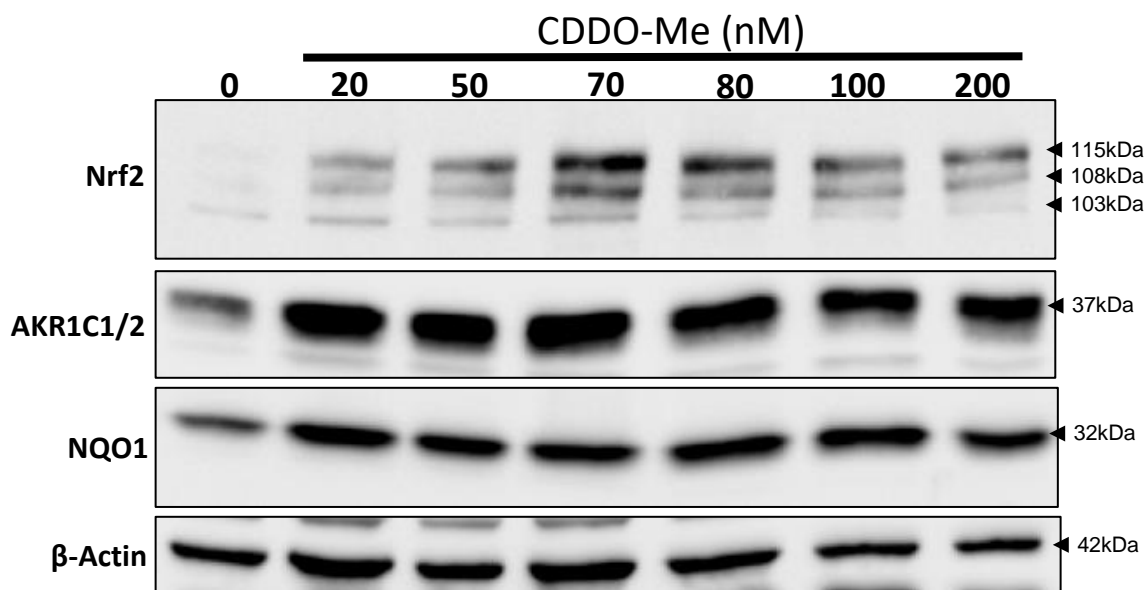


Figure 3-2: SUIT-2 cell lysate, following 24h exposure to CDDO-Me, probed for Nrf2 and downstream targets AKR1C1 and NQO1. Nrf2, β -Actin levels were ascertained as a control for loading. Representative image shown from three independent experiments.

Densitometry confirmed that each Nrf2 band increased in intensity, after normalising to β -Actin loading control (Fig. 3-3). The 115kDa and 108kDa bands increased to a peak of 56.2 and 22.6 times, respectively, their vehicle-treated abundance in response to being treated with 70nM CDDO-Me. The 103kDa band also reached a peak in response to 70nM CDDO-Me, however it only reached 2.5 times its vehicle-treated abundance. Higher concentrations of CDDO-Me (80nM, 100nM, 200nM) also resulted in upregulation of each Nrf2 band, however each higher concentration appeared to predominantly result in lower Nrf2 accumulation than 70nM.

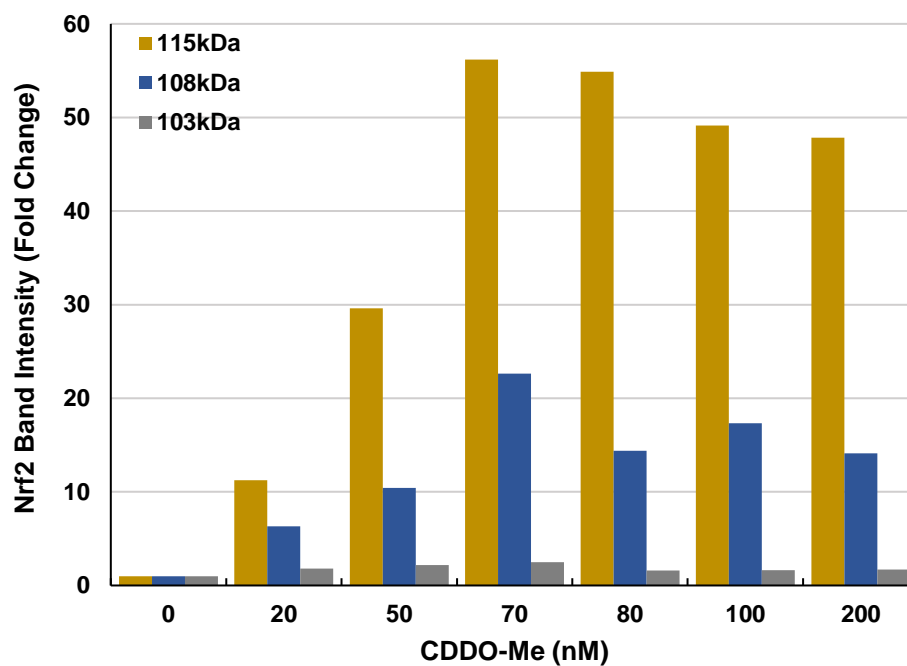


Figure 3-3: Densitometric analysis of Nrf2 bands (103kDa, 108kDa, and 115kDa) from Fig. 3-2. Band intensities were normalised to β -Actin loading control and expressed as fold change relative to vehicle only (0nM CDDO-Me) control.

Densitometry confirmed that AKR1C1/2 and NQO1 also increased in intensity (Fig. 3-4), after normalising to β -Actin loading control.

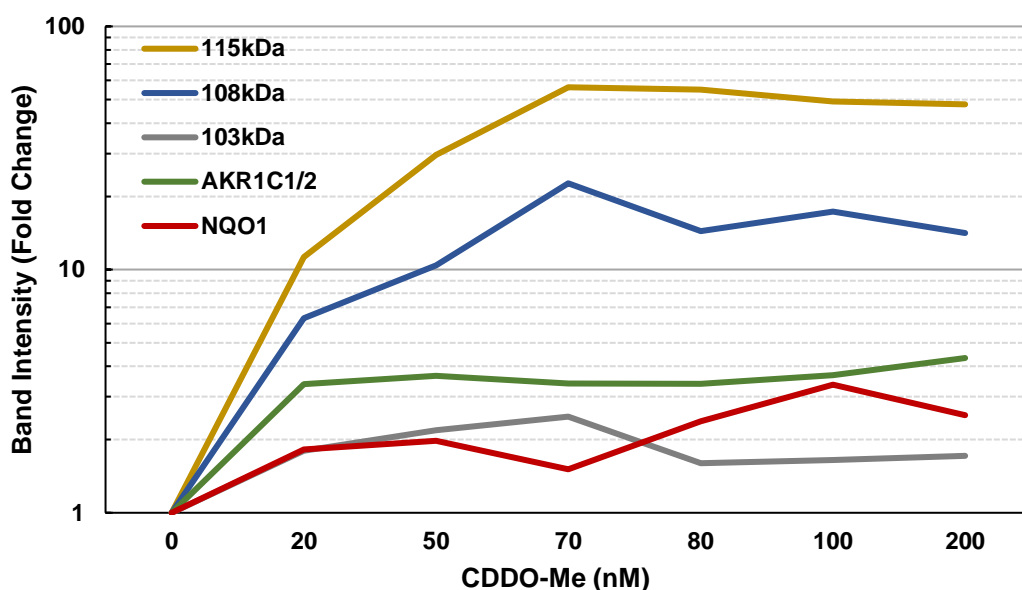


Figure 3-4: Alternative representation of densitometric analysis of Nrf2 bands (103kDa, 108kDa, and 115kDa) from Fig. 3-2, shown on a log₁₀ scale alongside densitometric analysis of AKR1C1/2 and NQO1, also from Fig. 3-2. Band intensities were normalised to β -Actin loading control and expressed as fold change relative to vehicle only (0nM CDDO-Me) control.

3.2.3 Identification of bands corresponding to newly-synthesised and stable Nrf2

In order to further explore the nature of the three Nrf2 antibody-reactive bands, cells were exposed to either the proteasome inhibitor MG-132 and/or the protein synthesis inhibitor cycloheximide (CHX), or the proposed Nrf2-inhibitor brusatol (+/- MG-132) for 24h, and their respective effects upon each Nrf2 band were investigated (Fig. 3-5).

As expected, treatment with brusatol and CHX each resulted in depletion of the 115kDa and 108kDa Nrf2 bands, however this was not the case for the 103kDa Nrf2 band. MG132 treatment resulted in the accumulation of Nrf2, with the 115kDa form most affected, indicating that the 115kDa form is the form most highly targeted for proteasomal degradation. Combined treatment of MG132 and either CHX or brusatol resulted in an increase in the 115kDa band relative to either CHX or brusatol alone, however the 108kDa band was not detectable in cells following the combined treatment with either MG132 and brusatol or MG132 and cycloheximide despite being detectable following treatment with

MG132 alone. As such it appears that 108kDa represents a newly synthesised form of Nrf2 which would not be present following treatment with an inhibitor of protein synthesis even if Nrf2 was prevented from being degraded. The 115kDa band appears to represent a longer-lived form of the protein, as it was not inhibited to as great an extent as the 108kDa band when treated with brusatol or cycloheximide alone, whereas it was accumulated when cotreated with MG132 and brusatol or cycloheximide. It therefore appears that the 108kDa form is converted to the 115kDa form by post-translational modification. Two possibilities of post-translational modification known to affect Nrf2 are phosphorylation and ubiquitination. As the 115kDa band in particular was overrepresented following inhibition of proteasomal degradation, which would result in the accumulation of ubiquitinated proteins, it may be that the 115kDa band represents a ubiquitinated form of Nrf2.

The band at 103kDa did not change during the course of this experiment. As it did not decrease with protein synthesis inhibition or increase with proteasomal degradation inhibition, this protein appears to be highly stable and slowly turned over. It may be that this is a non-specific band overlapping the previously validated Nrf2 band at 103kDa (Fig. 3-1, Fig. 3-2) which was previously not detectable, or it may be a stable long-lived form of Nrf2. However, it is not clear what this form of Nrf2 is. It may be an active phosphorylated form, which has a long half-life, however this would not be consistent with the low induction observed following treatment with CDDO-Me (Fig. 3-2). Although the 103kDa band has been seen to increase dramatically in response to CDDO-Me (Fig. 3-1), a consistent upregulation would be expected in response to an Nrf2 activator if the 103kDa band represents active Nrf2.

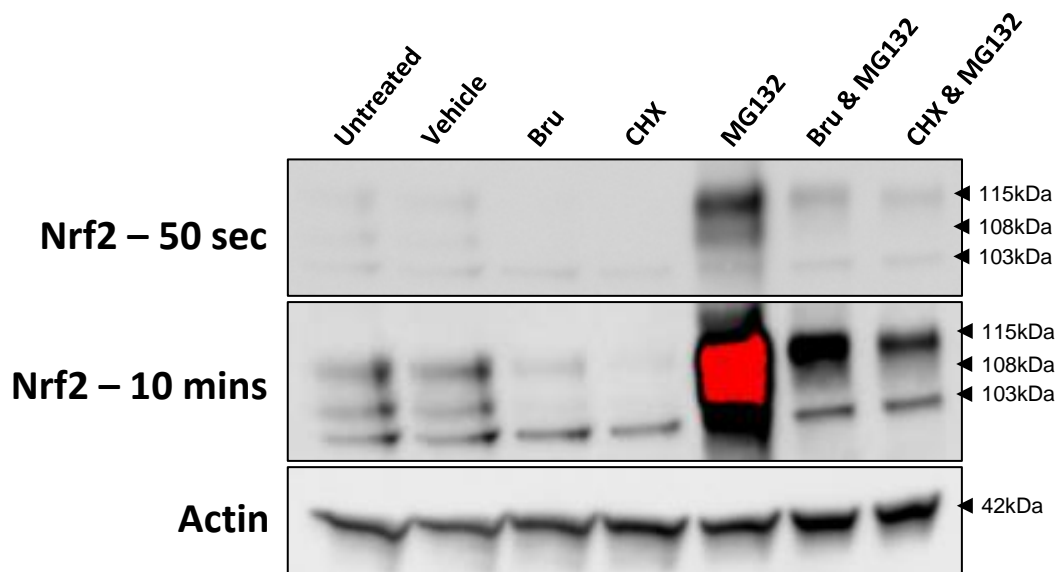


Figure 3-5: Nrf2 western blot following treatment with brusatol, cycloheximide and/or MG132. Different exposure times (50 sec and 10 min) are shown to account for the large differences in Nrf2 abundance between treatments. Red highlighted areas are overexposed and are not used for comparison at that exposure time. β -Actin levels were ascertained as a control for loading. Representative image shown from 3 independent experiments. Abbreviations: Bru, Brusatol. CHX, Cycloheximide.

3.2.4 Nrf2, NQO1 and AKR1C1/2 Proteins were Depleted Following Treatment with Gemcitabine

Having investigated the different forms of Nrf2 detectable by western blotting, I next sought to use the ability to identify these bands to determining how chemotherapy treatment affects Nrf2 abundance *in vitro*. Treatment with gemcitabine for 24h was seen to result in depletion of Nrf2 and its downstream targets in SUIT-2 and MIA PaCa-2 cells (Fig. 3-6). This effect was most noticeable in SUIT-2 cells (Fig. 3-6 A). 1 μ M gemcitabine was seen to result in a reduction of Nrf2 protein relative to 100nM and lower concentrations. NQO1 abundance was greatly reduced following 1 μ M gemcitabine treatment. AKR1C1/2 was also reduced relative to lower concentrations of gemcitabine-treated cells, however this was not to as

great an extent as NQO1. A further reduction of Nrf1, NQO1 and AKR1C1/2 was observed following treatment with 10 μ M gemcitabine. AKR1C1/2 was much more noticeably reduced following treatment with 10 μ M than with 1 μ M, with further reductions seen in Nrf2 and NQO1. The 108kDa and 115kDa bands of Nrf2 were not detectable following treatment 10 μ M or 100 μ M gemcitabine. However, the 103kDa band was not as heavily affected. Although it did noticeably reduce following 10 μ M gemcitabine treatment, this inhibition was not as great following 100 μ M treatment (although the band was still lower than following 1 μ M and lower concentrations of gemcitabine treatment). This followed the pattern of AKR1C1/2, which did not show great depletion until 10 μ M (unlike NQO1 and other Nrf2 bands) and did not show as strong depletion at 100 μ M.

The effects of gemcitabine treatment upon Nrf2, NQO1 and AKR1C1/2 abundance in MIA PaCa-2 cells (Fig. 3-6 B) was not as pronounced as upon protein abundance in SUIT-2 cells (Fig. 3-6 A). Each Nrf2 band from MIA PaCa-2 cells appeared downregulated following 24h 100 μ M gemcitabine treatment relative to vehicle treated control, however there was little effect at lower concentrations. Treatment with 100nM gemcitabine appeared to result in a marginal depletion of the 108kDa and 115kDa bands, and to a lesser extent at 1 μ M, however the 103kDa appeared to slightly increase in intensity. The inhibitory effects were not seen following 10 μ M gemcitabine treatment. AKR1C1/2 appeared to decrease following treatment with 1 μ M and 100 μ M gemcitabine, whereas NQO1 appeared to decrease following treatment with 100nM and 1 μ M gemcitabine. The reduction of AKR1C1/2 at 100 μ M may be attributed to the reduction in Nrf2 observed in the same samples, however it is not clear why AKR1C1/2 would be depleted to a similar extent following treatment with 1 μ M gemcitabine. The depletion of NQO1 following 100nM and 1 μ M gemcitabine treatment may be attributable to the small depletion of 108kDa and 115kDa Nrf2 at these concentrations, however it is not clear why NQO1 would not reduce following 100 μ M gemcitabine treatment which exerted a greater effect upon each Nrf2 band.

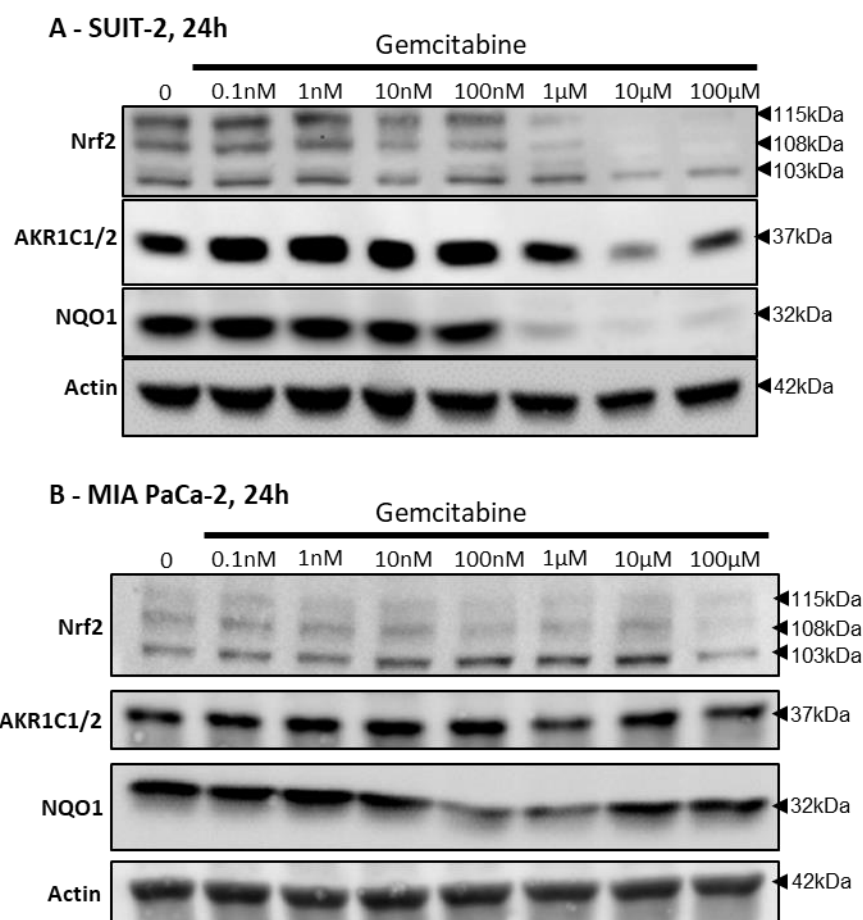


Figure 3-6: Western Blot of Nrf2 and downstream proteins from SUIT-2 and MIA PaCa-2 cells following treatment with gemcitabine. Representative images shown from three independent experiments.

3.2.5 Nrf2, NQO1 and AKR1C1/2 proteins were depleted following treatment with 5-FU

Treatment of SUIT-2 cells with 5-FU for 24h (Fig 3-7 A) resulted in a depletion of the 103kDa and 108kDa Nrf2 bands from 10μM and higher, with a depletion of the 103kDa Nrf2 band observed following 24h 1mM 5-FU treatment. There was little effect upon either AKR1C1/2 and NQO1. AKR1C1/2 did not appear to be affected at concentrations below 1mM, with only a small reduction observed following 1mM 5-FU treatment. 10μM 5-FU treatment appeared

to result in some depletion of NQO1, with each higher concentration having a greater inhibitory effect upon NQO1 abundance.

Similar effects of 24h 5-FU treatment were seen upon MIA PaCa-2 cells (Fig 3-7 B); 24h 10 μ M 5-FU treatment resulted in depletion of the 108kDa and 115kDa Nrf2 bands, however a lesser effect was seen to be exerted by as little as 100nM 5-FU. A small effect upon the 103kDa Nrf2 band appeared present in response to 100nM 5-FU in MIA PaCa-2 cells, however this effect did not intensify at higher concentrations. AKR1C1/2 and NQO1 abundance appeared almost entirely unaffected by 5-FU treatment in MIA PaCa-2 cells. Although there appeared to be some degree of depletion of AKR1C1/2 following treatment with 10 μ M 5-FU and higher, this was only a small effect. NQO1 in MIA PaCa-2 cells did not appear to be affected at any concentration analysed.

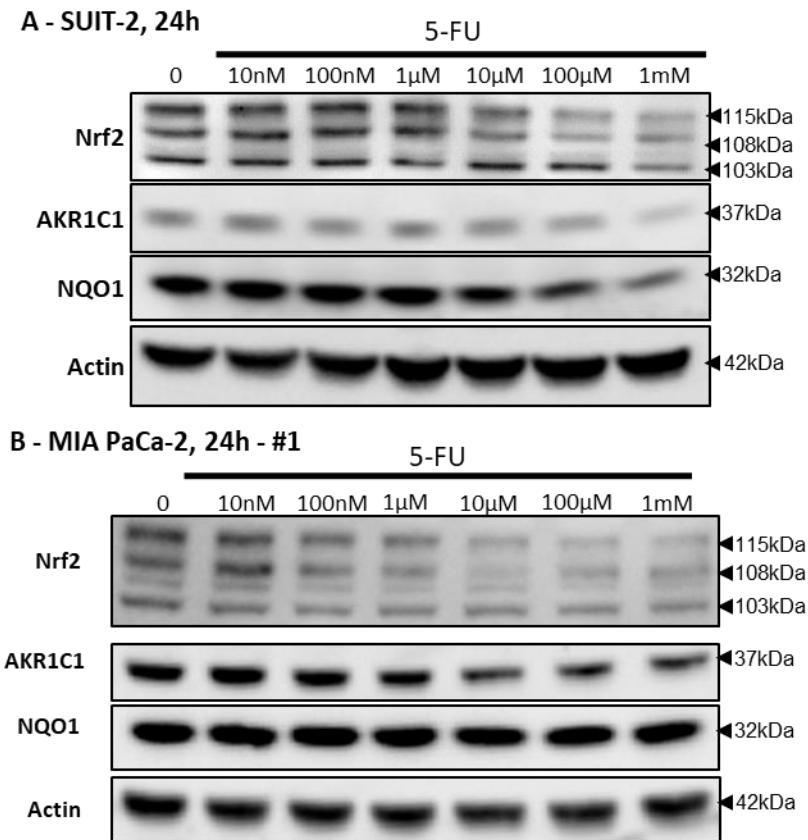


Figure 3-7: Western Blot of Nrf2 and downstream proteins from SUIT-2 and MIA PaCa-2 cells following treatment with 5-FU. Representative images shown from three independent experiments.

Chemotherapy depleted Nrf2 in PDAC cell lines (Fig 3-6, Fig 3-7), although it is not immediately clear why. One explanation for the observed decrease in Nrf2 abundance following chemotherapy exposure may be that the effects of chemotherapy reduce the ability of cells to induce Nrf2 activity. One of the dominant mechanisms of action of gemcitabine is to prevent cell division. Cellular metabolism is a major source of ROS, which activates Nrf2. Cell cycle arrest, although ultimately damaging to the cells, may cause a decrease in cellular metabolism and therefore reduce Nrf2 activation. To test this hypothesis, cells were incubated in serum-free medium for 24h to halt their growth and determine if this would result in reduced Nrf2 accumulation. Serum starvation did not appear to affect to Nrf2 abundance (Fig. 3-8), however the inhibitory effects of gemcitabine and 5-FU upon Nrf2

abundance were also not recapitulated during this experiment. This is discussed further in Section 3.2.6.

3.2.6 Cells Remain Capable of Accumulating Nrf2 whilst in the Presence of Gemcitabine and 5-FU

Although it was shown that gemcitabine and 5-FU treatment could result in the depletion of Nrf2 protein, it was not clear if this was an active inhibition or the removal of induction. The cause of Nrf2 depletion in response to chemotherapy could be that chemotherapy actively inhibited Nrf2 accumulation, such as by directly inhibiting Nrf2 selectively or by causing cells to be too damaged to synthesise proteins, or the cause could instead be that chemotherapy prevented the induction of Nrf2. To address this, SUIT-2 cells were cotreated with CDDO-Me and 100nM gemcitabine, 100µM gemcitabine, or 100µM 5-FU for 24 hours to determine if cells were still capable of synthesising and accumulating Nrf2 in the presence of chemotherapy (Fig. 3-8).

CDDO-Me resulted in Nrf2 accumulation regardless of the presence of any other drug. However, it seemed that 100µM gemcitabine limited this effect to some extent. Additionally, downstream targets, particularly NQO1, appeared to be prevented from being induced by CDDO-Me when treated in combination with gemcitabine. However, 5-FU treatment did not appear to prevent CDDO-Me induced accumulation of downstream targets. No evidence of a complete inhibitory effect of either gemcitabine or 5-FU on Nrf2 when combined with CDDO-Me was found. Although it appears that 100µM gemcitabine may inhibit the ability of cells to induce Nrf2 accumulation to some extent, this effect appeared small so does not appear to fully explain the large inhibitory effect of 100µM gemcitabine previously seen in SUIT-2 cells (Fig. 3-6). However, there did not appear to be a considerable inhibitory effect of 100µM gemcitabine upon Nrf2 when treated without CDDO-Me cotreatment during these

experiments. The lack of consistency in the effect of 100 μ M gemcitabine upon Nrf2 abundance may suggest that the effect is distant to Nrf2 rather than a direct inhibition. However, 100 μ M gemcitabine was seen to at least partly counteract the effects of CDDO-Me. For this reason it may be that 100 μ M gemcitabine may exert a direct inhibitory effect upon Nrf2, alongside reducing the induction of Nrf2 through alternative mechanisms. Although 100 μ M gemcitabine is considerably higher than concentrations of gemcitabine typically used *in vitro*, it implies the existence of an inhibitory mechanism which may be relevant under different conditions.

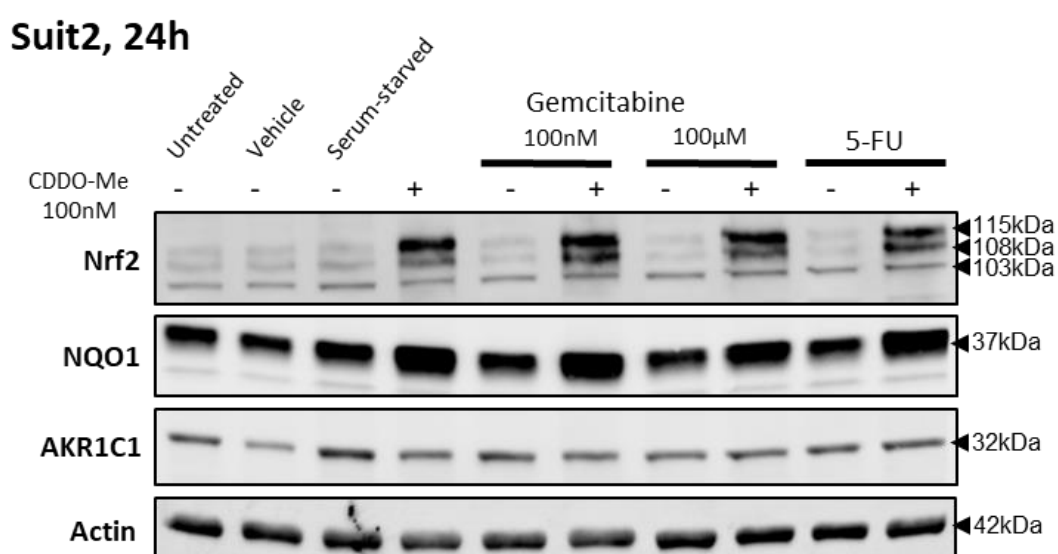


Figure 3-8: Western blot of SUIT-2 cells either drug/vehicle treated for 24h or cultured in FBS-free medium ('serum-starved') for 24h prior to harvest. Representative image shown from three independent experiments.

3.2.7 Validation of a luminescent reporter for the detection of Nrf2 activity in cultured cells

The effect of chemotherapy upon Nrf2 activity was investigated using a transfectable Nrf2-inducible luminescent reporter. The luciferase assay was first optimised using HEK293 cell line, a renal cell line exhibiting reliably high transfection rates. CDDO-Me and brusatol were used as positive and negative controls respectively to confirm the relationship of the 8xARE plasmid to Nrf2 activity. Due to the presence of two separate luminescent reporters (8xARE

firefly luciferase and *Renilla* luciferase control), a specificity analysis was performed (Fig. 3-9). Specificity analysis involved transfections of each luminescent reporter individually to confirm that efforts to detect one were not contaminated by a signal from the other. This also measured the efficacy of the firefly luciferase signal cancellation prior to *Renilla* luciferase measurement. The reading of *Renilla* luciferase when detecting Firefly luciferase (and vice versa) were close to blank and hundreds to thousands of times lower than when detecting the appropriate luciferase. As such, non-specific luciferase activity and residual firefly luciferase signal following quenching when measuring *Renilla* luciferase were not considered to noticeably affect the results of subsequent experiments.

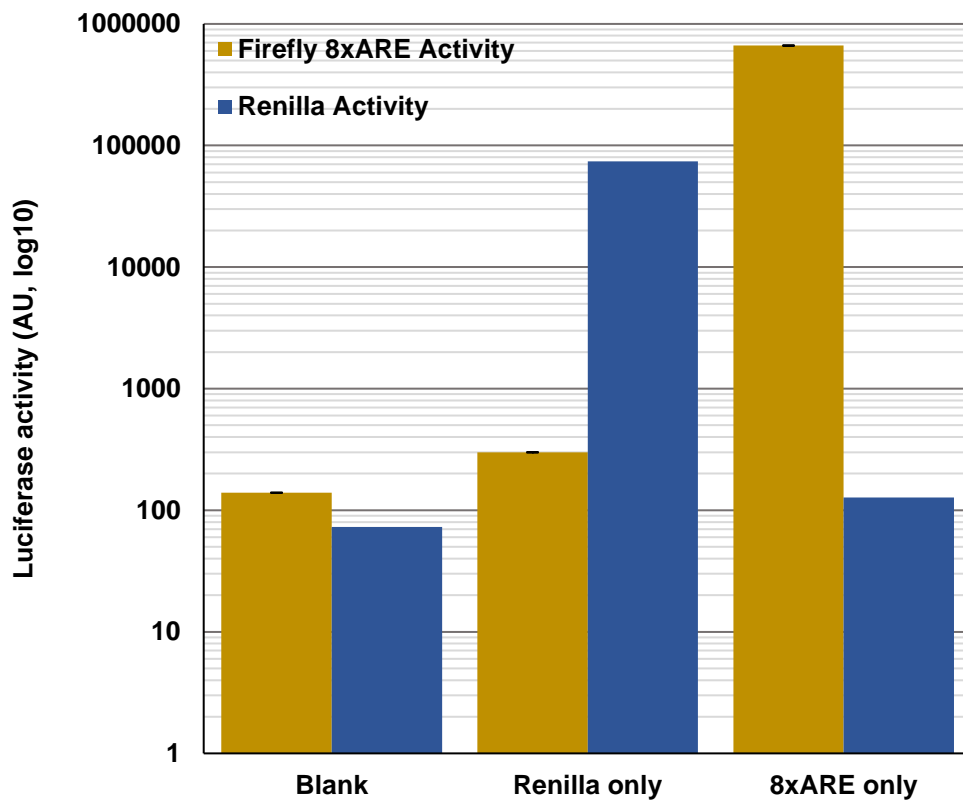


Figure 3-9: Assay specificity analysis. HEK293 cells were transiently transfected with *Renilla* Luciferase only and Firefly 8xARE (Nrf2Luc) Luciferase only. Dual-glo assay was performed in full on each to measure the extent of background and residual luciferase activity. +/- SEM. Abbreviations: AU, Arbitrary Units.

For the purposes of assay development and preliminary analysis, luciferase activity was measured once in HEK293 cells in response to chemotherapy and controls. Luciferase activity increased following 6h treatment with CDDO-Me and decreased following brusatol exposure relative to DMSO treated control in HEK293 cells (Fig. 3-10 A, B). However, the effect of brusatol may be due to directly inhibiting the synthesis of luciferase if brusatol is acting as a protein synthesis inhibitor. Although CDDO-Me treatment resulted in increased luciferase activity as expected, this was only to a small degree. It therefore appears that Nrf2 is not greatly inducible in HEK293 cells under these conditions.

Neither gemcitabine nor 5-FU significantly induced Nrf2 activity in HEK293 cells (Fig 3-10 B). However, HEK293 cells, a renal cell line, would not be expected to necessarily behave the same as PDAC cell lines.

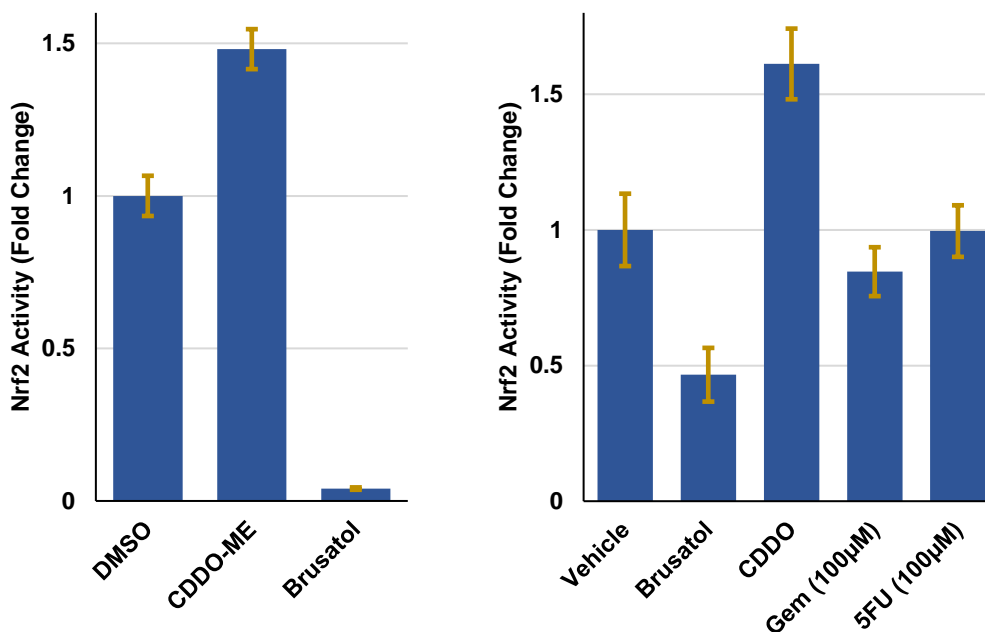


Figure 3-10 (A) Treatment of HEK-293 with brusatol, CDDO-ME and vehicle control (DMSO) following transient transfection of Nrf2 luciferase, N=1 (B) Treatment of HEK-293 with gemcitabine and 5-FU following transient transfection of Nrf2 luciferase, N=1. CDDO-ME and brusatol served as positive and negative controls of luciferase activity respectively. Error bars +/- SEM of technical replicates.

3.2.8 Gemcitabine and 5-FU induced Nrf2 activity in cultured cells

Following evaluation of the luciferase assay in HEK293 cells, Nrf2 activity in MIA PaCa-2, PANC-1 and SUIT-2 cells was analysed. MIA PaCa-2 and PANC-1 both showed either significantly increased activity or a trend towards increased activity in response to gemcitabine and 5-FU (Fig. 3-11), seemingly contrary to the effect of gemcitabine and 5-FU to deplete Nrf2 and downstream target abundance (Figs. 3-6, 3-7). However, the effect of gemcitabine and 5-FU to result in Nrf2 depletion was not consistently observed (Fig. 3-8).

Increasing concentrations of 5-FU each had a greater effect upon the induction of Nrf2 activity of MIA PaCa-2 and PANC-1 cells (Fig. 3-11).

The Nrf2 activity of SUIT-2 cells did not appear to be affected by gemcitabine or 5-FU, either positively or negatively.

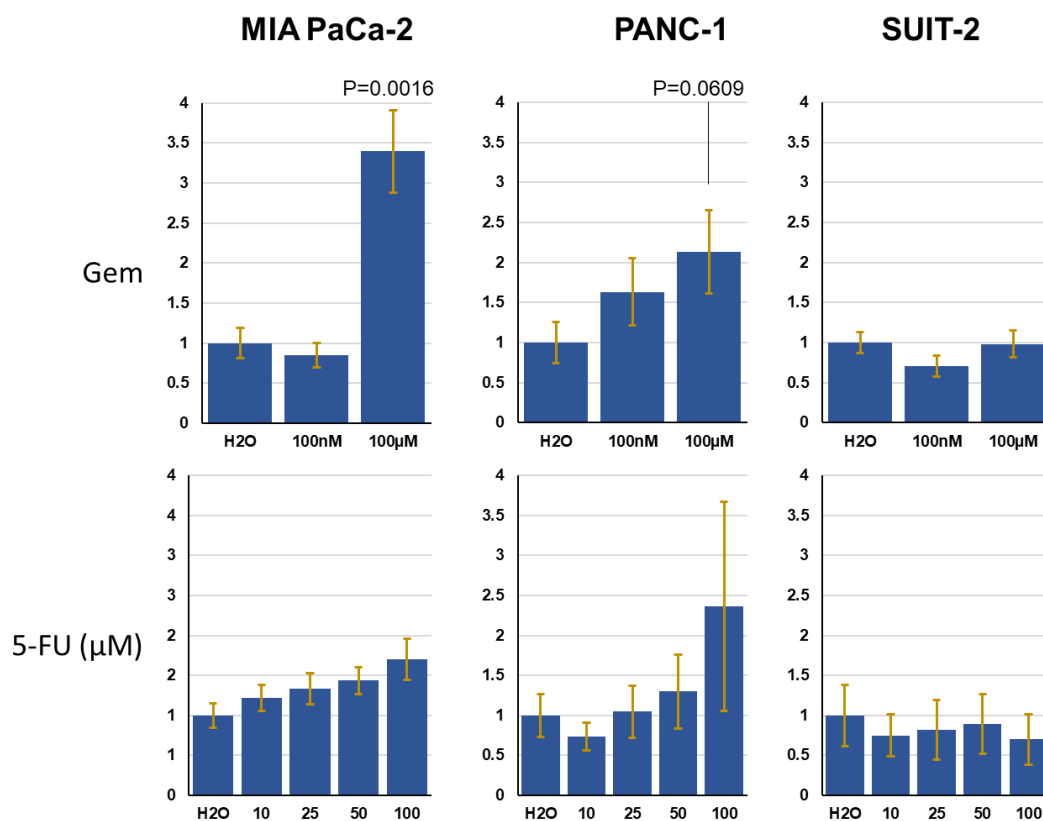


Figure 3-11 Luminescence readings of MIA PaCa-2, PANC-1 and SUIT-2 cells treated with gemcitabine (Gem) and 5-FU following transient transfection of Nrf2 luciferase. Work contributed to by MRes students Lewis Wignall and Chris Brown under my direct supervision. Data represent the mean of three individual experiments, each performed in triplicate. Error bars +/- SEM. Statistical analysis was performed using two-tailed *t*-test between each condition and vehicle control.

3.2.9 Validation of the Bioluminescent OKD48-mediated Nrf2 Reporter Mouse Model

To explore the effect of chemotherapy upon Nrf2 activity in an organism-wide system, a mouse model expressing the Nrf2-inducible OKD48 luminescent reporter (170) was used. This made it possible to determine how certain treatments would affect Nrf2 activity throughout the body, as cell culture could not recapitulate the variables that can affect the efficacy of drug treatment. These include physical boundaries to certain tissues, different cell types showing different resistance/sensitivity, and certain organs (such as the liver) receiving

blood supply and therefore a large amount of drug before it reaches the heart to circulate around the body. The OKD48 construct produces a luciferase-based reporter inducible by Nrf2 due to displaying three ARE sequences in its promoter region, and negatively regulated by Keap1 whenever Nrf2 is degraded (Fig. 3-12).

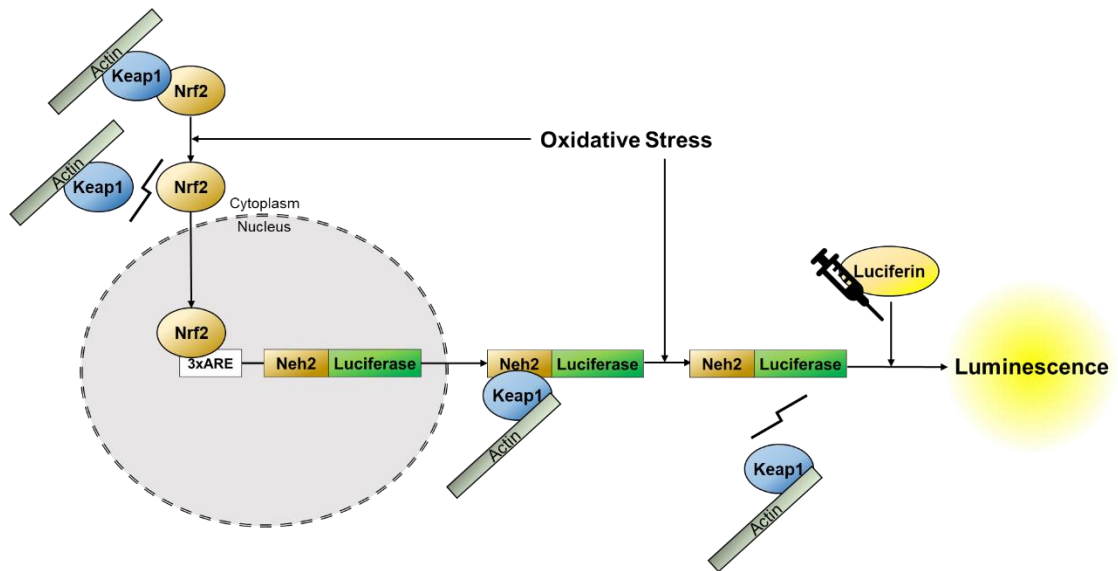


Figure 3-12: Graphical representation of the dual mechanisms utilised by the luciferase OKD48 3xARE Nrf2 activity reporter. OKD48 expression was activated by Nrf2 activity upon the release of Nrf2 from Keap1. The accumulation of OKD48 protein was inhibited under the same circumstances under which Nrf2 would be inhibited (Keap1-mediated under non-stressed conditions due to OKD48 comprising Neh2, the Keap1 binding region of Nrf2). Degradation of OKD48 under circumstances in which Nrf2 would also be degraded reduced the effects of aberrant expression of OKD48, and ensured that any OKD48 protein synthesised in response to Nrf2 activity would not continue to be present following cessation of that activity. OKD48 is therefore a sensitive reporter of Nrf2 and its abundance at any specific time is a reliable indicator of Nrf2 activity at that time.

The reporter assay was validated using CDDO-Me. As expected, luciferase activity hugely increased following exposure to the Nrf2 activator (Fig 3-13 A, B). Treatment with CDDO-Me resulted in substantially increased Nrf2 activity by 4h which was still highly elevated at 24h

(Fig. 3-13). However, there was only marginal sign of increased Nrf2 activity 1week post-CDDO-me treatment (Fig. 3-13).

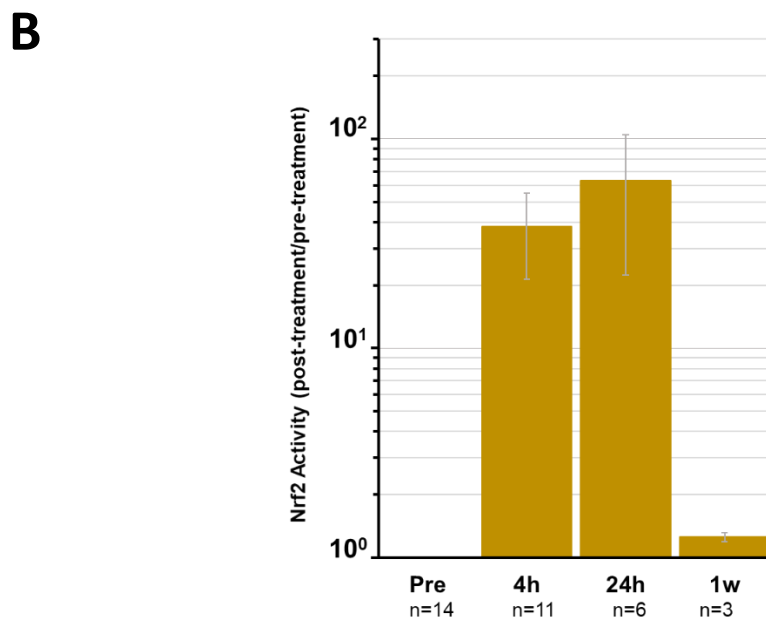
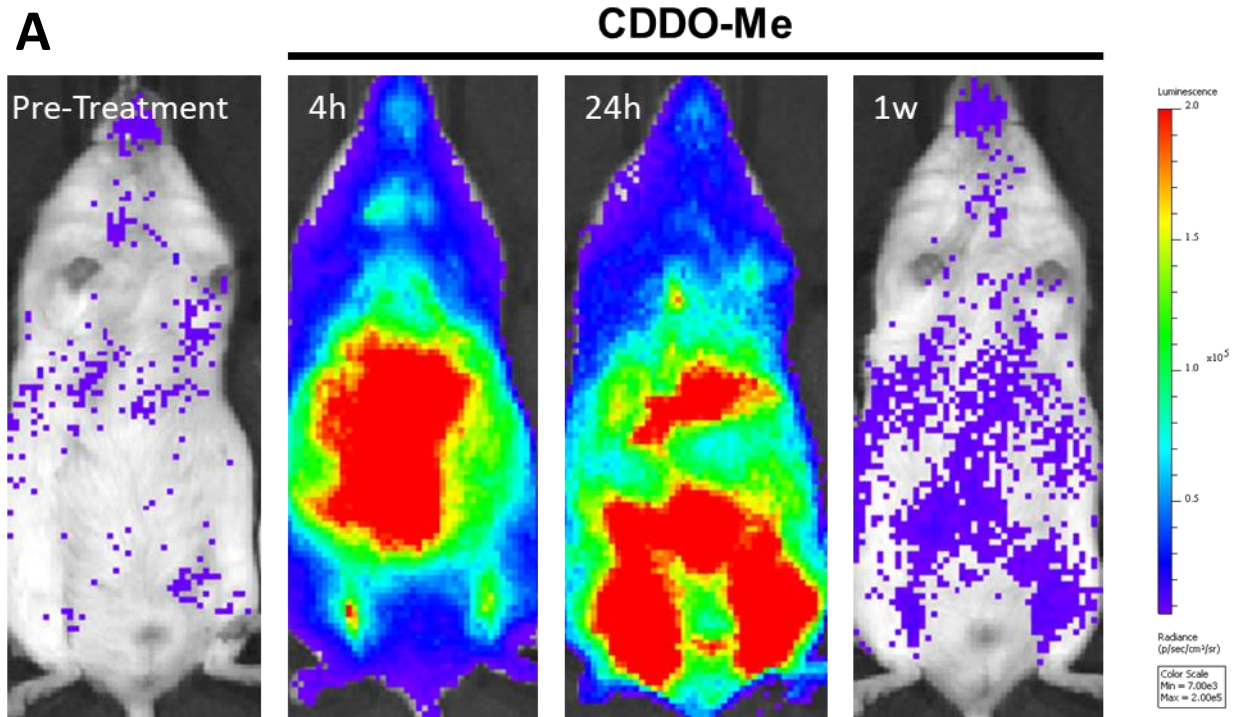


Figure 3-13: A: Representative image of a single OKD48^{+/+} mouse prior to treatment with CDDO-Me and at 4h, 24h and 1 week (1w) post-treatment. The location of intensity of radiance, as a marker of Nrf2 activity, is represented by coloured overlay. B: Mean of the average luminescence readings from CDDO-Me treated mice at 4h, 24h and 1 week (1w) normalised to pretreatment readings. Errors bars +/- SEM.

3.2.10 Gemcitabine and 5-FU did not consistently affect Nrf2 activity *in vivo*

Treatment with gemcitabine and 5-FU did not consistently have any noticeable effect, however (Fig. 3-14, Fig. 3-15). The location and intensity of Nrf2 activity was similar 4h post-treatment to pretreatment (Fig. 3-14), with small areas of localised induction occurring at 24h post-treatment. This effect was considerably lower than that exerted by CDDO-Me, and by other forms of treatment analysed using this model by our collaborators (169).

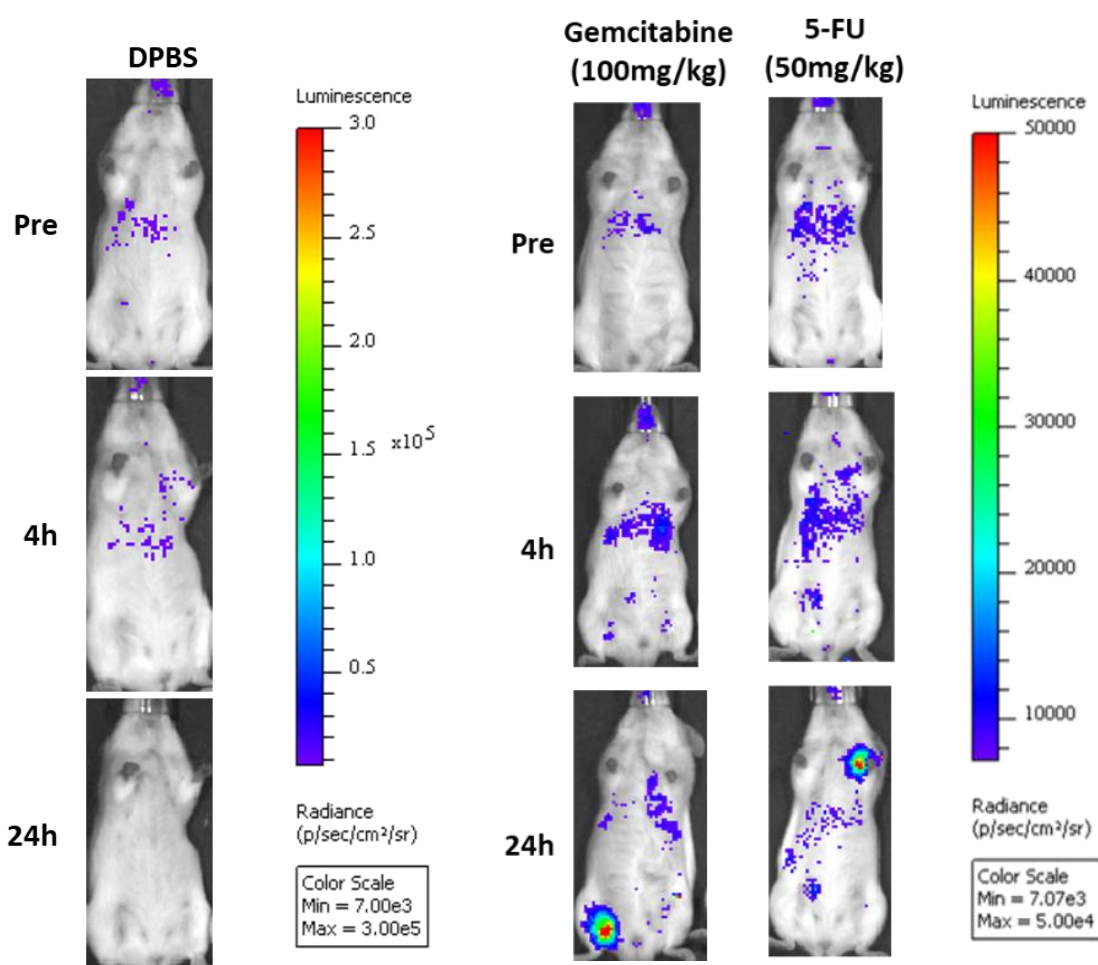


Figure 3-14: Representative images of mice treated with vehicle (DPBS) only, gemcitabine (100mg/kg), or 5-FU (50mg/kg). Small areas of localised Nrf2 activation were detected irregularly in all treatment arms as seen at 24h, however these were not to the extent or spread of activation following treatment with CDDO-Me.

Collaborators who have previously published work using this colony (169) had advised that the pelvis may intermittently produce a large signal without any apparent external induction. This was subsequently observed during this course of work. In some instances, mice would exhibit a large degree of Nrf2 activation which was highly specific to the pelvis. This was also observed in vehicle-only treated controls. This signal was as intense as CDDO-Me treated controls in some instances, although CDDO-Me induced Nrf2 activation throughout the body. Due to the lack of external stimulus and highly specific location of the activation, it appeared that these cases of Nrf2 activation were a result of intrinsic factors and reflected individual and time-based differences rather than an effect of drug treatment. As such, and consistent with advice I had received, it was decided that these signals were a confounding variable which could be removed from analysis. Additional analysis of Nrf2 activation was performed on both the upper and lower body whilst determining system-wide Nrf2 activation in affected animals.

Nrf2 activity following treatment with DPBS, either at 4h, 24h or 1w, exhibited mild increase and decreases relative to pretreatment Nrf2 activity (Fig. 3-15). This varied both within and between different time points. It was also observed that the distribution of Nrf2 activity was different at pretreatment to post-treatment time points. It therefore appeared that these differences were a result of the imaging process. IP injection of DPBS vehicle may have contributed to this effect, however this would likely be the same effect as exerted by IP injection of the same volume of DPBS to deliver luciferin during imaging. Although this effect sometimes appeared to be several fold-change, it was considerably lower than the effect exerted by the CDDO-Me positive control and by toxic agents in previous experiments by our collaborators (169). This is likely due to there being only low levels of Nrf2 activity in healthy tissue, so spontaneous variation or minor changes could result in a relatively large fold-change despite there still being low levels in absolute terms. Therefore, this was not

considered likely to impact upon effects exerted by chemotherapy, which as seen previously would produce considerably higher effect if they impacted Nrf2 activity.

1mg/kg and 5mg/kg 5-FU treatments (Fig. 3-15 A) showed a similar pattern with a greater trend towards minor increases. As similar inductions were seen in response to DPBS, the change in Nrf2 activity following 5-FU 1mg/kg and 5-FU 5mg/kg treatment appears to be either random variation or a response to injection and imaging. However, 50mg/kg 5-FU treatment resulted in 2 of 5 mice imaged at 24h post-treatment exhibiting higher average Nrf2 activity than lower concentrations of 5-FU did. Although one reading was only slightly higher than other conditions, the other was considerably out of the normal range. However, the other 3 of 5 demonstrated a similar pattern to that of DPBS-treated and lower 5-FU concentrations. Although the same mouse was considerably out of normal range 4h post-treatment, it was not to as great an extent and was the only one of 7 to apparently be affected. Whilst it may be the case that 50mg/kg 5-FU may occasionally result in substantially increased Nrf2 activity, as it occurred only a single time it could also be a rare spontaneous event unrelated to the drug which could have occurred in response to any treatment.

The effects of gemcitabine (Fig. 3-15 B) also appeared to be consistent with those of DPBS, however with fewer outliers than shown by 5-FU treatment (potentially related to lower numbers). One result at 24h post-treatment of 0.5mg/kg and, to a lesser extent, 50mg/kg gemcitabine appeared to be out of the normal range, however this was not to a large degree. The remainder of results appeared consistent with those of DPBS.

It does not appear that either gemcitabine or 5-FU consistently substantially affect Nrf2 activity of healthy tissues *in vivo*. Although a small number of large changes in Nrf2 activity following drug treatment were observed, these could not be replicated and were highly localised on imaging. These were rare events which could reflect spontaneous activity or

occasional response to imaging, with no evidence to suggest they occurred due to chemotherapy treatment.

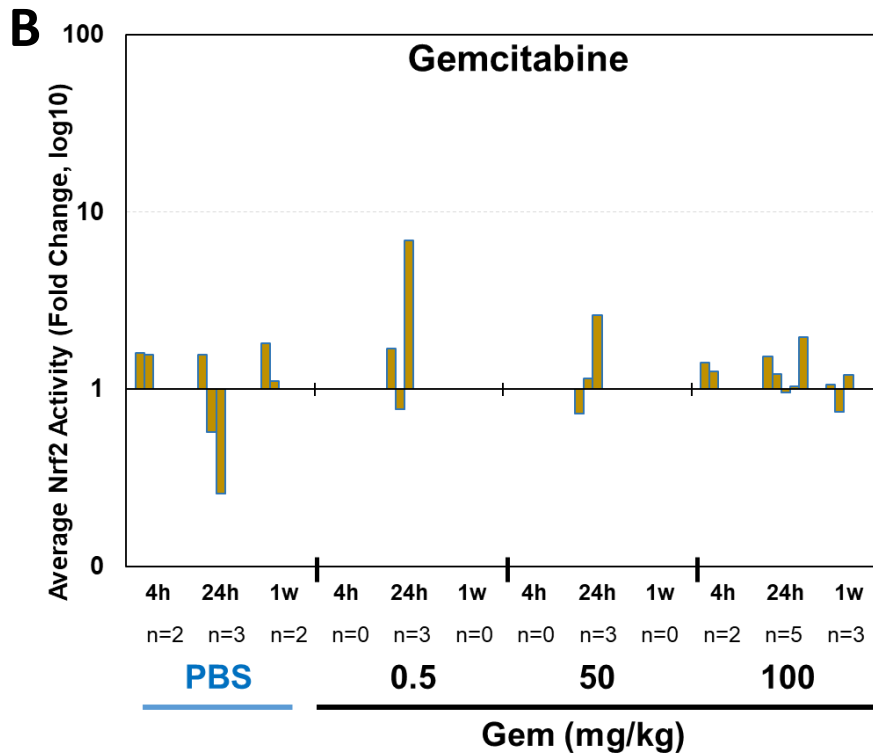
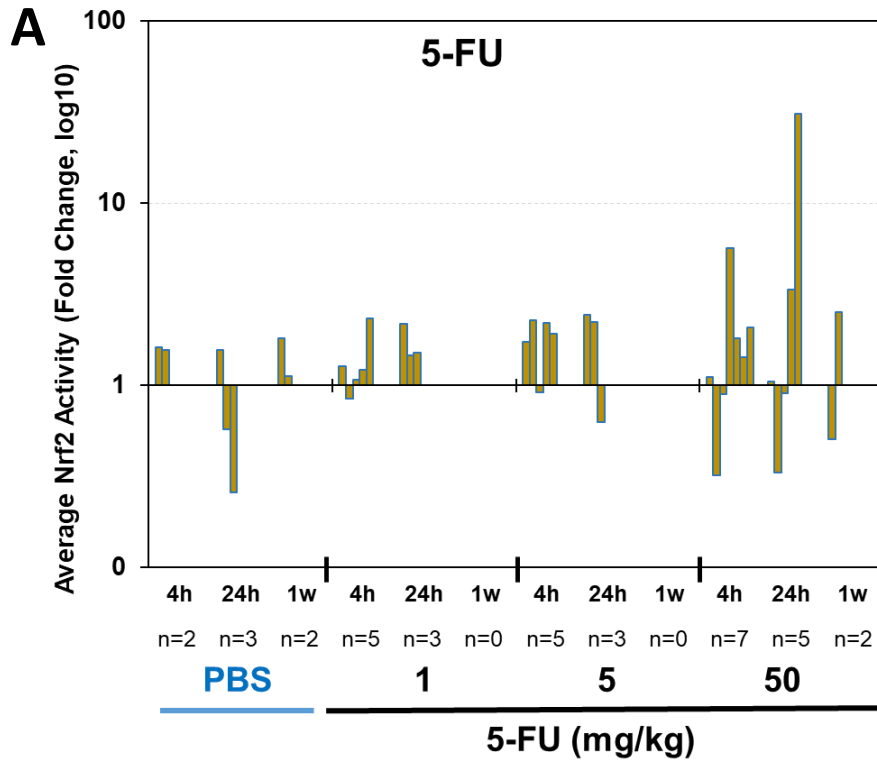


Figure 3-15: The fold change between the average pretreatment reading and the average reading at 4h, 24h and 1w post-treatment of 5-FU (A) or gemcitabine (B). The same DPBS controls are shown in both A and B for comparison purposes.

3.2.10 Gemcitabine and 5-FU did not affect NQO1 abundance *in vivo*

Ex vivo analysis to measure Nrf2 activity was performed via IHC. Previous work within this group has failed to identify a selective Nrf2 antibody for ICC/IHC (Fig. 3-16) (142). Poor specificity of the antibodies trialled precluded direct detection of Nrf2 during this work. Instead, NQO1 was detected by IHC (Fig. 3-17).

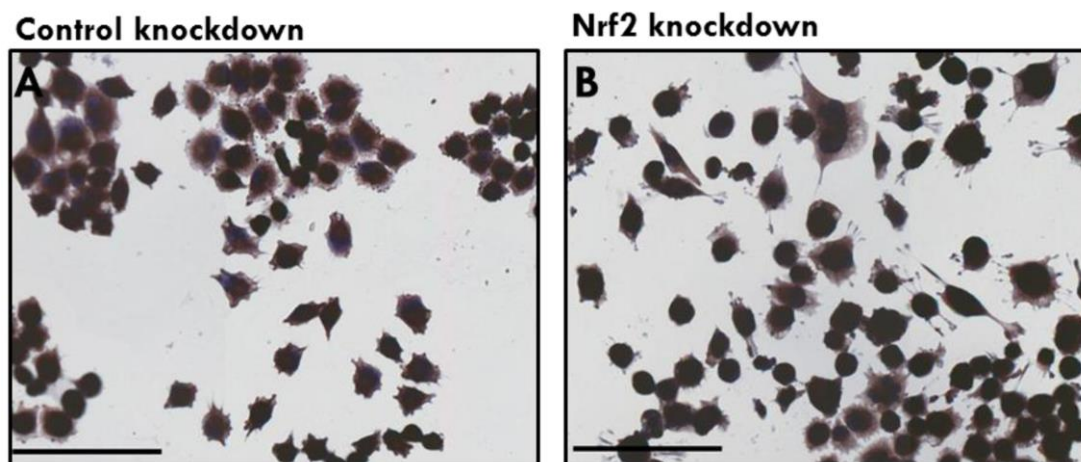


Figure 3-16: MIA PaCa-2 cells were treated with off-target (A, Control) or Nrf2 (B) siRNA on cover slips and subsequently stained via ICC for Nrf2 (brown). Figure adapted from Dr Thompson Gana's PhD thesis (142). Abbreviations: ICC, Immunocytochemistry.

The pancreas did not appear to exhibit as high a degree of expression of NQO1 as sections of liver or kidney did (Fig. 3-17). Although specific areas of detectable NQO1 were widely present, it was not as widespread or as intense as in liver or kidney tissue. This is likely due to the fact that the purpose of the liver and the kidney are directly related to detoxification, which NQO1 would be expected to contribute to.

Contrary to expectations, there also did not appear to be an effect of CDDO-Me upon NQO1 relative to DPBS-treated control (Fig. 3-17). However, there did appear to be a slight depletion of NQO1 abundance in each tissue analysed of mice treated with gemcitabine and 5-FU, relative to DPBS treated control.

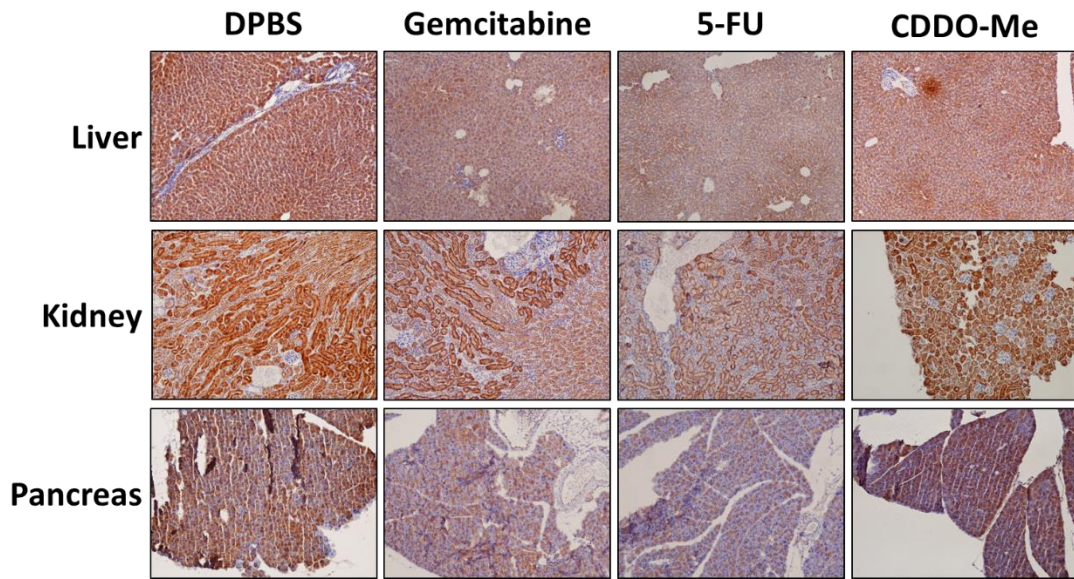


Figure 3-17: IHC sections of organs taken from Nrf2Luc mice 48h post drug-treatment. 100x magnification.

3.2.12 KEAP1 gene promoter was not found to be methylated in PDAC tumour patient Samples.

This group and collaborators previously reported low/lack of Keap1 protein expression in 70% of PDAC tumours (113). In order to determine whether methylation status of *KEAP1* promoter regions was the cause of the previously observed protein absence, the *KEAP1* methylation status of patient-matched tumour and acinar were investigated. Acinar tissue was selected as the closest available patient-matched healthy control, as healthy pancreatic duct tissue was not available and acinar tissue is related to duct tissue. Laser capture microdissection was utilised to dissect specific areas of cancerous and acinar tissue for further analysis, as tissue homogenisation or analysis of whole tumour would have resulted in tumour samples consisting predominantly of desmoplastic stroma. Following DNA extraction of microdissected tissue, bisulphite treatment and then PCR-mediated amplification, electrophoresis and subsequent imaging confirmed that *KEAP1a* and *KEAP1b* had been successfully extracted and amplified. Pyrosequencing was used to investigate the base changes resulting from bisulphite treatment at the CpG sites. Unmethylated cytosine in

the base sample was converted to uracil, which was replaced by thymine in subsequently produced strands during PCR. Methylated cytosine was unaffected, making it possible to sequence the segment and determine if the original sample contained methylated or unmethylated cytosine by the presence of cytosine or thymine, respectively, at a CpG site. It was discovered that the degree of methylation was low (Table 3.1 A), with very few CpG sites exhibiting a high frequency of methylation (Table 3.1 B).

Table 3.1: Methylation status of patient-matched PDAC tumour and healthy acinar tissue.

A. Methylation Index of two *KEAP1* promoter regions analysed in five sets of patient matched tumour and acinar tissue samples. Both regions in all samples from both tumour and acinar exhibited either low or no detectable methylation of *KEAP1*.

	Methylation Index (%)			
	<i>KEAP1a</i>		<i>KEAP1b</i>	
	Tumour	Acinar	Tumour	Acinar
1	0	8.2	0	0
2	0	0	1.19	0
3	8.2	0	0	1.8
4	0	0.5	0	0
5	0.7	0	0	0

B. Methylation status of specific CpG sites of two *KEAP1* promoter regions analysed in five sets of patient matched tumour and acinar tissue samples. No *KEAP1* promoter methylation was detected at the majority of CpG sites, with only one site exhibiting methylation in over 20% of cells.

	Percentage methylation (%)										
	<i>KEAP1a</i> CpG sites						<i>KEAP1b</i> CpG sites				
	1	2	3	4	5	6	1	2	3	4	5
Tumour 1	0	0	0	0	0	0	0	0	0	0	0
Acinar 1	0	0	0	0	49.34	0	0	0	0	0	0
Tumour 2	0	0	0	0	0	0	0	0	0	5.95	0
Acinar 2	0	0	0	0	0	0	0	0	0	0	0
Tumour 3	0	0	11.8	6.76	16.29	14.37	0	0	0	0	0
Acinar 3	0	0	0	0	0	0	0	0	8.96	0	0
Tumour 4	0	0	0	0	0	0	0	0	0	0	0
Acinar 4	0	0	0	3.33	0	0	0	0	0	0	0
Tumour 5	0	0	0	4.35	0	0	0	0	0	0	0
Acinar 5	0	0	0	0	0	0	0	0	0	0	0

Due to a weak signal from the sample reporting higher methylation (Acinar 1, *KEAP1a*) at CpG sites during pyrosequencing, the degree of methylation at this site may be overstated. This presents a problem in determining the ratio between methylated and unmethylated cytosines in the original sample, as a stronger signal is required to draw a reliable ratio. This issue may have been caused by low genomic DNA input, due to the issues associated with

gathering sufficient amounts of FFPE tumour tissue and the hazardous nature of the extraction and subsequent treatments. However, the majority of CpG sites exhibited little to no indication of methylation, and so this is considered unlikely to have affected the conclusion that *KEAP1* promoter methylation is not the cause of Keap1 protein absence observed in PDAC.

3.2.13 NQO1 SNP rs1800566 status did not correlate with the probability of developing resectable PDAC, or with prognosis in response to treatment

The clinical significance of modulation of the Nrf2-system was then investigated. Specifically, the effect of SNPs in Nrf2-related genes upon patient outcome was analysed. Previous unpublished work from this group by Dr Thompson Gana and Dr Claire Jenkinson has shown that changes in selected *NRF2* and *SRXN1* SNPs (rs2886162 and rs6053666, respectively) did not significantly correlate with patient outcome in advanced pancreatic cancer cases ($p=0.405$ and $p=0.632$, respectively) (142). This analysis was performed on samples obtained from the TeloVac and ViP clinical trials, both of which collected samples from advanced pancreatic cancer cases. However, the presence of the minor allele of an *NQO1* SNP (rs1800566) from the combined TeloVac and ViP trials was seen to correlate with improved patient outcome ($p=0.01$) (142). As such, I then investigated if the minor allele was associated with improved prognosis of patients with resectable PDAC.

The presence of the C609T *NQO1* SNP (rs1800566) was first investigated using genomic DNA extracted from cultured cell lines (Fig. 3-17). The use of various sample volumes and various masses of DNA in standard volume (5 μ L) were analysed for the purposes of assay optimisation in addition to determining cell line SNP status.

The results of each cell line (Fig. 3-17 C) appeared highly similar regardless of the masses (5ng, 10ng, and 25ng) of DNA used (Fig. 3-17 C). A low mass of DNA therefore did not appear to be a limiting component of the reaction, nor did an excess of DNA appear to be detrimental

to reaction efficiency. Both PANC-1 and MIA PaCa-2 cells were found to be homozygous for the major wild-type allele (Fig. 3-17 C). However, SUIT-2 cells were found to be heterozygous (Fig. 3-17 C).

A set of samples using 25ng of DNA but from a more dilute solution, therefore increasing the reaction volume, was also trialled (Fig. 3-17). This was to determine if available clinical samples could be used without additional concentration. However, the effect of this was to drastically reduce the efficacy of the reaction to levels below the negative control (Fig. 3-17). Although further optimisation may have addressed this, this was not pursued during the course of this work because the results also indicated that a concentration low enough to use all samples would be viable. A lower mass of DNA was required for a successful reaction than had been expected so larger volumes of sample would not be necessary in subsequent reactions.

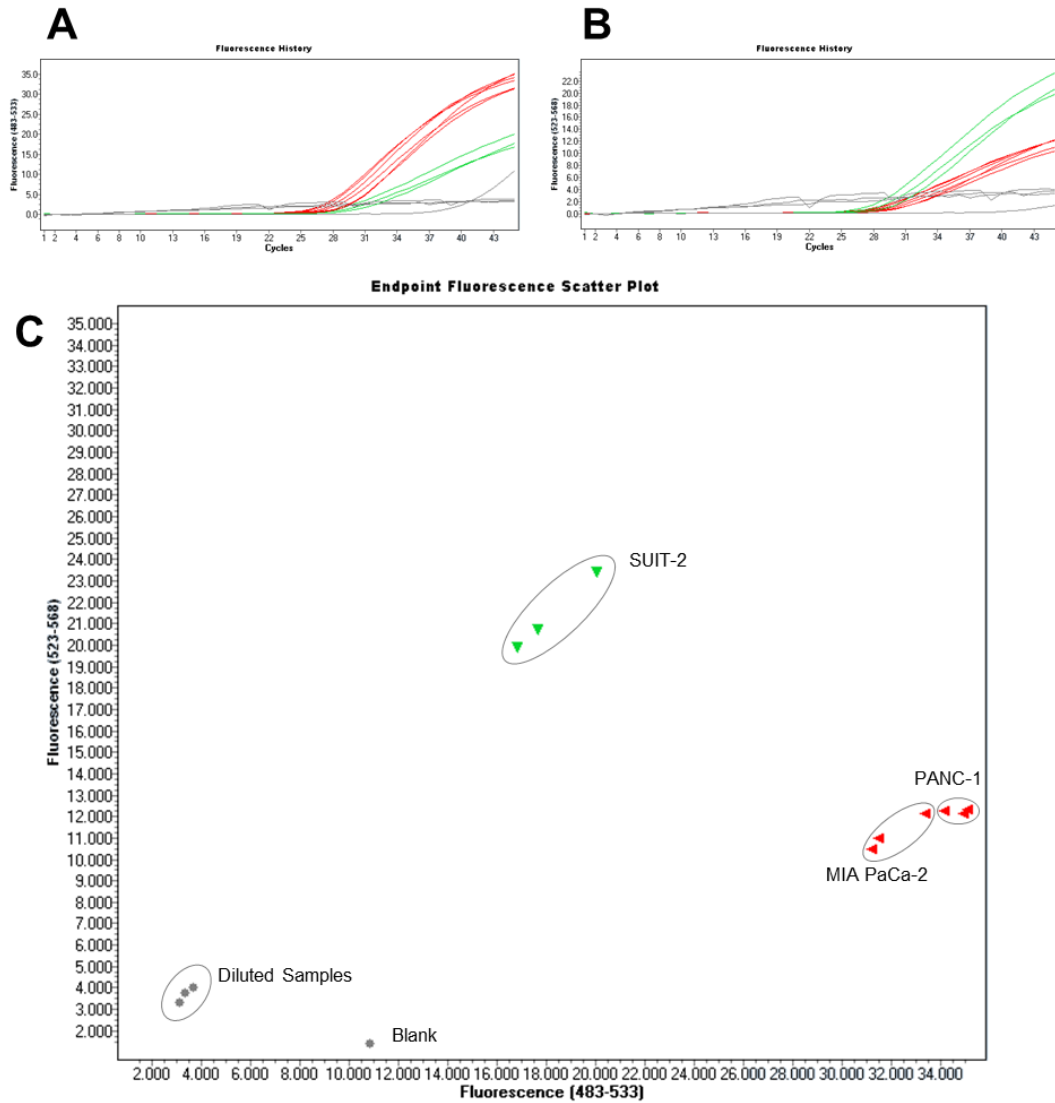


Figure 3-18: qPCR results to determine genomic NQO1 SNP status in MIA PaCa-2, PANC-1 and SUIT-2 cell lines under various conditions. Endpoint signals of fluorescence indicating C allele (A) and T allele (B) amplification were combined (C) to separate the two groups and colour coded (red – CT; green – TT). Positive results for each cell line are labelled. Negative results, including negative control, are shown in grey and labelled separately.

SNP analysis via qPCR of patient samples was performed blinded to patient information, including patient outcome (Fig. 3-18). Genotypes were matched to anonymised patient IDs and sent to Eftychia-Eirini Psarelli to correlate with survival time and perform statistical analysis (Fig. 3-19). ‘All interventions’ covers patients being treated with gemcitabine, GemCap, 5-FU, radiotherapy, 5-FU & radiotherapy in combination, or receiving no further

anti-cancer treatment (observation only). Due to small numbers of patients receiving other treatments, only gemcitabine and GemCap arms were used for further analysis.

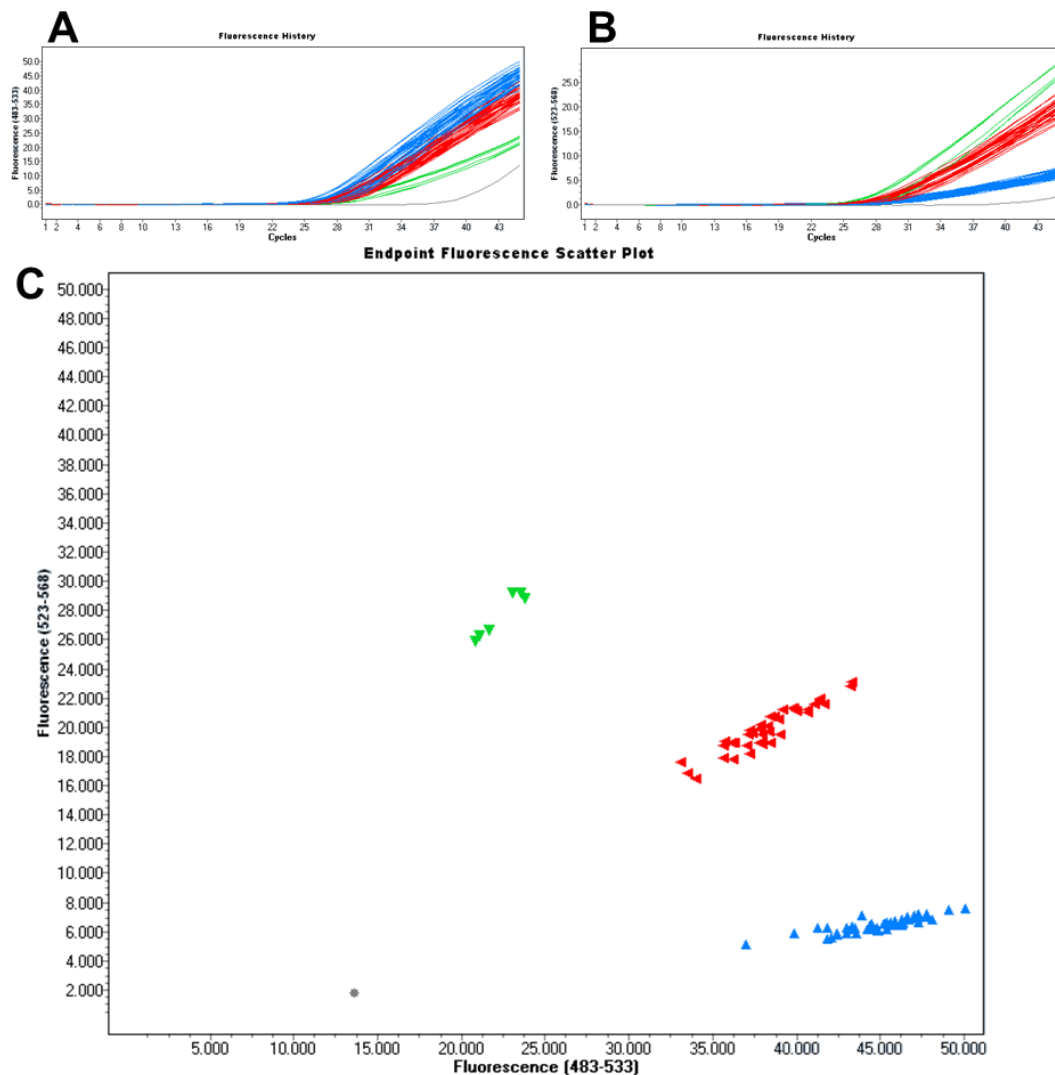


Figure 3-19: Representative images of qPCR results to determine genomic NQO1 SNP status in ESPAC patient samples. Endpoint signals of fluorescence indicating C allele (A) and T allele (B) amplification were combined (C) to separate the three groups and colour coded (blue – CC; red – CT; green – TT). Negative control is shown in grey.

Germline allelic distribution of rs1800566 among ESPAC patients with resectable pancreatic cancer was not significantly out of Hardy-Weinberg equilibrium, nor did it significantly differ from the allelic distribution expected from a European cohort (gnomAD, (168)) (Table 2).

Table 3.2: Hardy-Weinberg equilibrium was measured using χ^2 test comparing observed germline allele distribution of resectable cancer (ESPAC) and advanced cancer (TeloVac/ViP) to expected distribution based upon allele frequency. Allele distribution was also compared to a European cohort (gnomAD v2.1.1 (controls)).

Allele Frequency Source	Minor : Major	Expected (Observed)			χ^2	P
		CC	CT	TT		
ESPAC	0.204 : 0.796	158.40 (160)	81.192 (78)	10.40 (12)	0.386	.534
GnomAD	0.186 : 0.814	165.47	75.84	8.69	1.503	.221
TeloVac/ViP	0.195 : 0.805	96.56 (92)	46.78 (56)	5.67 (1)	5.875	.015
GnomAD	0.186 : 0.814	98.62	45.20	5.18	6.39	.011

This suggests that the SNP does not affect the probability of developing operable pancreatic cancer. This is in contrast to analysis of rs1800566 amongst advanced cases (ViP/TeloVac trials). SNP data obtained previously by colleagues in the laboratory, all Dr Thompson Gana and Dr Claire Jenkinson was similarly analysed and found to be significantly ($p=0.015$) out of Hardy-Weinberg equilibrium and different from a European cohort (168) (Table 3.2). Specifically, the minor homozygote (TT) allele was noticeably under-represented. Five samples across these studies were expected to exhibit the homozygous minor genotype, however only one was found. As the analysis of samples from the ESPAC study (Table 3.2), shows that genotype does not affect the probability of developing PDAC. It was therefore considered that these findings may suggest that the TT genotype delays or otherwise limits progression into an advanced inoperable state. If genotype affects disease progression it might be expected to affect survival time as well. To investigate whether this was the case, I undertook survival analysis. It was observed that NQO1 SNP status did not correlate with response to response to chemotherapy (gemcitabine or GemCap).

There was no significant difference in survival time between different genotypes, either of all patients or separated according to treatment (Fig. 3-19). However, there appeared to be

notable areas of separation in survival probability at various timepoints (such as ~15 months) for patients treated with gemcitabine although the overall differences were non-significant.

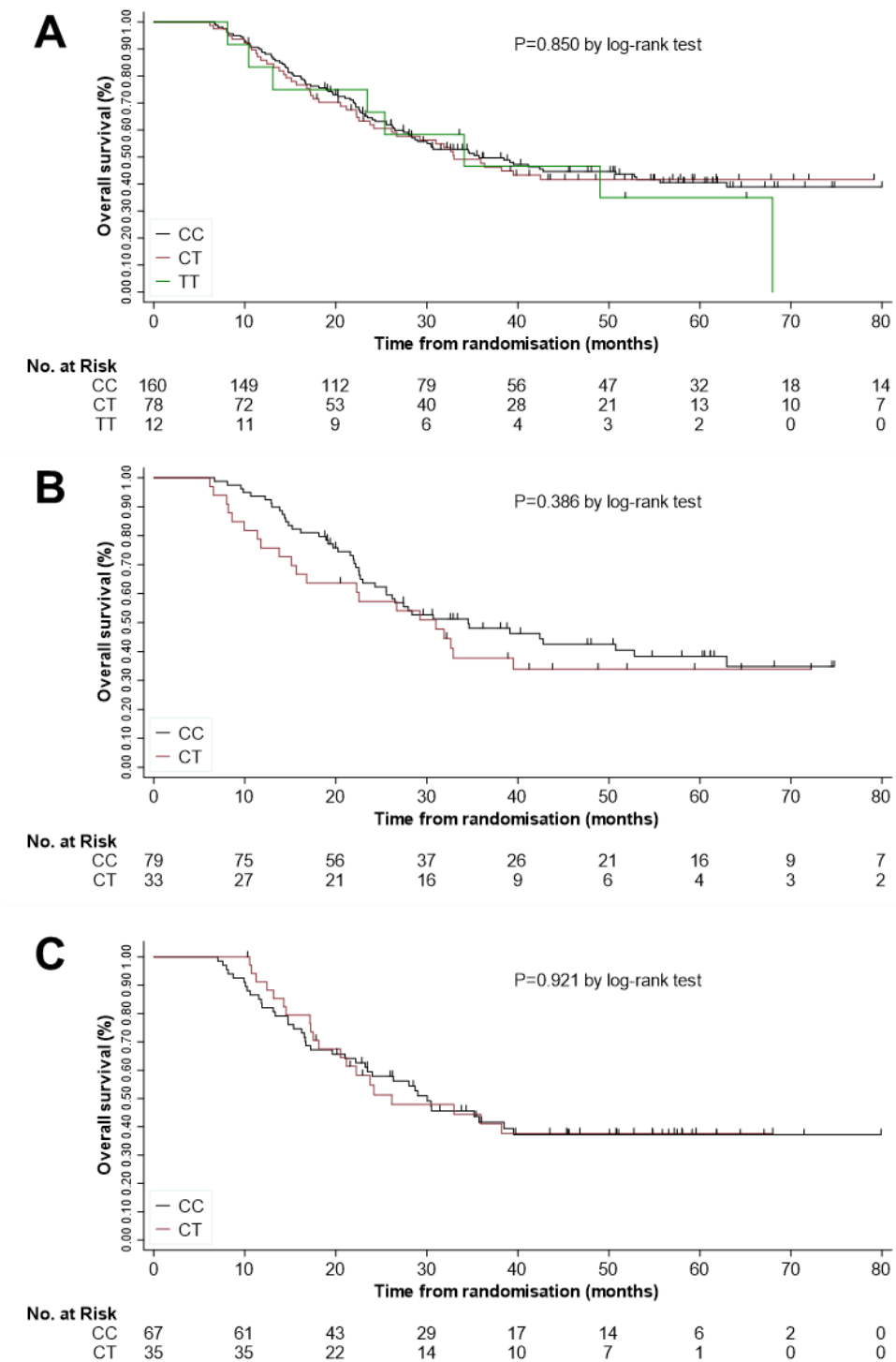


Figure 3-20: Kaplan-Meier plots of overall survival of patients according to NQO1 SNP (A), survival in response to gemcitabine treatment (B), and survival in response to GemCap treatment (C). TT genotype was excluded from individual arm analysis due to small numbers of patients.

In addition to the absence of an effect on overall survival trend, there was similarly no apparent effect of *NQO1* SNP status upon survival time (regardless of intervention) (Fig. 3-20).

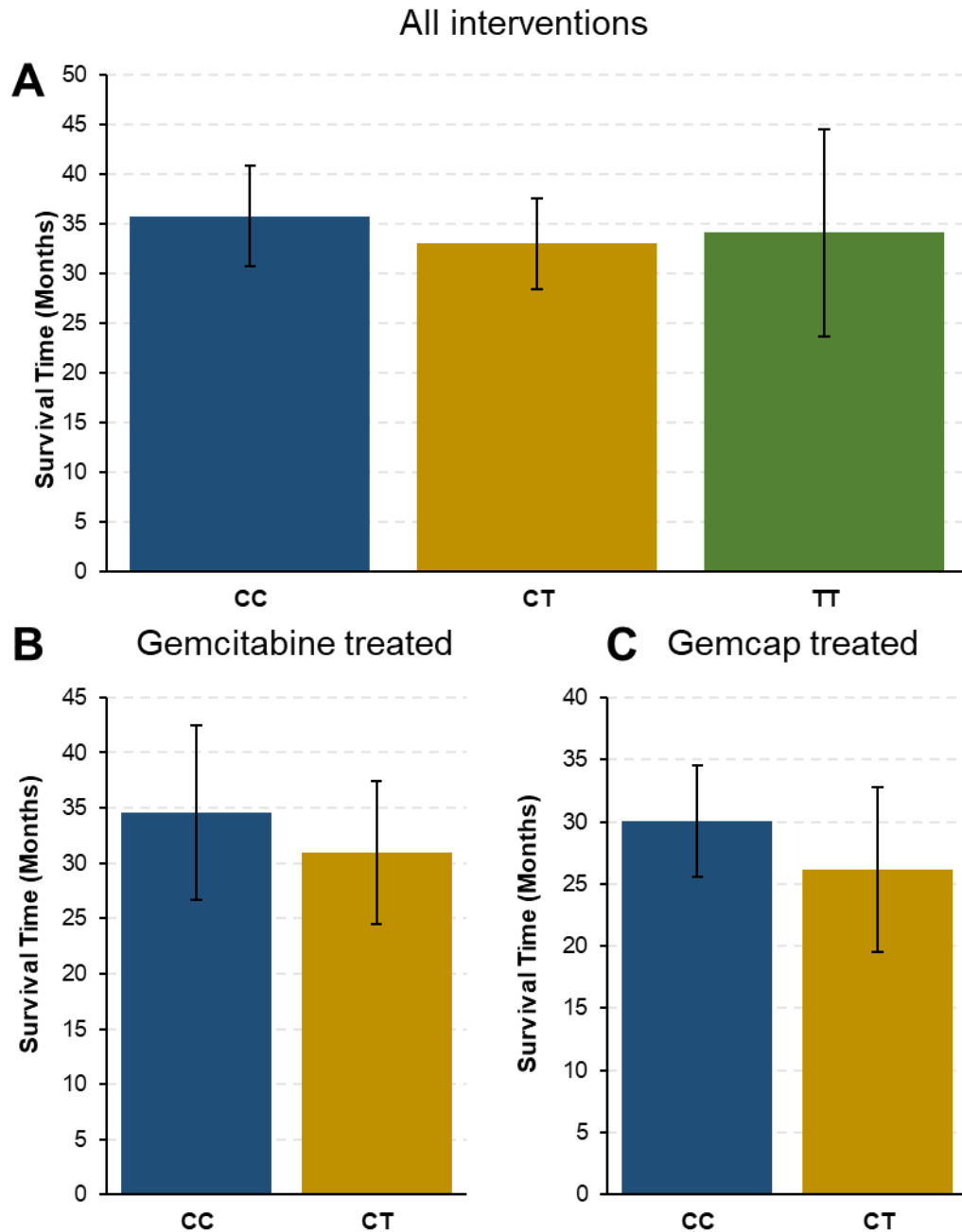


Figure 3-21: Median survival time (months) of patients of each germline *NQO1* genotype of any intervention (A), when treated with gemcitabine (B), or when treated with GemCap (C). Error bars +/- SEM.

3.3 Discussion

3.3.1 Nrf2 and downstream targets were not consistently affected by chemotherapy

Decreases in Nrf2 abundance and activity is associated with decreased viability of cancer cells and an increased sensitivity to chemotherapy (117, 172, 180). Our work has demonstrated decreases in Nrf2 and NQO1 abundance (Figs. 3-6, 3-7, 3-17) post-chemotherapy exposure, despite an increase in Nrf2 activity observed in cultured cell lines (Fig. 3-11). However, a lack of effect to induce Nrf2 activity was observed *in vivo* (Figs. 3-14, 3-15). Overall, these data suggest that Nrf2 does not contribute to acquired chemoresistance in PDAC or affect the Nrf2 activity of healthy tissues, and that the resistance conferred by Nrf2 is limited to intrinsic chemoresistance. Nrf2 therefore continues to be a promising target to reduce innate chemoresistance, however it does not appear that acquired chemoresistance is a consequence of Nrf2 modulation in pancreatic cancer.

3.3.2 NQO1 SNP was not associated with patient prognosis

The absence of effect of NQO1 SNP status upon survival time of patients with resectable PDAC (Fig. 3-19) could be attributable to small numbers of patients, particularly as there were too few TT patients to analyse in any individual arm. The cause of the absence of TT exhibiting patients with advance disease (Table 2, TeloVac/VIP) is not clear. If the TT genotype prevented/delayed progression into advanced pancreatic cancer an accumulation of patients exhibiting TT would be expected in the resectable cohort. Although the observed frequency of the TT genotype in individuals in the ESPAC trial (n=12) was marginally greater than the mathematically expected number (n=10.4), this was not statistically significant and the difference does not appear great enough to offset the lack of the TT genotype in the non-resectable cohort. Instead, it may hypothetically be the case that NQO1 genotype does not

directly affect progression but correlated with criteria affecting eligibility. The TT genotype may have contributed to ill health of patients suffering from advanced disease and therefore prevented their enrolment in the trial, whereas patients with resectable disease may have not been as heavily affected. If true this would suggest that NQO1 and potentially Nrf2 contribute to the improved wellbeing of patients with advanced pancreatic cancer. However, this has not been demonstrated and is a hypothetical explanation.

Differences in the eligibility and exclusion criteria make it difficult to draw conclusions by comparing individuals in separate trials. This may be addressed by either using directly compatible trials or a single trial covering all cohorts to be analysed, however that was not feasible for the purposes of this work. Additionally, if the effect of the TT genotype to exclude patients is linked to the stage of the disease as theorised, this would also not be addressed by using a single trial.

3.3.3 Future Work

Further work is required to explore the effects of multiple chemotherapy exposures and/or longer time points post-treatment. The reduction in Nrf2 abundance was an unexpected finding, however it may be that further Nrf2 depletion would render cells chemosensitive. It is also possible that tumours *in vivo* do not exhibit the same depletion in response to chemotherapy. There did not appear to be any effect of chemotherapy *in vivo* upon either Nrf2 activity or NQO1 abundance, and so the depletion of Nrf2 and downstream targets such as NQO1 occasionally (but not consistently) observed *in vitro* may not be relevant in a living organism. The effect of gemcitabine upon NQO1 abundance in tumour tissue is explored further in Chapter 5, along with the effect of brusatol.

During the course of this research, the OKD48 Nrf2-reporter model was used to examine the effect of chemotherapy upon Nrf2 activity in healthy mice over time. Similarly, the KPC model of PDAC was used to investigate the effect of frequent gemcitabine and brusatol treatment

upon NQO1 in tumour tissue (Chapter 5, Section 5.2.8). Breeding the two to generate a KPC model with OKD48 luciferase present was considered. This would have made it possible to study Nrf2 activity in tumours over time and in response to single or infrequent doses of chemotherapy. Unfortunately, this was not a feasible course of action. Efforts to produce a homozygous OKD48 transgenic mouse at this establishment had previously not been successful. Because of this, only a heterozygote and a wild type could be used for breeding so only half the small number of mice produced would typically be the suitable genotype. Similarly, KPC animals were heterozygous for 3 genetic alterations. As the parents would typically be heterozygous and each possess different alterations, only 1 in 8 animals produced would be predicted to be the correct genotype. The difficulty of breeding each line would mean that only one animal with the correct genotype, OKD48-KPC, would be expected to be born for every 16 produced from appropriate parents. This would not only be prohibitive due to financial and time constraints, but also raised ethical issues due to the large numbers of animals born which could not be used.

Despite the apparent effectiveness of targeting Nrf2, a reliable pharmacological method to do so remains elusive. As discussed during this thesis (Chapter 4), brusatol – previously among the most promising of potential Nrf2 inhibitors – is unlikely to be a direct Nrf2 inhibitor and displays substantial off target effects. Although it now appears unlikely that brusatol will be used primarily as an Nrf2 inhibitor in a clinical setting, it continues to be useful as one in a research setting as part of a careful experimental design.

Identification of the method by which Keap1 is depleted may provide the basis for therapies to restore it and therefore naturally inhibit Nrf2. Contrary to previous findings in PDAC cell lines (137), the majority of PDAC tissue genomic DNA analysed exhibited little or no methylation of the *KEAP1* promoter regions investigated (137). As such it does not seem likely

that methylation of the *KEAP1* promoter is the cause of the previously noticed absence of Keap1 protein in PDAC tissue (113). Alternative potential explanations include mutation of *KEAP1*, miRNA silencing and degradation of the Keap1 protein.

4 – The Mechanism of Action of Brusatol

4.1 Introduction

Brusatol is a commonly used Nrf2 inhibitor due to its ability to deplete Nrf2 protein (151, 152). It has also been observed that brusatol acts as a global translational inhibitor (159, 163, 164) and it was suggested that the effect of brusatol upon Nrf2 may therefore be due to its inhibition of protein synthesis, with Nrf2 being selectively affected due to its short half-life.

The mechanism of action of brusatol remains elusive partly due to the fact that a direct molecular target has not been identified. Currently the molecular basis of some of its effects have been identified, such as the inhibition of protein synthesis resulting from the disruption of the elongation process during translation (164). However, it is not clear how far downstream these effects are of the direct target of brusatol, or whether these effects are up- or downstream of the inhibition of Nrf2. It has also been seen that brusatol localises to the endoplasmic reticulum, which may give it the opportunity to act upon ribosomes directly (159).

Inhibition of Nrf2, such as through shRNA-mediated inhibition of expression, has been seen to result in a decrease of protein synthesis due to an accumulation of ROS (116). Additionally, brusatol treatment can result in ubiquitination of Nrf2 which is an alternative explanation for Nrf2 depletion (155). It may therefore be the case that brusatol targets Nrf2 and consequently inhibits protein synthesis (Mechanism A, Fig 4-1), rather than inhibiting all protein synthesis and resulting in the rapid depletion of short-lived proteins such as Nrf2 (Mechanism B, Fig 4-1). The purpose of this study was to investigate the previously unexplored possibility that brusatol is an Nrf2 inhibitor which inhibits protein translation as a downstream effect of this (Mechanism A, Fig 4-1). This was performed by analysing the effects of brusatol upon protein synthesis under various conditions and determining if the effects of brusatol upon viability could be mitigated by targeting two proposed mechanisms of action as described in Fig. 4-1.

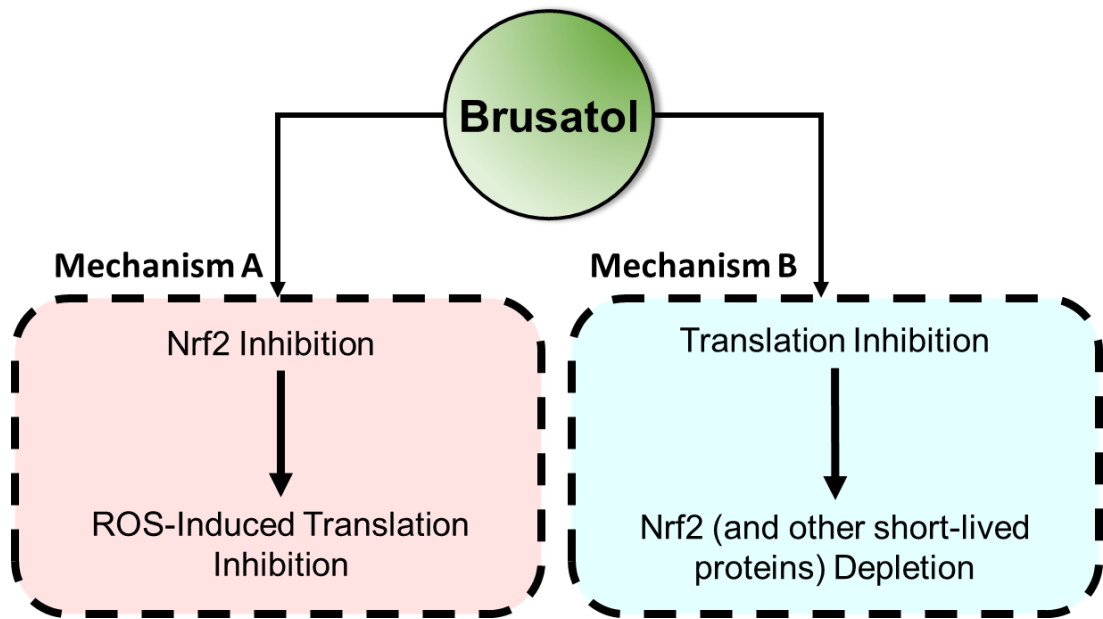


Figure 4-1: Two alternative proposed mechanisms of action of brusatol investigated during this course of work. Left, brusatol as a direct Nrf2 inhibitor with downstream effects upon protein translation. Right, brusatol as a direct inhibitor of translation resulting in the depletion of proteins such as Nrf2.

4.2 Results

4.2.1 Brusatol treatment inhibited protein synthesis and resulted in depletion of Nrf2

The ability of brusatol to inhibit protein synthesis was confirmed by protein synthesis analysis (Fig. 4-2). Protein synthesis analysis was performed as described in Chapter 2.4. In brief, SUIT-2 cells were treated with the drug of interest in complete 10% medium for 15 minutes. They were then treated with the drug of interest in serum-free methionine-free medium for 30 minutes. Reporter amino acid L-aza was then added for one hour before cell lysis. Protein synthesis analysis measured the degree of protein synthesis occurring in the presence of L-aza (a period of one hour during these experiments, following 45 minute drug treatment). Following cell lysis and protein preparation (Chapter 2.3), newly synthesised proteins were represented by bands on a PVDF membrane (Fig. 4-2, 4-3). The intensity of bands therefore

corresponded to the degree of protein synthesis, and an absence of bands corresponded to a lack of detectable protein synthesis.

Brusatol treatment reduced protein synthesis to seemingly undetectable levels (Fig. 4-2) and noticeably decreased the abundance of Nrf2 (Fig. 4-2). The protein synthesis inhibitor cycloheximide had the same effect as brusatol upon both protein synthesis and Nrf2 (Fig. 4-2 A). Dose-response analysis showed that all detectable protein synthesis was inhibited at 80nM Brusatol with only minimal synthesis detected at 50nM. Greater degrees of protein synthesis inhibition were seen to correspond to increasing depletion of Nrf2. Low levels of Nrf2 were detected long after the half-life of uninduced Nrf2, suggesting that some Nrf2 was dissociated from Keap1 and active either as a result of brusatol treatment or as basal functionality.

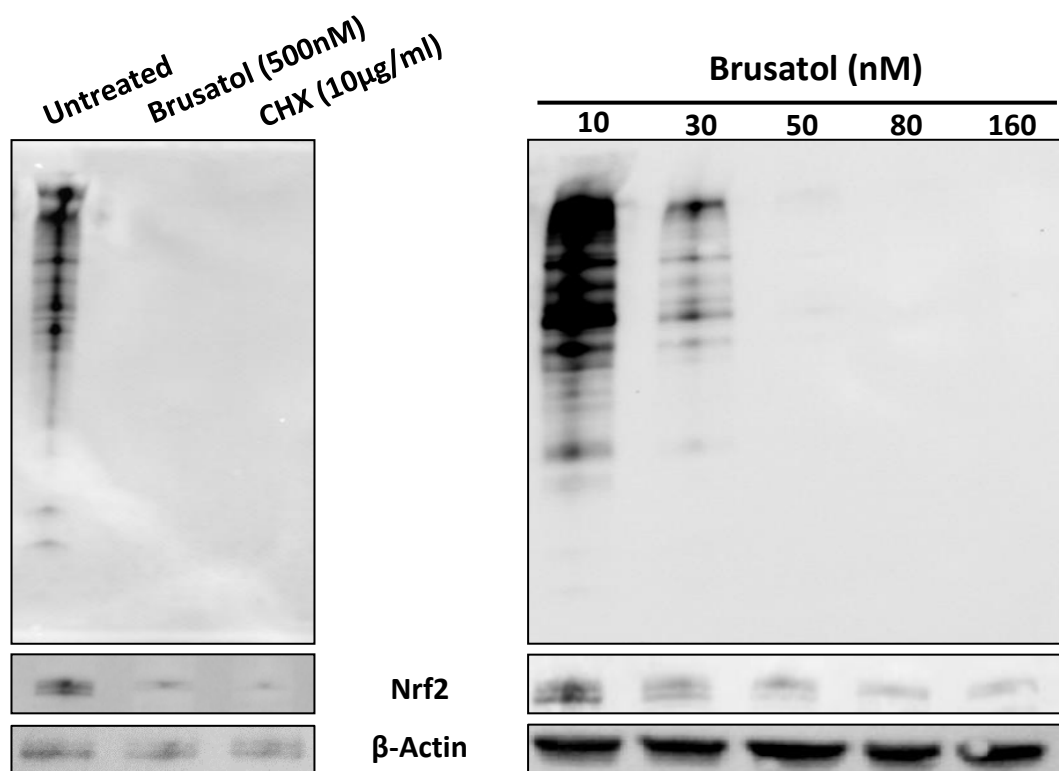


Figure 4-2: Brusatol inhibited nascent protein synthesis (cycloheximide treatment shown as a positive control) within SUIT-2 cells. The maximal effect was observed at 80nM. Abbreviation: CHX: Cycloheximide.

4.2.2 CDDO-Me-mediated accumulation of Nrf2 did not mitigate the effects of brusatol upon protein synthesis

CDDO-Me is a highly selective Nrf2 activator acting through interaction with Keap1 and causing a subsequent release of Nrf2, and so was used in this study for the purposes of mitigating Nrf2 inhibition and depletion (181, 182). Protein synthesis analysis following pretreatment with CDDO-Me was used to determine if an accumulation of Nrf2 could mitigate the effects of brusatol (Fig. 4-3). It was found that CDDO-Me did not mitigate the inhibitory effects of either brusatol or CHX on protein synthesis. Furthermore, it appeared that CDDO-Me treatment resulted in reduced protein synthesis. The effect of brusatol upon protein synthesis therefore appears to be either the cause of or unrelated to Nrf2 depletion, rather than a result of Nrf2 depletion.

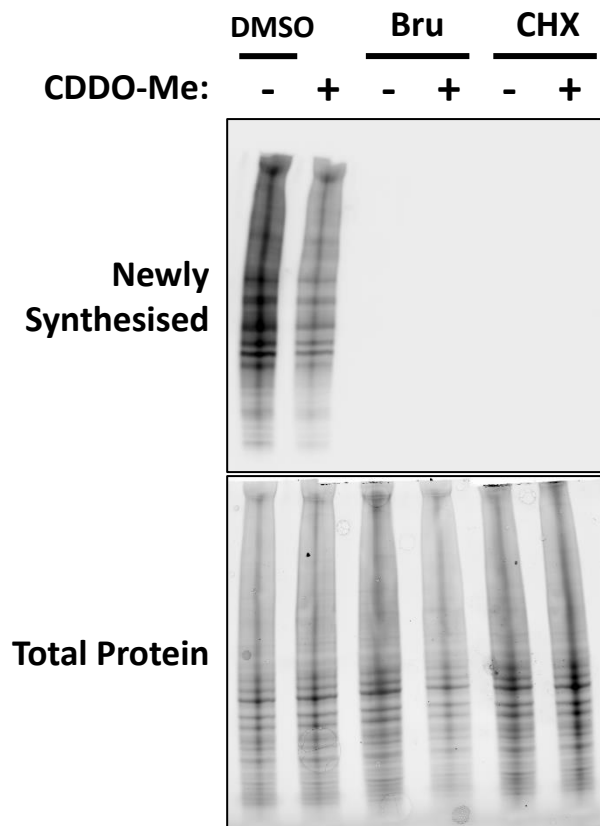


Figure 4-3: The effect of CHX (10 μ g/mL) and brusatol (100nM) on protein synthesis following 4 hour CDDO-Me pretreatment. Newly synthesised protein shown as a visualisation of the degree of protein synthesis. Total protein loaded shown as loading control. Abbreviations: Bru: brusatol. CHX: cycloheximide.

4.2.3 CDDO-Me-mediated accumulation of Nrf2 did not mitigate the effects of brusatol upon cell viability

Although Nrf2 depletion appears to be a result of protein synthesis inhibition, the specific mechanism by which brusatol treatment exerts its toxic effects is unclear. It has previously been observed that brusatol treatment can cause the accumulation of ROS, an expected result of Nrf2 depletion and a possible cause of loss of viability (101). Brusatol appears to inhibit the expression of all proteins, however many of these may potentially be less

important for cell survival, and/or with a longer half-life so would be less affected by protein synthesis inhibition. I therefore hypothesised that Nrf2 depletion may ultimately contribute to brusatol-induced toxicity even though Nrf2 depletion does not appear to be the primary target nor a specific mechanism of action of Brusatol. As such, MTT assays were performed to investigate the effect of brusatol upon cell viability and determine if the effect could be mitigated through compensation of a loss of Nrf2.

CDDO-Me pretreatment was used to mitigate any subsequent depletion of Nrf2. Following CDDO-Me pretreatment, cells were exposed to brusatol, CHX and H₂O₂ for short periods of time (between 10 minute and 2 hours, plus 48h for maximal effect) before medium was replaced. This was to account for the possibility that treatment could overwhelm any accumulated Nrf2 and downstream targets by the time of analysis. Cellular viability was measured using MTT assay 48h following treatment. H₂O₂ treatment was used to compare against chemically induced cell viability inhibition, which Nrf2 would be expected to defend against. However, although CDDO-Me pretreatment appeared to defend cells against the effects of H₂O₂ treatment in at least some instances (Fig. 4-4 A, C), it did not appear to defend cells against the effects of brusatol or cycloheximide (Fig 4-4).

Although CDDO-Me pretreatment showed strong trends to mitigate H₂O₂ toxicity, this was only statistically significant in MIA PaCa-2 cells treated for 10 minutes (Fig. 4-4 A). This trend was observed following most treatment durations of MIA PaCa-2 cells and all treatment durations of SUIT-2 cells. However, CDDO-Me pretreatment did not appear to be protective against H₂O₂ treatment of PANC-1 cells.

The effect of brusatol and CHX were not significantly mitigated by CDDO-Me pretreatment. CDDO-Me pretreated cells often exhibited a tendency for lower viability following drug treatment than their non-pretreated counterparts (Fig. 4-4 A, B). However, SUIT-2 cells were

an exception to this. CDDO-Me pretreatment of SUIT-2 cells showed a trend towards an increase in viability relative to cells treated with brusatol or CHX alone.

Brusatol appeared to act more slowly than cycloheximide despite resulting in a similar final effect at 48h (Fig. 4-4 B, C). The reduced response of short treatments of brusatol relative to the same treatment durations of cycloheximide was seen in PANC-1 and SUIT-2 cells (Fig. 4-4 B, C) but was most pronounced upon SUIT-2 cells (Fig. 4-4 C). The same effects of cell viability of MIA PaCa-2 cells were seen in response to the same durations of brusatol and CHX treatment (Fig. 4-4 A), however.

These differences may suggest that the two chemicals exert distinct mechanisms of action. However, it may also be the result of how quickly each chemical could reach their targets, even if they act through a shared mechanism.

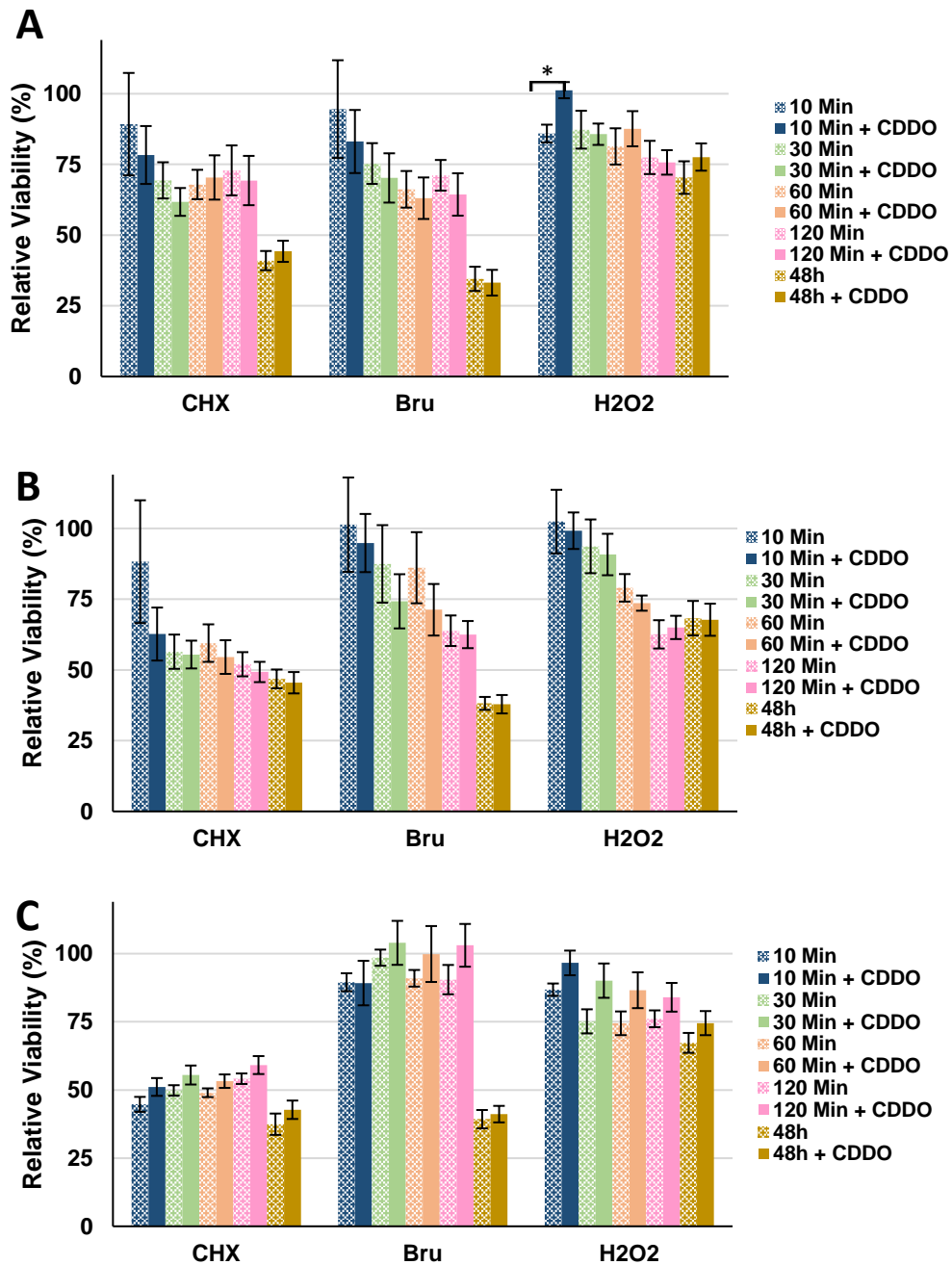


Figure 4-4: Relative viability of MIA PaCa-2 (A), PANC-1 (B) and SUIT-2 (C) cells with CHX, Bru or H₂O₂ for various periods of time either with (solid colour) or without (patterned colour) 4h CDDO-Me pretreatment. Viability was normalised to a vehicle control with the same 4h CDDO-Me pretreatment (with/without). Statistical analysis was performed using *t*-test between pretreated and non-pretreated for each drug and timepoint, with Bonferroni correction to account for multiple comparisons. * *p*-value below 0.0033. Each bar is the mean of three experiments each performed in triplicate. Error bars +/- SEM. Abbreviations: CHX: cycloheximide. Bru: Brusatol. CDDO: CDDO-Me.

4.2.4 ML385 did not inhibit Nrf2 activity below baseline activity

Taken together, the findings of this chapter so far appear to indicate that that Nrf2 depletion is a non-specific and secondary effect of brusatol, and that Nrf2 depletion is not the cause of brusatol cytotoxicity in the conditions analysed. However, efforts to identify alternative Nrf2 inhibitors have been met with limited success. ML385, a commonly used inhibitor of Nrf2 (166, 183-185), was considered as an alternative to brusatol to be used during the course of this research. However, luciferase-based Nrf2 activity analysis (as described in Chapter 3, Section 3.2.8) showed that Nrf2 activity following ML385 exposure to cells in culture did not significantly differ from Nrf2 activity in vehicle (DMSO) treated pancreatic cancer cells (Fig. 4-5).

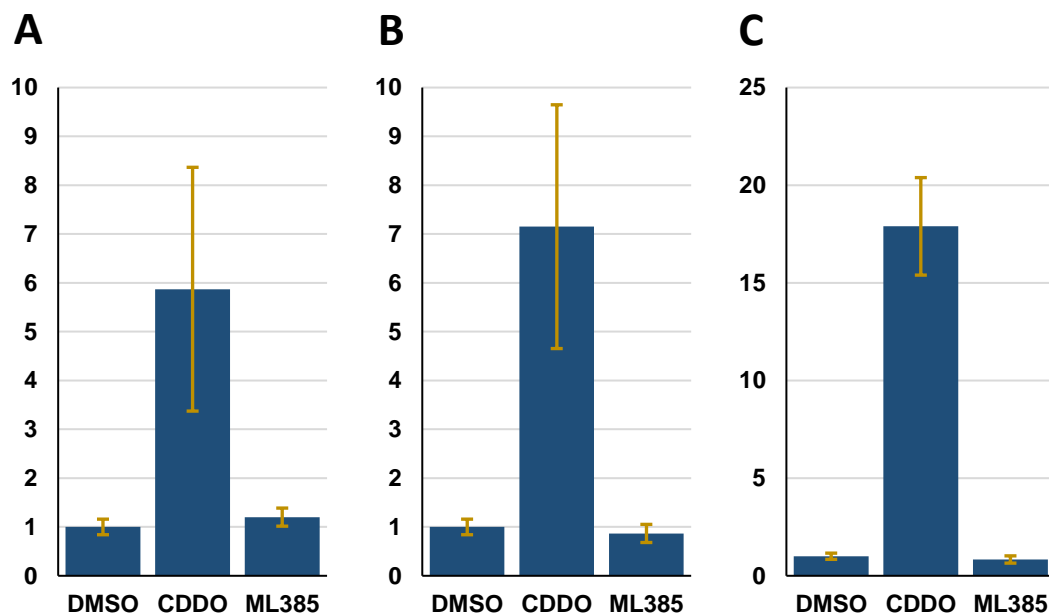


Figure 4-5: Treatment of MIA PaCa-2 (A), PANC-1 (B) and SUIT-2 (C) cells with CDDO-Me and ML385 following transient transfection of Nrf2 luciferase. Data are the mean of three experiments, each performed in triplicate. Work contributed to by MRes student Lewis Wignall with my direct supervision and input. Error bars +/- SEM.

ML385 has been found to exert its inhibitory effect upon Nrf2 by inhibiting the DNA binding domain, Neh2, of Nrf2 (166). To address the possibility that Nrf2 activity was at a minimum and could not be inhibited further, the effect of ML385 on CDDO-Me treated cells was explored. No significant inhibition by ML385 on CDDO-Me induced Nrf2 activity was found (Fig. 4-6). In each cell line treated with ML385 and CDDO-Me, the level of induced Nrf2 activity compared to that seen with CDDO-Me alone was reduced, although it did not reach statistical significance. Although Nrf2 activity was consistently reduced following combined ML385 and CDDO-Me treatment compared to treatment with CDDO-Me alone, the effects observed were mild. Consequently, ML385 was not explored further during the course of this work.

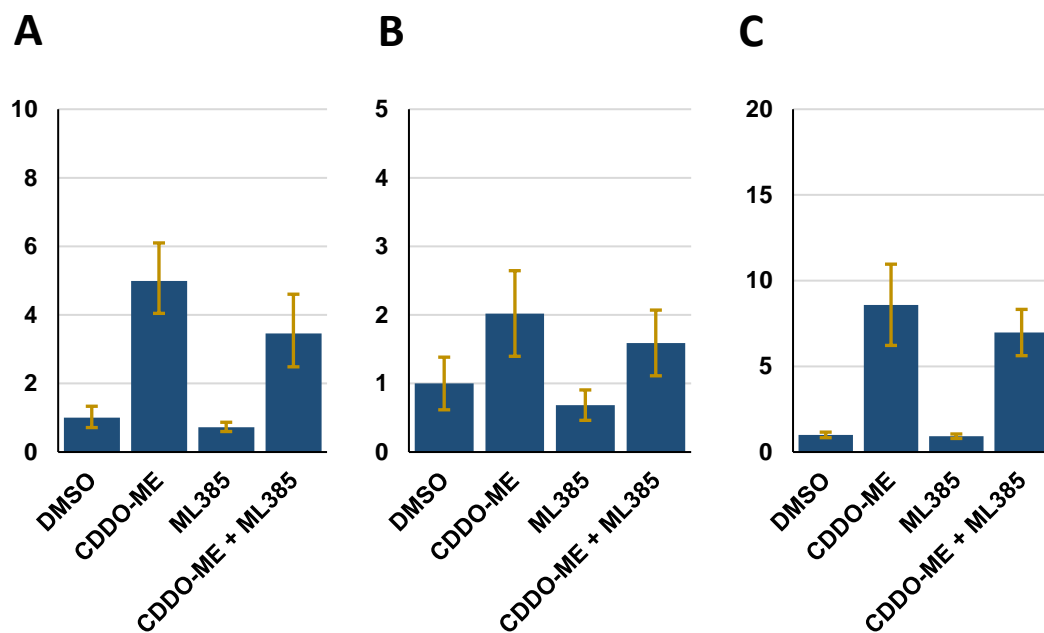


Figure 4-6: Treatment of MIA PaCa-2 (A), PANC-1 (B) and SUIT-2 (C) cells with CDDO-Me, ML385 and combination following transient transfection of Nrf2 luciferase. Data are the mean of three experiments, each performed in triplicate. Work contributed to by MRes student Chris Brown with my direct supervision and input. Error bars +/- SEM.

Why no significant effect of ML385 was observed, inconsistent with published literature, is not clear. Although it is known that ML385 is selective for *KEAP1* mutated cells whereas the

cell lines used here do not exhibit loss-of-function KEAP1 mutations (113, 166), this would seem to be due to unstressed wild-type *KEAP1* cells exhibiting minimal Nrf2 activity already available to inhibit. It is not clear why an inhibitor of the DNA binding-domain of Nrf2 would not prevent Nrf2 upregulating downstream targets such as the luciferase plasmid, regardless of *KEAP1* mutation status, once Nrf2 was activated through other means (CDDO-Me treatment, in this instance). Despite not being significant there was a trend of ML385 to reduce Nrf2 activity in CDDO-Me treated cells relative to CDDO-Me treated alone, so it may be that ML385 inhibited Nrf2 activity but not to a great extent under these conditions. Further optimisation may have elucidated the reasons for the perceived lack of effect of ML385 and may have resulted in a method to use ML385 to inhibit Nrf2 in pancreatic cancer cells more effectively. However, time constraints did not allow for this during the course of this work.

4.3 Discussion

Brusatol continues to be widely used as an Nrf2 inhibitor (153-155, 160-162). Although it has been hypothesised that this effect is a result of brusatol acting as a global protein synthesis inhibitor, protein synthesis inhibition is also an expected consequence of Nrf2 inhibition. Additionally, the well described effect of brusatol upon Nrf2 is a reasonable candidate for the cause of the cytotoxicity exhibited by brusatol regardless of whether it is a direct or downstream effect. This study focused upon determining the mechanism of action of brusatol and to what extent, if any, depletion of Nrf2 is responsible for the anti-tumour effects exhibited.

These data suggest that inhibition of Nrf2 is not the dominant mechanism of action by which brusatol exerts its toxic effects. However, brusatol has been seen to potently result in the depletion of Nrf2 (Fig. 4-2). The inhibition of a pro-survival pathway would normally be

expected to result in toxicity, and it is known that inhibition of Nrf2 through alternative means such as siRNA-mediated depletion has been seen to result in diminished viability of pancreatic cancer cells (113). It therefore seems likely that although the inhibition of Nrf2 by brusatol may hypothetically result in inhibition of viability, other toxic mechanisms render this redundant in the cell lines analysed. However, the effect of Nrf2 depletion being more significant in other cell lines, diseases or conditions cannot be discounted.

The findings of this research suggest that the primary effect of brusatol is not to directly inhibit Nrf2, and that the observed effect on Nrf2 is a consequence of protein synthesis inhibition. Additionally, the mechanism by which brusatol inhibited cell viability did not appear to be dependent upon Nrf2 depletion. Minimising the loss of Nrf2 by causing its accumulation and mitigating the effects of its loss through supplementation of antioxidants demonstrated no protective effect against brusatol. Despite this it is well known that the loss of Nrf2 activity is associated with decreased cellular survival and increased chemosensitivity (113, 116, 130, 134, 186). Whilst this appears to be redundant in the cell lines exposed to brusatol during this study, these findings confirmed that brusatol inhibited Nrf2. Although the effect to inhibit Nrf2 appeared redundant under these conditions, since it was observed that cell viability was inhibited by brusatol following CDDO-Me-induced accumulation of Nrf2, it does not exclude the possibility that Nrf2 depletion by brusatol is toxicologically relevant in other cell lines and/or diseases.

Although inhibition of Nrf2 is an attractive therapeutic target, efforts to identify pharmacological inhibitors have been met with minimal success. Although brusatol has been shown to rapidly result in depletion of Nrf2 protein and do so selectively to short-lived proteins, the inhibition of protein synthesis appears to cause other effects which are relevant to cytotoxicity. As demonstrated, it appears that the effect of brusatol – arguably the most widely used Nrf2 inhibitor currently available – upon Nrf2 is secondary to its effect upon

protein synthesis. This is consistent with conclusions previously drawn from the observation that brusatol inhibits protein synthesis (159, 163). Recently developed examples of alternative Nrf2 inhibitors include ML385, demonstrated to inhibit Nrf2 and be particularly cytotoxic to *KEAP1* mutated cells (166). However, luciferase reporter assay of Nrf2 activity showed that ML385 had only a mild effect (Fig. 4-6). ML385 appeared to slightly offset the effect of CDDO-Me (Fig. 4-6), however it did not reduce basal levels of Nrf2 activity (Fig. 4-5) in the cell lines analysed. As ML385 does not appear to be a potent inhibitor of Nrf2 activity under these conditions and did not demonstrate any anti-tumour properties, it was not considered for further analysis. However, there are other recently identified Nrf2 inhibitors (135, 174, 175, 187). These include camptothecin, which caused an inhibition of Nrf2 expression in a variety of cancer cell lines, and is already available as a form of chemotherapy (175). Further research is required to fully understand their mechanisms of action, the presence and significance of any off-target effects, and the feasibility of using them therapeutically.

In addition to reliably depleting Nrf2, the indirect and additional effects demonstrated by brusatol appear to contribute to its cytotoxicity to pancreatic cancer cells, and so remains a promising potential chemotherapy. Additionally, brusatol has already been seen to be a potent anti-cancer agent *in vitro* and *in vivo*, including against pancreatic cancer models (151-154, 157, 162). Although the extent of Nrf2 involvement in the efficacy of brusatol in previously published work cannot be guaranteed, and the effect of Nrf2 depletion did not appear to be a necessary component of the effects of brusatol during the course of this work, brusatol has still shown considerable promise as an anti-cancer agent and so continued to be the focus of this work.

5 – Analysis of Brusatol as a Form of Chemotherapy

5.1 Introduction

The prognosis of most common forms of cancer has improved over time, however PDAC patient outlook has improved only minimally over several decades (32, 56, 188). In 2017 it was demonstrated that combination of capecitabine with gemcitabine modestly improved the prognosis of patients eligible for surgical resection patients (a 10% increase in survival time), representing one of the largest improvements in treatment of non-selected patients since the introduction of gemcitabine (52). The poor prognosis of PDAC has been attributed in part to chemoresistance (28, 55, 68, 189). Use of an agent to mitigate this chemoresistance and so render tumours responsive to chemotherapy, or other forms of treatment, is therefore an attractive avenue for research.

The *Brucea javanica* extract brusatol is a quassinoid shown to exhibit anti-cancer properties (152, 190). It has been demonstrated to render cancer sensitive to multiple forms of therapy, such as radiotherapy and chemotherapy (101, 159, 190). Brusatol is a widely used Nrf2 inhibitor and it was previously commonly thought that Nrf2 inhibition conferred its cytotoxic properties (101, 152, 158, 190). However it has also been observed that all protein synthesis is inhibited in response to brusatol treatment (159, 163). Although a molecular mechanism of action has not been fully elucidated, it appears that brusatol acts primarily by inhibiting protein synthesis and that this has the consequence of preventing Nrf2 production and accumulation (159, 163). The exact direct cause of the cytotoxicity exerted by brusatol and the extent to which specific effects, such as protein synthesis inhibition and Nrf2 depletion, contribute is unclear, however Nrf2 and the antioxidant system have been directly implicated in brusatol-mediated cytotoxicity (101, 152).

Brusatol research has produced promising results as an anti-cancer therapy. *In vivo* analysis has previously shown it to be well tolerated by animals and an effective treatment against models of cancer (including pancreatic cancer), either as a single agent or in combination

therapies (112, 151, 157, 176, 191). It has been shown to work synergistically with first line treatments such as 5-FU and gemcitabine, and to have comparable effects to standard chemotherapy in orthotopic xenograft models of the disease in terms of efficacy and toxicity (157). However, its efficacy against spontaneous tumours in a genetic model of PDAC, such as the KPC model, has not previously been reported.

I hypothesised that brusatol could be a cytotoxic agent against PDAC tumour cells both *in vitro* and *in vivo*. Additionally, brusatol function is expected to remove the ability of cells to upregulate chemical defence and cell survival pathways such as Nrf2 and downstream genes. I therefore hypothesised that brusatol may be a chemosensitiser that could improve the efficacy of other chemotherapies in addition to exerting its own cytotoxic effects.

5.1.1 Models of drug synergy

In basic terms, drug synergy refers to a combination of drugs or chemicals working more effectively than its individual components, whereas antagonism refers to the combination working less effectively than its individual components. However, the strict definition of drug synergy, and how to measure it, varies depending upon the intent and context. This is because whether the effect of a combination is more or less effective than its individual components depends upon what effect the combination is being compared against and why. For example, if two hypothetical drugs work through a similar mechanism of action then they could be considered antagonistic. The two drugs have overlapping effects so therefore either one competitively prevents the other from acting fully. Although each drug may greatly inhibit cell viability (in the case of toxic agents) when added individually, if that effect has already been achieved by one drug then the addition of a second drug is unlikely to yield as great an absolute effect as if that drug was added alone. This concept of synergy postulates that drugs act additively if they act completely independently of one another. Synergy therefore refers to a greater effect than expected of them working independently whereas

antagonism refers to a less pronounced effect than expected if they worked independently. This definition of synergy is typically used in experiments designed to investigate the mechanisms of action of the drugs of interest, of which the degree of toxicity is a reporter of individual drug potency in the combination. The Bliss Independence Model is a widely used measure of synergy which follows the previously described definition of synergy, which assumes that drugs acting independently and non-competitively yield an additive response (192).

It is also simultaneously possible that the same combination of drugs produces a greater effect than either could alone. If a concentration of each drug is used which would individually give their maximum effect, then even if only a slight increase in effect is observed when used together there would seem to be some benefit to the combination. This could therefore be considered synergistic despite, as previously explained, also being considered antagonistic under a model such as Bliss measuring drug independence. This definition of synergy is typically used in situations in which the extent of the effect is the primary interest. The Highest Single Agent (HSA) and/or Loewe Additivity Model (192) is often used when using this definition of synergy, in which the absolute effect of a combination is to be investigated instead of the effect on relative efficacy of either individual drug. HSA and Loewe Additivity Model both define synergy based upon an increase in final efficacy of the drugs, however they do so in separate ways. Whereas HSA assumes that the addition of a second drug producing a greater response than either does alone at the concentration used in the combination is synergistic, Loewe Additivity Model compares the effect of a combination to what would be expected if the drug was compared to itself.

Not only can the definition and method of measuring synergy vary, but whether the same result is considered antagonistic or synergistic may differ depending upon the method used.

As such, multiple models of drug synergy were utilised to examine the interaction between the effects of drugs on cell viability.

5.1.2 Licensing for *in vivo* work

The use of protected animals for scientific experiments is regulated under UK law by the Animals (Scientific Procedures) Act 1986 (ASPA). This legal framework comprises multiple forms of licence issued by the Home Office, all of which must be obtained prior to starting any form of work regulated by the act. The three main forms of licence are establishment, project (PPL) and personal (PIL). Before experiments may begin, the work must be covered by each relevant form of licence. The institution at which the work is to be performed must have obtained an establishment licence covering the use of protected animals. The project of work itself must also be covered by a PPL, which requires that the specific procedures to be performed are detailed and justified. Each individual performing experiments with animals must obtain a PIL.

The PIL certifies that the researcher has completed academic training to make them aware of their responsibilities and how to care for the animals, as well as has been trained how to handle them. However, a PIL does not immediately permit an individual to perform *in vivo* experiments. Practical training and supervision to competence is first required before regulated procedures can be performed.

A PIL and PPL were applied for to enable the *in vivo* work detailed in this thesis to be performed. Academic and practical training was given prior to the successful application for a PIL, and subsequent training to competence was performed following the granting of one. In addition to this, a substantial contribution was made by me to the preparation of a successful application to be granted a PPL. For a PPL to be granted the potential detriment caused to animals must be justified by the potential benefits of the research, and the 3Rs

(Replacement, Reduction and Refinement) must be followed. In brief, the 3Rs refer to avoiding the use of animals wherever possible (replacement), minimising the numbers of animals required when they must be used (reduction), and taking care to minimise suffering and the risks of adverse events (refinement).

A PPL application was prepared for the purposes of seeking Home Office approval to perform experiments involving KPC mice. The primary intention of this licence was to investigate the effects of brusatol and other potential pancreatic cancer therapies to upon the survival of tumour-bearing KPC/KC mice. This involved the treatment of mice with drugs of interest (which was brusatol during the course of this work), which had toxicity information already well established clinically or *in vivo*, and procedures that would directly contribute to this aim such as ultrasound imaging of mice to detect tumours.

The strict framework surrounding animal research is vital for ethical and scientific reasons. It improves the scientific value of research through limiting the number of confounding variables, by ensuring poor treatment would not affect the animal and therefore the results of the experiment. As such, the PPL application relied heavily upon methods and limits set by pre-established guidelines. Specifically, the Laboratory Animal Science Association (LASA) best practice guidelines for administration of substances was used to establish limits on methods and volumes of drug delivery. Although the first drug intended to be trialled was brusatol, a licence to test any new potential drug to treat PDAC was sought. However, it was explicitly stated that any drug/chemical to be used must have been used *in vivo* previously. A pharmacokinetic analysis is typically performed to determine safe limits of a novel agent to be trialled *in vivo* for the first time. It was decided that this would not form part of this licence due to the substantial ethical justification required and the low probability of needing to use one. This decision was partly due to ethical considerations so that the use of an unsafe untested substance would be avoided, but also because the focus of this and future work

was to identify agents that have already shown promise *in vivo* and therefore a safe working concentration is already known. Although the agent would be novel in regard to its usage in a genetic model of PDAC, it would likely have been used *in vivo* in other circumstances. Previous *in vivo* work may have investigated the treating of xenografts or GEMMs of other cancer types, or the drug may have been used clinically to treat a different condition.

5.2 Results

5.2.1 Brusatol inhibited cell viability

Brusatol inhibited the viability of PDAC cell lines with an IC₅₀ ranging from 8.56nM to 25.98nM dependent upon cell line (Fig. 5-1). IC₅₀ of gemcitabine and 5FU were also established for the purposes of subsequent synergy analysis to determine if brusatol and standard chemotherapies acted synergistically, additively, or antagonistically *in vitro*. Analysis of MTT assays demonstrated that brusatol, 5-FU and gemcitabine each individually decreased cell viability (Fig. 5-1). Brusatol appeared to almost entirely inhibit cell viability at high concentrations. 5-FU had a considerably higher IC₅₀ than gemcitabine and brusatol.

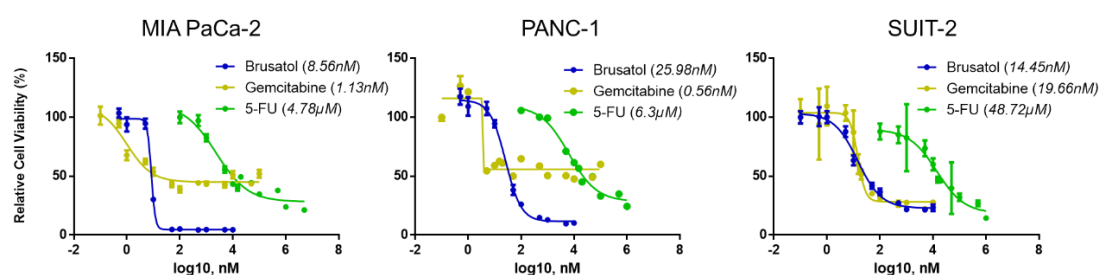


Figure 5-1: MTT analysis of MIA PaCa-2, PANC-1, and SUI-2 cells treated with brusatol, gemcitabine or 5-FU for 48h prior to MTT assay. Representative image of three independent experiments, mean IC₅₀ shown in italics.

The Loewe Additivity Model and the HSA were utilised to determine if brusatol in combination with gemcitabine or 5-FU yielded improved results in terms of inhibiting cell

viability relative to an increase in the single drug concentration. Bliss Independence Model was used to help determine if the chemicals affected cell viability independently of one another. Zero Interaction Potency ('ZIP') is a relatively recently created model (192) which aims to incorporate the concepts of both Bliss and Loewe. Synergy analysis was performed and figures generated using SynergyFinder in R Studio (193). The following figures (Figs. 5-1:5-4) display the degree of synergism/antagonism of each drug combination as calculated by each model. The relationship between the effects of each drug is represented by a colour code. The cell of a drug combination being coloured red shows that the combination acted synergistically, whereas blue shows antagonism. The intensity of colour corresponds to the degree of synergism/antagonism, with additivity (neither synergistic nor antagonistic) being represented by the cell being shaded white. Dark grey indicates an inability to accurately calculate synergy/antagonism as a limitation of the model under those circumstances.

5.2.2 Brusatol and gemcitabine act predominantly additively or antagonistically during co-treatment

Gemcitabine and brusatol were seen to act predominantly additively across different cell lines and models of synergy, with large areas of antagonism although there were small areas of synergy (Fig. 5-2). The results suggesting antagonism of gemcitabine and brusatol were largely consistent for each cell line. Low to moderate doses of each drug were usually seen to act antagonistically, with additivity being seen at higher doses.

Whether or not synergy was detected appeared less consistent between different cell lines. Low concentrations of brusatol appeared to act independently and synergise with gemcitabine in MIA PaCa-2 cells (Fig. 5-2 A), however this effect appeared milder in PANC-1 cells (Fig. 5-2 B) and was only additive or mildly antagonistic in SUIT-2 cells (Fig. 5-2 C).

Bliss and ZIP analysis showed that low concentrations of brusatol inhibited MIA PaCa-2 viability through a mechanism independent to that of gemcitabine (Fig. 5-2 A), and that the two mechanisms acted in synergy. However, higher concentrations of brusatol were seen to act antagonistically. HSA and Loewe showed that brusatol and gemcitabine acted either antagonistically or additively, with no evidence of synergy.

Brusatol and gemcitabine were seen to act predominantly additively with only minor synergy or antagonism upon PANC-1 cell viability (Fig. 5-2 B). An exception was a fairly low (20nM) dose of brusatol with most concentrations of gemcitabine when analysed by the Loewe Additivity Model. These findings suggest that the drugs may be acting independently and typically produce a net additive final response, although specific low doses of brusatol appear to be an exception to this.

Gemcitabine and brusatol combinations were seen to act either antagonistically or additively upon SUIT-2 cells at most concentrations of each drug (Fig. 5-2 C). This was true for each model of synergy, suggesting that there were overlapping effects (as measured by Bliss) which resulted in a lower final response upon viability. However, the antagonistic effect upon final efficacy appeared to be milder than the degree their effects overlapped (as measured by Bliss). The antagonistic effect was most pronounced following treatment with lower concentrations of each drug, with higher and moderate concentrations yielding either less antagonistic or additive responses. ZIP analysis was an exception with showed greatest, though relatively mild, antagonism at moderate concentrations upon SUIT-2 cells.

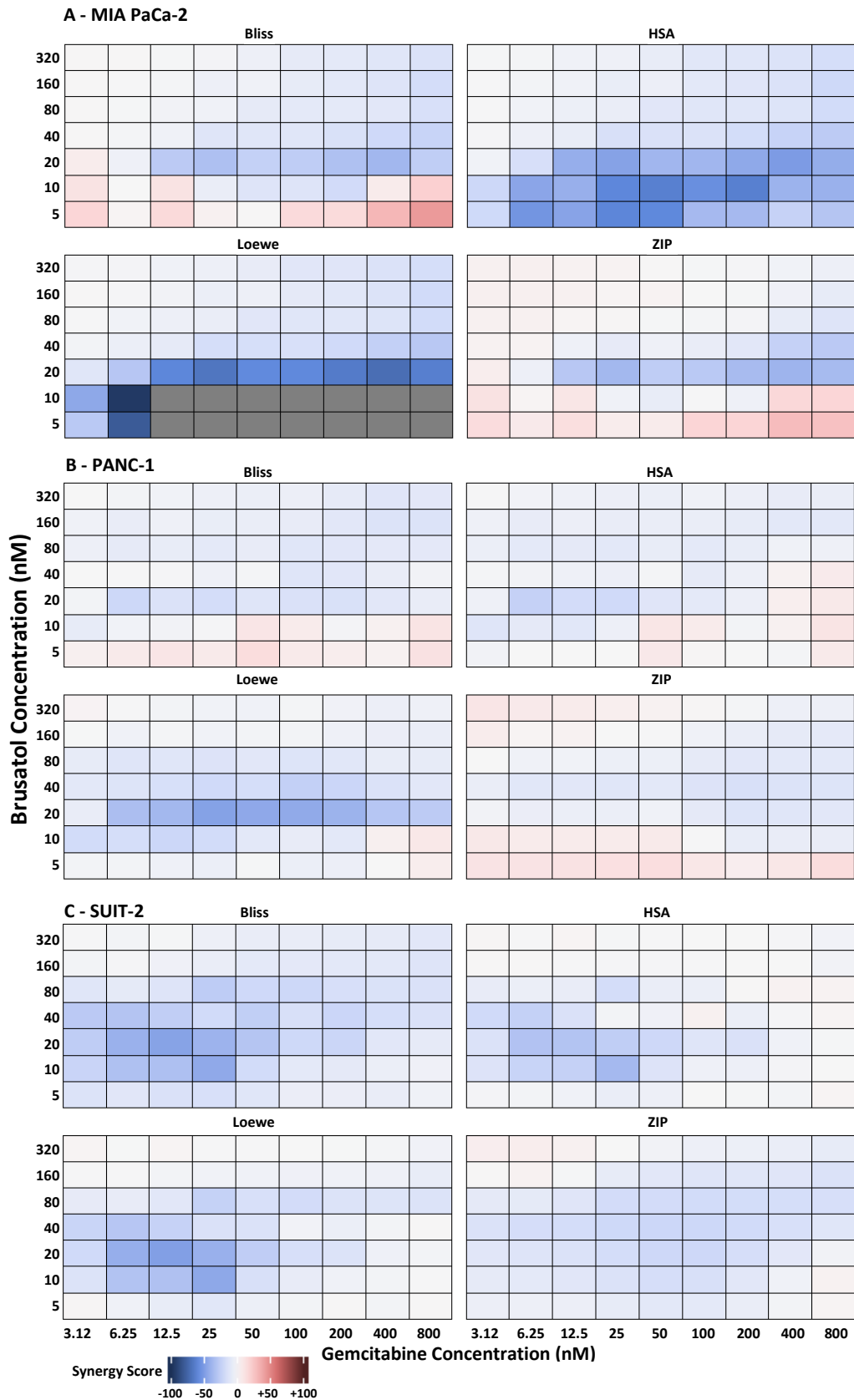


Figure 5-2: Synergy analysis of MIA PaCa-2 (A), PANC-1 (B) and SUIT-2 (C) cells treated with gemcitabine and brusatol, visualised using Bliss, HSA, Loewe and ZIP models of synergy. Images represent one preliminary experiment. Abbreviations: HSA, Highest Single Agent. ZIP, Zero Interaction Potency.

5.2.3 Brusatol and 5-FU act predominantly additively or antagonistically during co-treatment

5-FU and brusatol combinations appeared to be mostly additive or antagonistic across different models and cell lines (Fig. 5-3). Low concentrations of brusatol was seen to act antagonistically with 5-FU of MIA PaCa-2 cells, as measured by Loewe and HSA (Fig. 5-3 A). However, high concentrations of 5-FU appeared to synergise with low concentrations of brusatol upon MIA PaCa-2 cells in terms of increasing effect relative to the concentration used (HSA) rather than when compared to adding more of the same (Loewe) (Fig. 5-3 A). The Bliss model also showed overlapping effects of relatively low concentrations of brusatol with 5-FU, however the lowest concentration showed a small degree of synergy in contrast to the intense antagonism reported by Loewe (Fig. 5-3 A).

Moderate doses of brusatol and 5-FU appeared to act mildly antagonistically according to each model against PANC-1 cells (Fig. 5-3 B). The effects were otherwise mostly additive or mildly synergistic upon PANC-1 cells, depending upon concentration and model. ZIP in particular showed broad, though mild, synergy of low concentrations of 5-FU with low and high concentrations of brusatol (Fig. 5-3 B).

Brusatol and 5-FU predominantly acted additively upon SUIT-2 cell viability. One combination (3.12 μ M 5-FU, 20nM Brusatol) consistently exhibited notable antagonism in each model except ZIP, with adjacent combinations showing a lesser degree of antagonism.

Combinations of 5-FU and brusatol exhibited a similar pattern across each cell line and usually with general agreement across the different models of synergy. Antagonism was found mostly following treatment with low concentrations of brusatol (though not the lowest, which was often additive or synergistic), although the concentration of 5-FU it affected varied between cell lines. Higher doses of brusatol appeared to be additive with 5-FU, with evidence of mild synergism in some cases.

Combination treatments of PANC-1 cells appeared to show the greatest degree of synergism/antagonism. Although combination therapies of MIA PaCa-2 cells and SUI-2 cells tended to result in a similar pattern of synergy/antagonism to PANC-1 cells, the results of PANC-1 synergy analysis were more pronounced. This suggests that the effects of drugs to inhibit, enhance or overlap in terms of efficacy is more pronounced in the PANC-1 cell line than in others. This may be related to PANC-1 cells appearing more resistant to gemcitabine than MIA PaCa-2 and SUI-2 cells, although PANC-1 cells did not exhibit any higher resistance to brusatol or 5-FU.

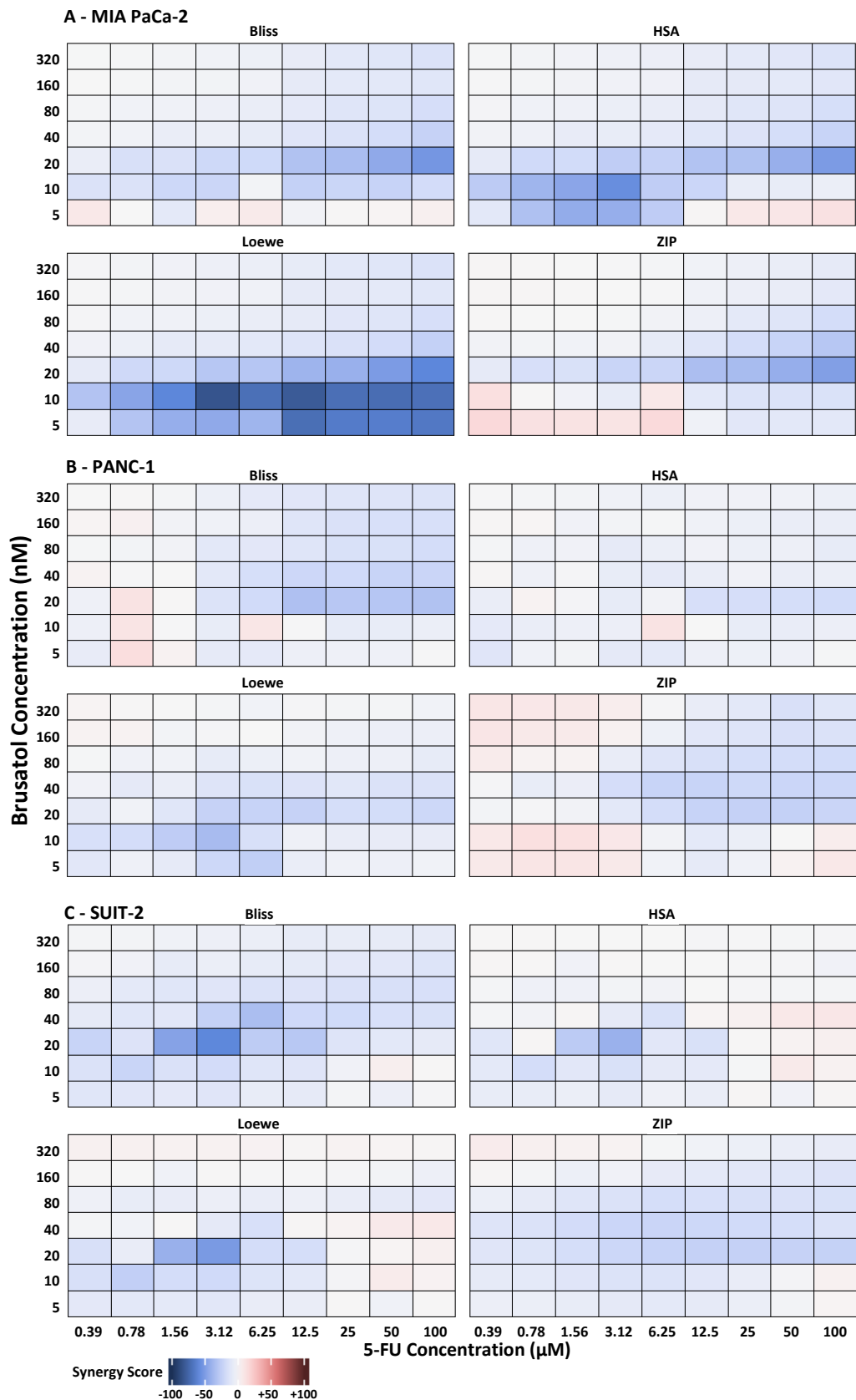


Figure 5-3: Synergy analysis of MIA PaCa-2 (A), PANC-1 (B) and SUIT-2 (C) cells treated with 5-FU and brusatol, visualised using Bliss, HSA, Loewe and ZIP models of synergy. Images represent one preliminary experiment. Abbreviations: HSA, Highest Single Agent. ZIP, Zero Interaction Potency.

5.2.4 Brusatol pretreatment sensitises PDAC cell lines to chemotherapy

Despite not appearing to synergise with gemcitabine or 5-FU consistently strongly during co-treatment, stronger synergistic effects were seen when treating with brusatol prior to treating with gemcitabine or 5-FU (Figs. 5-4, 5-5). This was particularly the case when 5-FU treatment followed brusatol pretreatment (Fig. 5-5). This suggests that although brusatol may not be immediately synergistic as a simultaneous combination therapy with gemcitabine or 5-FU, brusatol may be a useful chemosensitiser to be used prior to conventional chemotherapy. Different models of synergy gave broadly similar results, with one notable exception (Fig. 5-3 B) in which Loewe additivity reported antagonism between gemcitabine and low concentrations of brusatol whereas other models reported mild synergy.

5.2.4.1 Brusatol pretreatment sensitises PDAC cell lines to gemcitabine

The effect of brusatol pretreatment upon MIA PaCa-2 cells subsequently treated with gemcitabine was largely additive (Fig. 5-4 A), with areas of synergy or antagonism. Specifically, low concentrations of brusatol with high concentrations of gemcitabine appeared synergistic, whereas low concentrations of brusatol with low concentrations of gemcitabine appeared antagonistic.

Bliss, HSA and ZIP each reported synergy between brusatol pretreatment and subsequent gemcitabine treatment of PANC-1 cells, particularly following low doses of brusatol pretreatment (Fig. 5-4 B). However, the Loewe additivity model of the same results reported notable antagonism when treating PANC-1 cells with low concentrations of brusatol.

Brusatol pretreatment appeared to enhance the efficacy of subsequent gemcitabine treatment upon SUIT-2 cells at high concentrations of either drug with low-intermediate concentration of the other, however a high concentration of both resulted in very mild antagonism (Fig. 5-4 C).

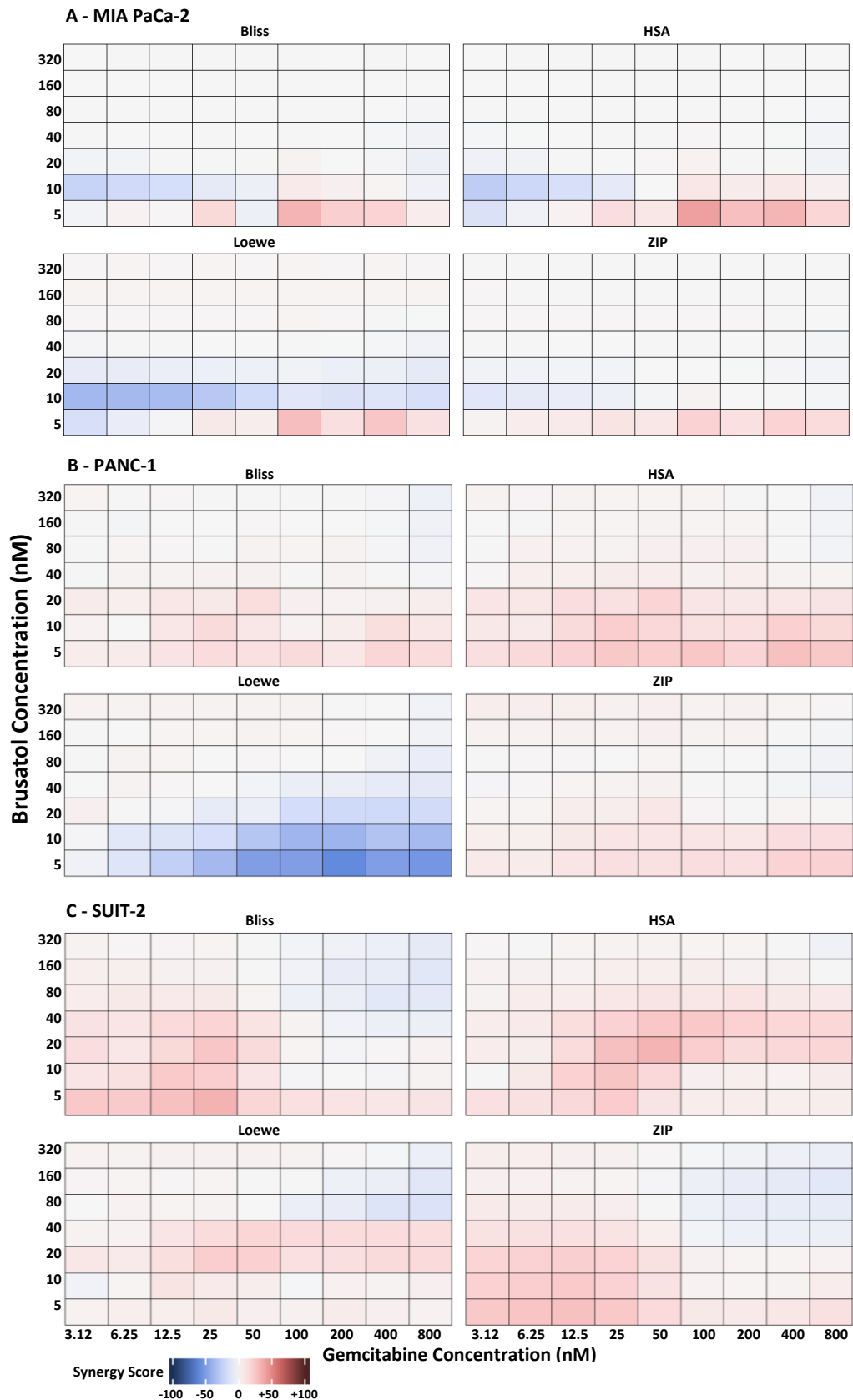


Figure 5-4: Synergy analysis of MIA PaCa-2 (A), PANC-1 (B) and SUIT-2 (C) cells treated with gemcitabine following 24h brusatol pretreatment, visualised using Bliss, HSA, Loewe and ZIP models of synergy. Representative images of three independent experiments. Abbreviations: HSA, Highest Single Agent. ZIP, Zero Interaction Potency.

5.2.4.2 Brusatol pretreatment sensitises PDAC cell lines to 5-FU

Low doses of brusatol followed by 5-FU treatment were seen to synergistically inhibit the viability of MIA PaCa-2 cells (Fig. 5-5 A). Higher concentrations of brusatol produced an additive result, with no evidence of antagonism. High concentrations of brusatol appeared to act antagonistically with high concentrations of 5-FU upon PANC-1 cells (Fig. 5-5 B). Lower-intermediate concentrations acted synergistically however, with additive responses seen at various other combinations.

Brusatol pretreatment appeared broadly, though mildly, synergistic with subsequent 5-FU treatment upon SUI-2 cells (Fig. 5-5 C). However, antagonism was seen at high concentrations of each drug when analysed using Bliss and ZIP models, although HSA and Loewe reported mild synergism or additivity. This suggests that the combination of drugs did not produce an effect through acting independently of one another, however this did not prevent the overall effect upon viability to be increased.

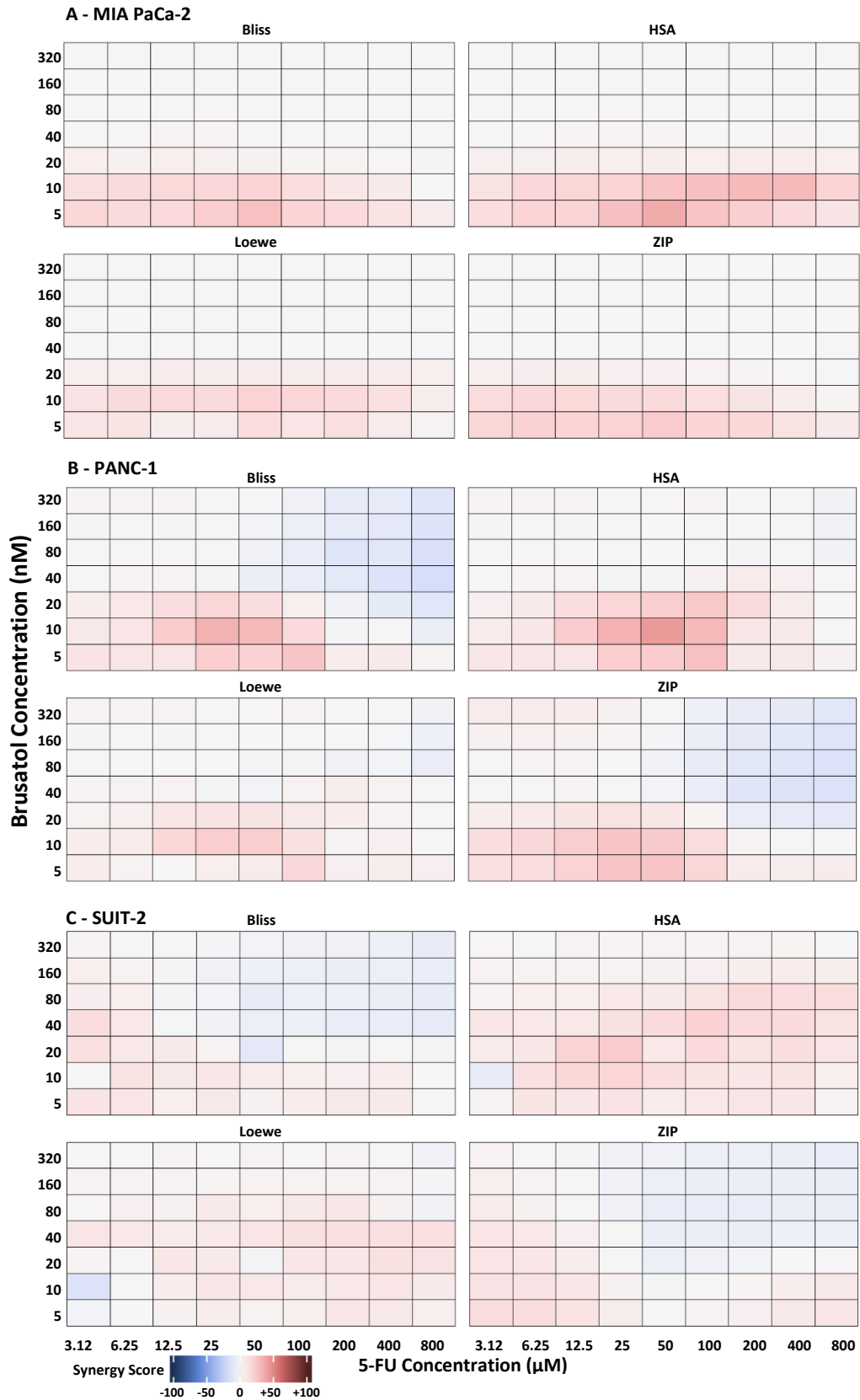


Figure 5-5: Synergy analysis of MIA PaCa-2 (A), PANC-1 (B) and SUIT-2 (C) cells treated with 5-FU following 24h brusatol pretreatment, visualised using Bliss, HSA, Loewe and ZIP models of synergy. Representative images of three (MIA PaCa-2, SUIT-2)/two (PANC-1) independent experiments. Abbreviations: HSA, Highest Single Agent. ZIP, Zero Interaction Potency.

5.2.5 Brusatol, gemcitabine and 5-FU each inhibited the colony forming capabilities of pancreatic cancer cells under certain conditions

Two different forms of clonogenic assay (194) were utilised to investigate different effects of gemcitabine, 5-FU and brusatol upon the ability of pancreatic cancer cells in culture to establish colonies. Preseeding treatment investigated the ability of cells to form colonies after having been treated with chemotherapy for 24h before being replated for clonogenic assay, to determine the mid to long-term effects of chemotherapy upon cells, i.e. to determine potentially lethal- and sublethal damage repair. Post-seeding treatment investigated the ability of cells to form colonies whilst in the presence of chemotherapy, to determine the effects of active drug treatment upon a process occurring at the point of chemotherapy exposure. The different forms of clonogenic assay exhibited different results (Fig. 5-6).

5.2.5.1 Pretreatment of pancreatic cancer cells with brusatol or 5-FU impaired subsequent colony formation

The effect of 5-FU applied prior to clonogenic seeding of cells showed a pronounced inhibition of colony formation which was not observed to the same extent following gemcitabine treatment (Fig. 5-6). This inhibition primarily appeared to inhibit the size of colonies, although a reduced number was also present. Brusatol also appeared to inhibit the growth of colonies relative to vehicle-only or gemcitabine treated cells. This was predominantly to a lesser extent than that of 5-FU, however brusatol appeared to exert a greater inhibitory effect than 5-FU on MIA PaCa-2 cells.

5.2.5.2 Post-clonogenic seeding treatment of pancreatic cancer cells in culture with brusatol, 5-FU or gemcitabine impaired subsequent colony formation

Treatment with gemcitabine and 5-FU shortly after clonogenic seeding resulted in almost complete inhibition of colony formation of each cell line analysed. Although brusatol treatment also resulted in a pronounced inhibitory effect, a small number of colonies was still present in most wells (Fig. 5-6).

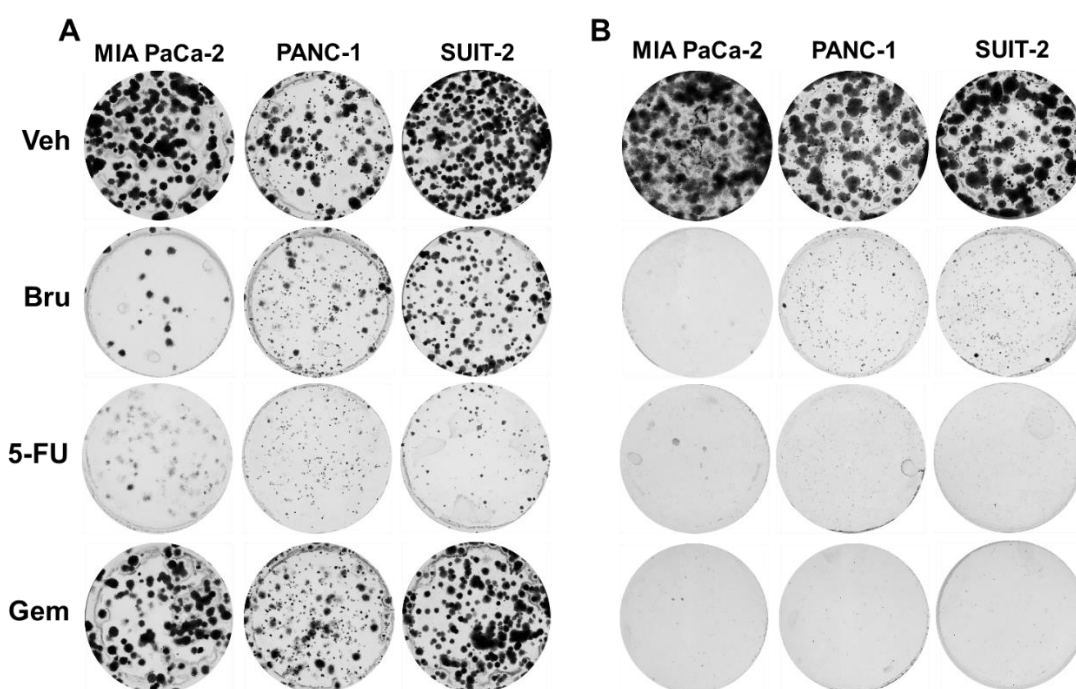


Figure 5-6: Clonogenic assay of MIA PaCa-2, PANC-1 and SUIT-2 cells treated with brusatol, 5-FU, gemcitabine or vehicle (H₂O). A: Cells were treated for 24h prior to replating for clonogenic seeding. B: Cells were treated following clonogenic seeding until analysis. Representative images from three independent experiments, each performed in triplicate.

The colonies derived from cells treated with gemcitabine, 5-FU, brusatol and vehicle (H₂O, DMSO) prior to clonogenic seeding (Fig. 5-6 A) were counted using Colony Counter plugin for ImageJ. The colonies derived from cells exposed to chemotherapy following seeding (Fig. 5-6 B) were not analysed using automatic quantification due to the lack of detectable colonies in the majority of wells. The number and size of each colony was recorded and used to

calculate average colony size and the total coverage of colonies per well. (Fig. 5-7). It was confirmed that the number of colonies was reduced and the size of each colony was reduced following treatment with 5-FU. This was significant in all cell lines except the number of colonies of MIA PaCa-2, which showed a noticeable non-significant decrease in colony numbers in response to 5-FU treatment.

Neither brusatol nor gemcitabine were seen to significantly affect the number or size of colonies, with the exception of a significant decrease in the size of SUIT-2 colonies following gemcitabine treatment. However, brusatol treatment consistently resulted in a non-significant decrease in colony size and number in each cell line. Similarly, gemcitabine treatment typically resulted in a non-significant decrease in colony size and number (particularly of SUIT-2 cells, in which a significant effect of gemcitabine was found upon colony size), however this effect did not appear to be present upon MIA PaCa-2 cells.

5.2.5.3 Brusatol, gemcitabine and 5-FU inhibited total colony growth depending upon cell line

The combined effect of drugs upon the number and size of colonies was therefore analysed by comparing the total coverage of colonies between the different drug treatments. This allowed for a milder effect upon both sets of observations (number and size of colonies) to be more readily detectable than by analysing them separately, whilst still contributing to the same conclusion regarding the effect of the drugs upon colony viability. In each cell line, total coverage of the well by colonies was most strongly affected by 5-FU, with a greater effect observed than upon number or size of colonies individually. Additionally, both gemcitabine and brusatol were found to significantly result in decreased growth of SUIT-2 colonies across the well. Brusatol was found to significantly limit the total coverage of PANC-1 colonies, with a non-significant reduction observed following gemcitabine treatment upon PANC-1 and following brusatol and gemcitabine treatments upon MIA PaCa-2.

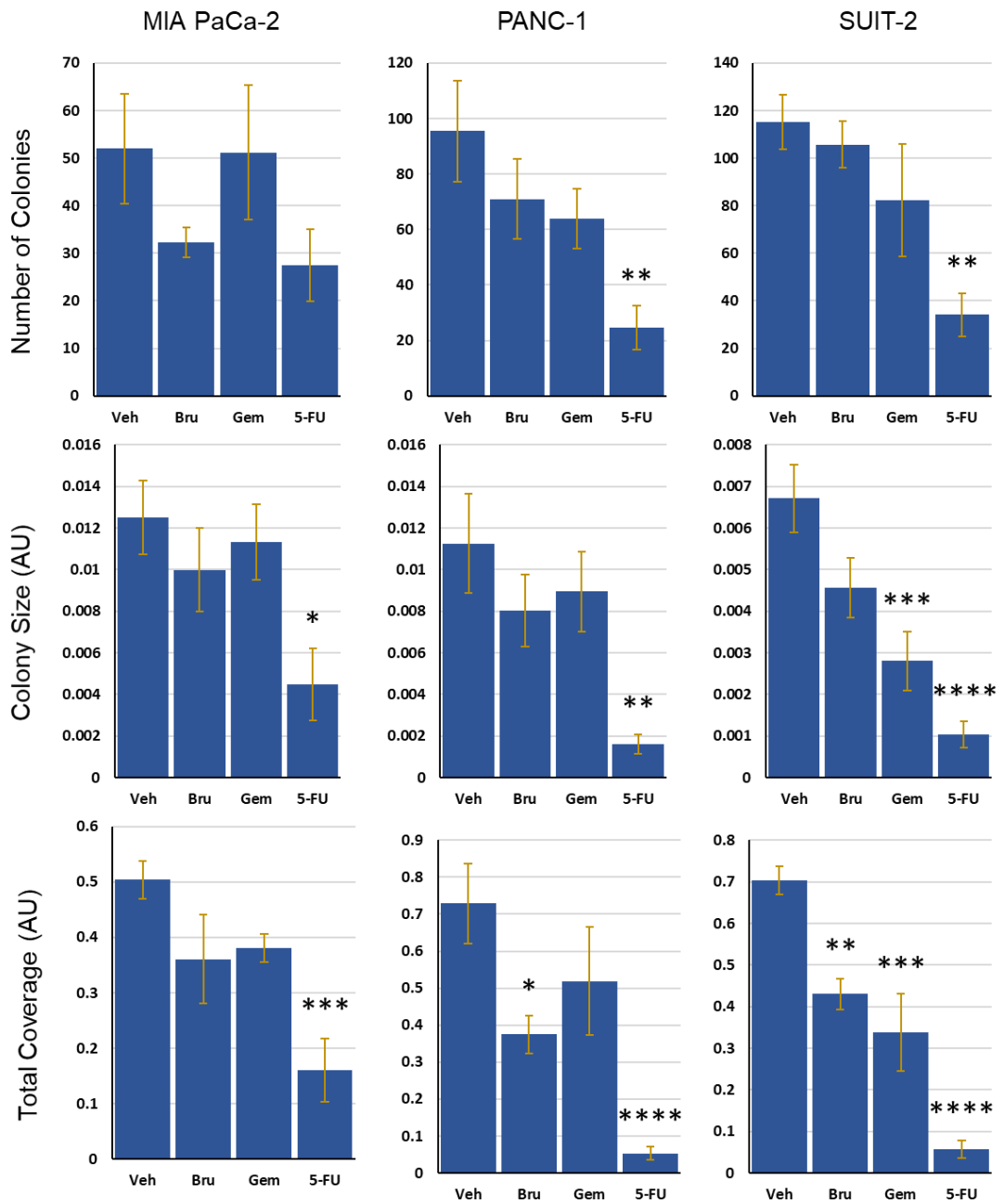


Figure 5-7: Quantification of clonogenic assay of MIA PaCa-2, PANC-1 and SUIT-2 cells treated with brusatol, 5-FU, gemcitabine or vehicle (DMSO, H₂O). Cells were treated for 24h prior to replating for clonogenic seeding. Data represents the mean of 3 experiments each performed in triplicate, +/- SEM. Statistical analysis was performed using Dunnett's multiple comparisons test of a one-way ANOVA for each analysis. *= $p < 0.05$; **= $p = 0.01$; ***= $p < 0.001$; ****= $p < 0.0001$ relative to vehicle control. Abbreviations: Veh, vehicle; Bru, brusatol; Gem, gemcitabine.

5.2.6 Brusatol, but not gemcitabine or 5-FU alone, inhibits the motility of pancreatic cancer cells

It has previously been suggested that brusatol inhibits EMT through the downregulation of Twist and vimentin, and the upregulation of E-cadherin (157). Inhibition of EMT may suggest that brusatol may prevent metastasis from occurring in addition to its other observed anti-cancer effects (167). To investigate this possibility, the effect of brusatol and conventional chemotherapy (gemcitabine and 5-FU) upon cell motility was measured using a wound-healing assay.

The results of the wound healing assay showed that brusatol appeared to prevent migration of MIA PaCa-2 and PANC-1 cells almost entirely (Fig. 5-8). It appeared that 5-FU may have had some effect relative to vehicle-treated, however the inhibition of motility was not as pronounced as that of brusatol. Gemcitabine did not appear to exert a noticeable effect. The effect of brusatol persisted when used in combination with either gemcitabine or 5-FU.

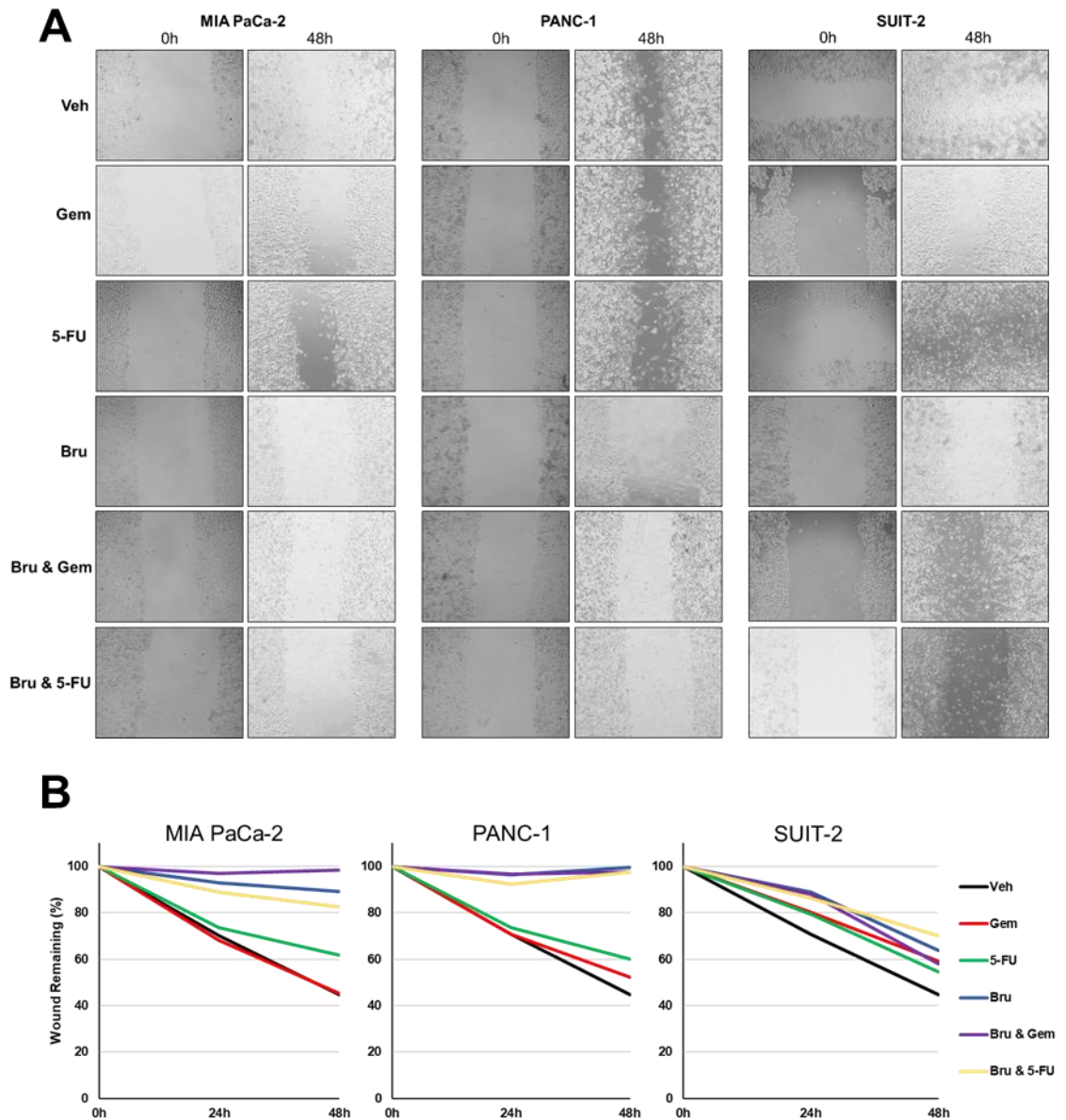


Figure 5-8. Wound healing assay of MIA PaCa-2, PANC-1 and SUIT-2 cells treated with combinations of gemcitabine, 5-FU and brusatol. A: Representative images of monolayer wounds of three independent experiment at the time of treatment (0h) and 48h following treatment for each cell line and drug combination. B: Quantification of mean cell migration of three independent experiments at 24h and 48h, normalised to 0h (100% wound size). Abbreviations: Veh, Vehicle (H₂O). Gem, Gemcitabine. Bru, Brusatol.

Brusatol appeared to result in a larger degree of cell damage than gemcitabine and 5-FU during the course of imaging. A larger amount of debris was present following brusatol treatment which was not evidenced to as great an extent following other treatments,

although there was still a large number of seemingly viable cells. To reduce the possibility that reduced cell number could directly affect the results of migration assay, the measurement of wound size was calibrated so that a wall of cells would be detected as the border of the wound even if there were gaps between them. It may be that the effect of brusatol on the remaining live cells was to inhibit motility by resulting in the observed cell damage rather than a direct effect on migratory machinery.

5.2.7 Continuous brusatol treatment from an early timepoint in KPC GEMM tumour development did not improve prognosis

KPC mice of a mixed background (C57BL6/129J) were divided into three treatment arms. Mice in each arm received a single form of treatment (brusatol, gemcitabine, or DPBS vehicle control).

Treatment started at 9 weeks of age, shortly before most mice were expected to have developed tumours (10 weeks). This timepoint was to maximise the likelihood that they exhibited, or would soon exhibit, early tumours at the point of initial intervention rather than advanced tumours or precursor lesions only. This was intended to reduce the opportunity for brusatol to act upon precursor lesions such as PanINs so minimised the possibility that any observed effects were the result of brusatol acting as a chemopreventative agent rather than a chemotherapeutic agent. A later time point at which all mice could confidently be expected to possess tumours was not chosen due to the rapid nature of PDAC progression and the nature of this study as an early intervention analysis. However, the maximum lifespan, and range of lifespans, of KPC animals during this study was unexpectedly large so it is likely that most animals did not possess tumours at the time of intervention. The unexpected survival time prompted us to confirm that the animals were actually KPC animals. The four longest survivors were selected for the purposes of validation, as they were considered to be the

most likely to have been incorrectly genotyped as KPC. Genotyping by Transnetyx confirmed that the mice were heterozygous for LSL-KrasG12D, LSL-Trp53R172H, and Pdx-1-Cre, and therefore were KPC mice.

KPC mice treated with gemcitabine (Fig. 5-9) showed the best survival time, although any difference in survival between gemcitabine- and vehicle-treated mice did not reach statistical significance. This is consistent with previous research comparing gemcitabine-treated and vehicle-treated KPC mice (195-197).

Brusatol treatment was not associated with a change in survival time from either gemcitabine or vehicle. Unlike survival time following gemcitabine-treatment, there was no indication of a non-significant trend away from vehicle-treated.

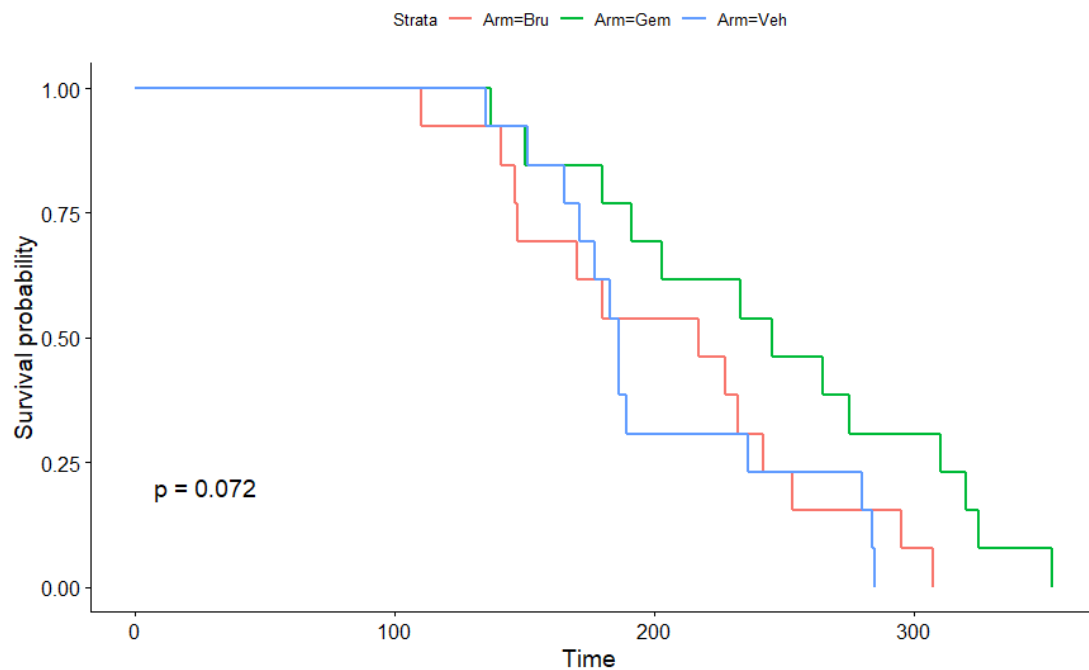


Figure 5-9: Kaplan-Meier analysis of the absolute survival time of brusatol, vehicle and gemcitabine treated KPC mice. No individual arm reached statistical significance (gemcitabine v vehicle $p=0.057$, brusatol v vehicle $p=0.63$).

5.2.8 Long term treatment of brusatol or gemcitabine did not appear to affect NQO1 abundance in KPC tumours

The abundance of NQO1 was measured in tumours using IHC to investigate if treatment affected NQO1, with a particular focus on determining if brusatol inhibited NQO1 in tumours. NQO1 was detected in all samples analysed, particularly in ductal cells whereas staining was typically mild or undetectable in stromal tissue (Fig. 5-10). NQO1 was still detectable following treatment with brusatol, and in one instance all of the tissue within the tumour exhibited intense staining for NQO1 (Fig. 5-10).

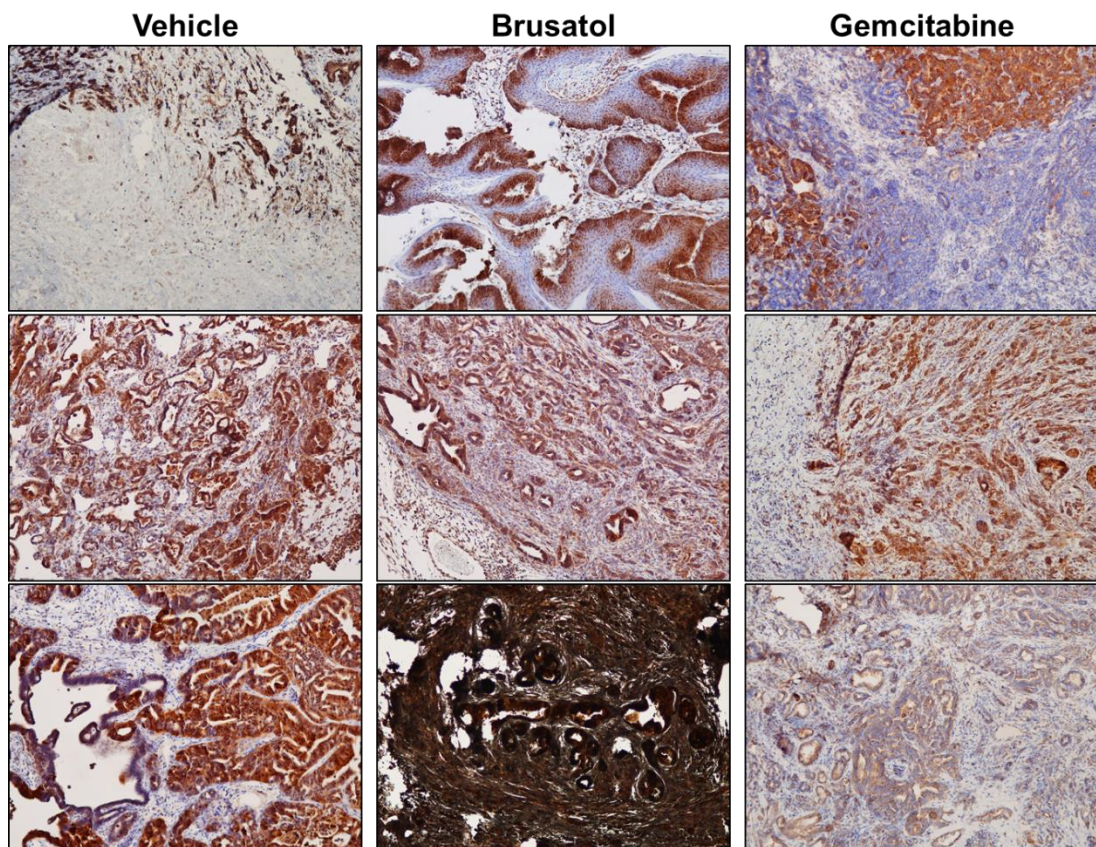


Figure 5-10: IHC of NQO1 in dissected tumours of KPC mice treated with vehicle (DPBS, 4% DMSO v/v), brusatol or gemcitabine. Images of tumours from three separate mice per treatment arm are shown.

5.3 Discussion

Previous research has shown that brusatol is a promising anti-cancer therapy which is well tolerated during *in vivo* experiments (112, 151, 157, 176, 191). Due to the lack of particularly effective chemotherapy for the treatment of PDAC, brusatol may be worthy of consideration for subsequent trials to determine its efficacy compared against and in combination with chemotherapy *in vivo*.

5.3.1 Synergy analysis identified brusatol as a chemosensitiser in pancreatic cancer

Synergy analysis determined that 24h pretreatment with brusatol synergised with subsequent gemcitabine and 5-FU treatment (Figs. 5-3, 5-4), suggesting that brusatol may be a useful form of chemotherapy as a chemosensitiser. This is despite the fact that cotreatment with brusatol and gemcitabine or 5-FU resulted in a largely antagonistic effect (Figs. 5-1, 5-2)

A modified synergy assay was used during the course of this work to measure the effect of pretreatment with brusatol, therefore measuring its efficacy as a chemosensitiser as well as an inhibitory agent in its own right. Although brusatol was seen to only mildly synergise with and often act antagonistically with gemcitabine and 5-FU when treated simultaneously, brusatol pretreatment most commonly appeared synergistic with relatively few combinations resulting in (mostly mild) antagonism. These findings suggest that brusatol may therefore be a useful chemosensitiser to be used in combination with other forms of chemotherapy, rather than either a standalone chemotherapy or as part of a simultaneous cotreatment regimen.

The applicability of synergy analyses *in vitro* to clinical and *in vivo* usage depends upon multiple factors. The dosage at which a treatment is used often depends upon how well it is tolerated by the patient, rather than its maximal effect upon the tumour. Methods to increase the effect of medication may therefore appear promising but not necessarily usable

in situations where the maximal effect of a drug is not the limiting factor of treatment. Whilst two drugs may work synergistically, if the healthy tissue toxicity of both drugs overlaps (and if the synergy is present in healthy tissues as well as cancerous tissue these toxic side-effects may be amplified) it may not be feasible to utilise them in combination therapies. Conversely, even if two drugs appear to function antagonistically, if they do not contribute to the same healthy tissue toxicity this may allow them to be used in combination at the highest concentrations that each would be used individually. This could allow a higher response than otherwise possible by using a single drug monotherapy. Further work will be required to identify if this is the case for the synergy observed between brusatol pretreatment and subsequent 5-FU and gemcitabine treatment.

5.3.2 Brusatol inhibited colony formation efficiency of pancreatic cancer cell lines

Gemcitabine, 5-FU and brusatol are well characterised as being toxic agents. As such their ability to inhibit colony formation is to be expected, particularly when applied following clonogenic seeding to a small number of cells, as was observed in Fig. 5-6 B. The great effect seen by 5-FU compared with little apparent effect of gemcitabine may suggest that 5-FU exerts longer term effects upon cells which would render them less capable of forming colonies. This effect may either be to render viable cells incapable of colony formation (such as through targeting replication), however it may also be the case that 5-FU resulted in slower cell death which resulted in a greater proportion of non-viable cells being seeded.

The effect of drug treatment following clonogenic seeding does not appear to be entirely attributable to conventional toxicity. Whereas these drugs prevented colony formation almost entirely, MTT assay and microscopy confirms that they would not typically render the whole population of cells unviable. It may therefore be that the effect of brusatol and particularly 5-FU upon pancreatic cancer cells was to render them less capable of long-term survival and proliferation despite surviving the initial exposure.

5.3.3 Brusatol inhibited motility of pancreatic cancer cell lines

Brusatol was seen to prevent pancreatic cancer cell lines from migrating (Fig. 5-8), except for SUIT-2 cells which appeared unaffected by it. This was in contrast to gemcitabine and 5-FU which did not appear to have any noticeable effect. As discussed in Section 5.3.1, brusatol pretreatment synergised with subsequent chemotherapy treatment to inhibit cell viability. The wound healing assay data showing that brusatol inhibited the motility of pancreatic cancer cells may suggest another mechanism by which brusatol may have clinical usefulness in combination with other forms of chemotherapy. Although inhibition of cell viability may target tumour cell survival directly, a drug which could reduce their ability to metastasise could be of therapeutic benefit regardless of its effects upon viability. However, although this preliminary data was promising, a wound healing assay does not accurately reflect cells ability to migrate *in vivo*. Further work would be required to investigate the effect of brusatol more fully upon metastatic ability of pancreatic cancer cells.

5.3.4 Early intervention brusatol monotherapy did not improve prognosis in KPC GEMM of PDAC

The KPC mouse model of pancreatic cancer faithfully recapitulates the human form of the disease (88). As such it is a highly useful tool for studying PDAC biology and therapies. However, it must be noted that the treatment plan performed during the course of this research, which involved twice weekly treatments until endpoint, differs from one that would be used clinically. The treatment plan used during the course of this work was designed for the purpose of investigating if brusatol would exert an effect at any timepoint, from early intervention onwards.

The numbers of animals used during this pilot study were decided based upon previous literature which suggested a more consistent prognosis for KPC mice. The larger degree of variation than expected may have contributed to the lack of a significant finding of survival

time of gemcitabine treated mice despite a trend towards improved survivability among the gemcitabine treated cohort. Despite the lack of a significant improvement in survivability of gemcitabine-treated KPC mice relative to vehicle treated, the effect of gemcitabine appeared more pronounced during this course of work than in many previous studies (195-197). This may be due to the longer period of treatment due to early intervention, the regular treatment until endpoint and the longer lifespan of the KPC mice during this study compared to others.

Brusatol has not previously been used extensively *in vivo* so limited data is available regarding its toxicity and side effects, especially for frequent long-term administration as in this study. Because of this, a more conservative concentration of brusatol (2mg/kg) was used in the treatment of KPC mice during this work. This concentration has been seen to be effective in the treatment of orthotopic xenografts of PDAC cell lines. The effect of daily 1mg/kg and 2mg/kg brusatol injections upon xenografts of PANC-1 and Capan-2 cell lines in mice, either with or without gemcitabine or 5-FU, was investigated, and it was found that brusatol of either concentration delayed tumour growth (157). Although a higher concentration (4mg/kg) was considered and has been used successfully previously (176), it was only used in relatively short studies. It was important not to use too high a dose for multiple reasons. If extended treatment resulted in toxic effects to the mice, this would have severe scientific and ethical consequences. However, this course of work has shown that the concentration of brusatol used can be given frequently for many months without any signs of side effects, suggesting that a higher dose may be feasible which may have a more pronounced effect on tumours.

Another potential explanation for the lack of effectiveness of brusatol may relate to the tumour microenvironment. PDAC is characterised by a dense desmoplastic stroma which may have prevented brusatol from reaching cancerous cells in the tumour. Further work may

investigate the tumour samples obtained during the course of this work to determine if brusatol had reached the tumour, however this was not possible during this study due to time constraints. If brusatol is found not to have reached the tumour, further work improving the delivery of brusatol may be a promising avenue of research. Brusatol was seen to sensitise cells to gemcitabine and 5-FU *in vitro* (Figs. 5-4, 5-5), suggesting that it may be a useful chemosensitiser *in vivo*. Combination therapies were considered for the course of this work, however this was not feasible due to the low numbers of KPC animals available. The data regarding the safety of brusatol obtained by this work may be an important foundation for any further studies investigating brusatol combinations.

5.3.5 Brusatol did not appear to affect NQO1 abundance in KPC tumours

Brusatol did not appear to inhibit NQO1 expression in KPC tumour tissue, particularly as the highest NQO1 expression detected was in the tumour of a mouse treated with brusatol (Fig. 5-8). *In vitro* work demonstrated that brusatol potently inhibited protein synthesis (Chapter 4, Section 4.2.1), so it appears unlikely that the accumulation of NQO1 (or any other protein) would be directly attributable to brusatol. Similarly, the absence of a consistent effect upon NQO1 abundance among the tumours of mice treated with brusatol would seem to suggest the response was not a direct result of brusatol treatment. Instead, it may be that brusatol did not have a detectable effect upon NQO1 abundance in tumour tissue and the abundance of NQO1 instead reflects either random variation. This is consistent with previous unpublished work within this group upon human tumour samples, which demonstrated varying intensities of NQO1 staining in tumour and stromal cells ((142), Fig. 5.13).

5.3.6 Future work

Further work may expand upon these findings to determine if more clinically relevant treatment plans involving brusatol (such as treatment at a later stage, less frequent treatment or in response to tumours of a certain size) can affect duration of survival. Future

work may use higher concentrations of brusatol and/or brusatol in combination with other forms of therapy.

5.2.3.7 Overview

The findings of this work suggest that brusatol is a promising chemotherapeutic agent for multiple reasons. It potently inhibits cell viability, sensitises cells in culture to subsequent 5-FU and gemcitabine treatment, and inhibits cell motility more than conventional chemotherapies (gemcitabine and 5-FU). However, these effects did not appear to improve the prognosis for KPC mice treated with brusatol. This result may not be due to the potential biological efficacy of brusatol upon cancer cells, and may instead reflect a low dosage of brusatol reaching the tumour (either due to a higher concentration of brusatol during treatment required in order to be effective, or the tumour stroma acting as a physical boundary). Further work may therefore try to remove these issues, and/or use brusatol in combination with gemcitabine/5-FU as a chemosensitiser.

6 – Discussion

6.1 Overview

The survivability of most common cancers has increased noticeably and steadily over time (11). However, the prognosis for pancreatic cancer patients has seen only minimal improvement and remains particularly dismal. Despite this the incidence of pancreatic cancer is rising, and it is soon expected to become the second leading cause of cancer related deaths (33). It is therefore vitally important to improve the understanding of this disease and provide a foundation for new therapies and/or methods of earlier diagnosis.

The primary objective of this work was to investigate if brusatol could be used as a chemotherapeutic agent, particularly through its previously discussed (Chapter 1, Section 1.7.2.2) inhibition of Nrf2 (151, 152). Understanding if brusatol could modulate Nrf2 for the treatment of PDAC required further investigation of the role of Nrf2 in PDAC and the effects its modulation might have, and how specific an Nrf2-inhibitor brusatol is (in addition to its overall efficacy as chemotherapy). The project was therefore split into the three main aims detailed in previous chapters. These aims were to investigate the role of Nrf2 in pancreatic cancer (Chapter 3), explore the relationship between Nrf2 and brusatol (Chapter 4), and analyse the efficacy of brusatol as a form of chemotherapy (Chapter 5). Together, the completion of these aims has cast light on the role of Nrf2 in response of pancreatic cancer to chemotherapy and shown how brusatol affects Nrf2 in the context of pancreatic cancer.

In brief, the findings of this work suggested that acquired chemoresistance of PDAC in response to chemotherapy was not attributable to Nrf2 induction (Chapter 3). Although brusatol strongly inhibits Nrf2 (Chapter 4, section 4.2.1), it does not do so specifically and there are considerable off-target effects which contribute to the anti-cancer properties exhibited by brusatol (Chapter 4, section 4.2). It was found that brusatol exhibited multiple promising potential anti-cancer mechanisms *in vivo*; these included acting as a chemosensitiser for subsequent gemcitabine/5-FU therapy (Chapter 5, Section 5.2.4),

inhibiting the colony forming capacity of pancreatic cancer cells (Chapter 5, Section 5.2.5) and strongly inhibiting the motility of pancreatic cancer cells (Chapter 5, Section 5.2.6). However, I did not find any evidence that brusatol treatment, at the concentrations used was effective against pancreatic cancer *in vivo* (Chapter 5, Section 5.2.7). This does not rule out the possibility that different brusatol-based regimens may have a beneficial effect. It may also be possible that different forms of cancer would respond otherwise to the treatment regimen described here. Our findings may therefore provide a foundation for future work involving brusatol therapy.

6.2 Nrf2 in Pancreatic Cancer

The role of Nrf2 and its downstream targets in cancer has previously been difficult to elucidate. Nrf2 has been described as both a tumour suppressor and an oncogene due to its role in preventing damage to cells, which could prevent carcinogenesis of a healthy cell but also protect cancerous cells from cellular stress, including chemotherapy (106, 114, 180). The balance of these effects must be considered when describing the role of Nrf2 in cancer, however in the context of an already existing cancer Nrf2 can typically be thought of as cancer-promoting (106, 180, 198).

Previous research has made a compelling case for the involvement of Nrf2 in cancer and the response to chemotherapy (99, 102, 109, 112, 113, 115-117, 130, 132, 134, 186, 199), suggesting that Nrf2 and downstream targets may be useful as biomarkers to predict response to treatment or that modulation of the Nrf2 pathway may improve treatment response. The fact that Nrf2 contributes to chemoresistance of various types of cancer, including pancreatic cancer, is well established (99, 102, 113, 117, 130, 186). For instance, Nrf2 has been found to be overexpressed in pancreatic cancer due to a lack of inhibitor Keap1, and that inhibition of Nrf2 renders cells vulnerable to chemotherapy (113). As such,

inhibition of Nrf2 through pharmaceutical methods is an attractive prospect for the treatment of PDAC. However, the work undertaken here has suggested that the Nrf2 pathway and its involvement in PDAC is more complicated than anticipated.

It had been expected that Nrf2 would be induced by chemotherapy, but this was not uniformly the case (Chapter 3), and Nrf2 downregulation was observed. Nrf2 and its downstream targets were not found here to contribute to acquired chemoresistance. This is in contrast to the contribution of Nrf2 to innate chemoresistance reported for various cancers including PDAC (99, 102, 117, 132, 134, 172). Modulation of Nrf2 to reduce the innate chemoresistance of PDAC therefore remains a promising avenue of research, however a method to inhibit Nrf2 reliably and specifically has not yet been widely validated. The two Nrf2 inhibitors investigated during the course of this work were brusatol and ML385 (Chapter 4). As discussed, brusatol strongly inhibited Nrf2 but appeared to do so through inhibition of protein synthesis and therefore the synthesis of other proteins. Conversely, there was no conclusive evidence that ML385 inhibited Nrf2 significantly under the conditions of this work (Chapter 4, Section 4.2.4).

6.2.1 NQO1 in Pancreatic Cancer

Surgical resection is currently the only potential curative option for PDAC, yet PDAC disease is usually too advanced at the time of diagnosis for the patient to be eligible for surgical resection of the tumour (23). As such, the discovery of new biomarkers to help predict PDAC development may make it possible to detect PDAC earlier and improve patient prognosis. Similarly, the identification of biomarkers which can predict response to treatment may make it possible to improve patient prognosis by identifying the most effective form of therapy. As Nrf2 is known to contribute to PDAC response to therapy (113), it was hypothesised that the deactivating SNP of NQO1 (rs1800566), one of the downstream targets of Nrf2, may be useful for either earlier detection or the response to treatment. However, it was found that the loss-

of-function NQO1 SNP rs1800566 was not associated with an increased risk of PDAC. Neither did it affect patient prognosis (Chapter 3, Section 3.2.13). This appears to be contrary to the hypothesis that NQO1 would be protective against carcinogenesis, as well as that it would protect tumours from chemotherapy. Previous research has shown that the TT genotype of NQO1 rs1800566 was associated with poorer outcome following chemotherapy in breast cancer patients (200). It has also been found non-small-cell lung carcinoma (NSCLC) patients exhibiting the TT genotype have a poorer response to chemotherapy (201). Additionally, a greater proportion of individuals exhibiting the TT genotype was present compared to controls. This suggests that the TT genotype promotes the risk of developing NSCLC (201). However, it has also been observed that the TT genotype was associated with a decreased (31%) risk of developing oesophageal cancer (147). The role of NQO1 rs1800566 appears to vary between different forms of cancer, and therefore the absence of a significant finding between NQO1 SNP status and PDAC prognosis during the course of this work is not necessarily surprising.

NQO1 protein levels appeared to be downregulated by chemotherapy (gemcitabine and 5-FU) *in vitro* and *in vivo*, as shown in Chapter 3. This suggests that NQO1 does not contribute to acquired chemoresistance of PDAC, however NQO1 has been seen to be overexpressed in PDAC tissue (202). This suggests that NQO1 may contribute to innate chemoresistance despite not being induced by chemotherapy. NQO1 appeared highly variable in pancreatic tumour tissue (Chapter 5, Section 5.2.8), consistent with findings in human PDAC (142)

6.3 Brusatol

6.3.1 Mechanism of Action and Nrf2

While this work was ongoing, papers emerged indicating that brusatol does not inhibit Nrf2 as specifically it was once thought to do. Published literature (159, 163, 164) and the results of this research, described in Chapter 4, show that brusatol is an inhibitor of protein synthesis

and that Nrf2 depletion appears to be a downstream effect of this. However, its effects still appear to be selective to Nrf2, and brusatol continues to be widely used as an Nrf2 inhibitor (112, 153-155, 162). Brusatol has also been demonstrated to be an effective anti-cancer agent, including in pancreatic cancer cell xenografts (101, 112, 151, 152, 154, 157, 159, 162). Additionally, attempts to identify an alternative Nrf2 inhibitor have been met with limited success. ML385, another widely used inhibitor of Nrf2, did not appear to substantially inhibit Nrf2 activity under the conditions of this project (Chapter 4, Section 4.2.4). Previous published research has shown that ML385 inhibits Nrf2 activity through binding to Neh1 of the Nrf2 protein and preventing Nrf2 from binding to DNA sequences (166). Although our findings did not demonstrate a significant effect of ML385, there was a trend towards lower Nrf2 activity in cells treated with both CDDO-Me and ML385 compared to those treated with CDDO-Me alone (Chapter 4, Section 4.2.4). Despite this, the lack of inhibition below basal activity and the non-significant inhibition of CDDO-Me activated Nrf2 meant that ML385 was not suitable for our purposes.

6.3.2 Efficacy of brusatol as chemotherapy

The anti-cancer properties exhibited by brusatol have been investigated during the course of this work. In particular, the effects of brusatol on cell viability, on models of migration, and its efficacy in an *in vivo* GEMM of PDAC (KPC). Brusatol was seen to potently inhibit cell viability, as well as cell migration and the ability to form colonies. Whilst these combined facts suggest that brusatol may have usefulness as an anti-metastatic therapy against cancer cell migration, these *in vitro* assays do not and are not intended to fully recapitulate metastatic disease. Instead, they analyse specific mechanisms of cancer motility and replicative viability post-chemotherapy treatment. These assays have shown that brusatol inhibits two mechanisms (motility and the ability to establish colonies *in vitro*) that may contribute to metastases, however there are many more factors that will influence

metastatic disease. My findings may therefore provide a foundation for further *in vivo* work, specifically investigating the effect of brusatol and metastasis.

6.3.2.1 Efficacy of brusatol as chemotherapy *in vivo*

Although brusatol appears to have a potent effect against cancer *in vitro*, this was not recapitulated in overall survival in a KPC mouse model. However, there were no signs of toxicity or side effects as a result of brusatol exposure despite the long-term treatment plan. It has therefore been demonstrated that frequent long term brusatol exposure of this dosage is not necessarily harmful to mice, which may be useful in future analysis.

By the nature of the experimental design as an early intervention analysis, mice were exposed to brusatol at the early stages of tumour development. However, tumours took longer to develop and did not follow the same predictable timespan as previously described (83, 203, 204). As such, it is likely that animals were treated earlier during tumour development than anticipated. It is possible that early therapy induced early chemoresistance resulting in decreased sensitivity to later doses, however this is in contrast to the fact that gemcitabine still appeared to exert some effect.

6.3.2.2 Brusatol toxicity *in vivo*

There are relatively few published studies investigating brusatol *in vivo*, and the majority of previously published work has investigated the use of brusatol in the short term (154, 162). However, the long-term nature of *in vivo* experiments performed during the course of this work required many treatments over several months. It was therefore decided that a moderate dose of brusatol (2mg/kg) would be used during each treatment to limit the risks of toxicity resulting from frequent high doses, although a higher dose may have exerted a stronger anti-cancer effect. This was for scientific as well as ethical reasons, as drug-induced toxicity would likely result in early withdrawal from the study and therefore prevent useful results being obtained. However, this research showed that brusatol did not appear to exert

any toxic effects at this dosage even when administered regularly over a long time period. It may therefore be possible to use a higher dose of brusatol without producing any toxic effects whilst potentially exerting a greater anti-cancer effect. It may also be possible to use this dosage (2mg/kg) of brusatol in combination therapies for the treatment of KPC mice, or in the treatment of other conditions.

6.3.2.3 Clinical Relevance

Brusatol did not appear to affect survival time of the KPC GEMM of pancreatic cancer (Chapter 5). However, the effect of a treatment upon a mouse model cannot be assumed to relate directly to clinical usage against human pancreatic cancer. The human disease is unpredictable and appears to be influenced by many factors, whereas the KPC model is highly predictable and all affected animals developed the disease due to the same initial genetic alterations. The heterogeneous nature of human pancreatic cancer may mean that patients would respond differently than KPC mice. Although the KPC GEMM faithfully recapitulates features of human pancreatic cancer and is one of the most reliable forms of model of human PDAC, the fundamental differences previously described contribute to variation between the behaviour and response to therapy of the human disease and the KPC GEMM. This is underlined by the fact that gemcitabine is typically not effective against KPC tumours (195-197), whereas gemcitabine treatment of human PDAC significantly improves prognosis (28).

Although GEMMs are currently among the most representative preclinical tools available for cancer research, it is also important to note that the differences between clinical treatment of PDAC and the treatment regimen utilised during this preclinical research means that the results of this research cannot immediately be directly related to PDAC patients. The purpose of this research was to analyse the activity of brusatol against pancreatic cancer throughout its progression, not as a fully representative preclinical trial targeted at a specific stage and under specific circumstances. By nature of being a GEMM, it was known in advance that KPC

mice would develop pancreatic tumours and were treated at an early timepoint (at which mice were predominantly expected to exhibit late pre-cancerous lesions or early stage primary tumours). Chemoprevention and early interventions are not currently viable options for pancreatic cancer patients due to the lack of known specific risk factors, as well as the commonly advanced stage of the disease at diagnosis. The effect of the treatment regimen performed during the course of this work may not mimic that of a patient exhibiting more advanced or metastatic disease at diagnosis, or the effect on PDAC post-resection. Further work may build upon these findings by performing a preclinical trial with treatment from an established point (such as tumour size measured by ultrasound) and/or incorporating combination arms in which brusatol is administered with other forms of chemotherapy. This could not be performed during the course of this work, partly due to practical constraint but also as these findings were required to understand the efficacy of brusatol to better plan how to use it in a clinically-relevant treatment regimen.

Brusatol may have the potential to treat other forms of cancer which may be more sensitive to its effects, however other cancers were not the focus of this work. Similarly, human pancreatic cancer cases are unpredictable as opposed to the highly predictable nature of KPC GEMMs. It may be that more specific analysis of brusatol against KPC tumours may yield more promising results.

6.3.2.4 Limitations

The use of cell culture has a number of inherent limitations. Cells taken from tissue and grown in culture undergo various changes which may limit their ability to represent tumour tissue (73). This is partly because the activity of cells *in vivo* is a product of interactions with other cells and physiological systems (77, 80, 205). This may be partly offset by the use of organoids, a form of 3D cell culture using multiple cell types intended to recapitulate basic biological structures (77, 80, 205). Although the use of organoids was considered during this

course of work, their use was prevented by financial and practical constraints. Organoid culture is a specialised technique requiring considerable time, money, and prior training. Instead, here cell culture assays were designed, focused upon responses relevant to individual cells rather than biological systems. *In vivo* models were used when a systems-wide analysis was particularly beneficial, such as the response of Nrf2 activity in an organism in response to chemotherapy, and the efficacy of brusatol against pancreatic tumours. These *in vivo* models were considered preferable to analysis of organoids for these purposes.

Although the KPC GEMM is among the most reliable models of pancreatic cancer, there were a number of limitations relating to its use. One is that all mice expressed oncogenic KRas and p53 from an early point during development which resulted in tumours developing early in their lifespan. This does not reflect the development of human disease, which typically involves the gradual acquisition of a variety of mutations over a long period of time and results in disease development relatively late in life. Similarly, each mouse developing pancreatic tumours due to the same genetically determined cause may have reduced the variability of the disease between different individuals and therefore reduced the opportunity for different responses to treatment.

Unlike human PDAC, survivability of the KPC GEMM is not usually significantly improved by gemcitabine treatment (195-197). This suggests that other drugs which would have a significant effect upon human disease may also not appear significantly effective upon KPC mice.

The numbers of mice required for each arm limited the number of arms that could be used. The largest number of mice possible were assigned to each arm in an effort to mitigate the lack of significant effect upon KPC survival of a drug known to be effective in humans, which would become even weaker with smaller numbers. This contributed to the decision not to have an arm treated with both gemcitabine and brusatol in combination. Following the

findings that the 2mg/kg brusatol monotherapy was ineffective, further work taking place to investigate if higher doses of brusatol or gemcitabine and brusatol in combination would be effective were merited. However, due to the unexpectedly long lifespan of the mice in the first experiment, time and financial constraints prevented subsequent experimentation.

6.4 Future Research

The findings of this work have cast light on the involvement of Nrf2 in pancreatic cancer and the use of brusatol as a chemotherapeutic agent. Although no evidence of an effect of brusatol against pancreatic cancer was found *in vivo*, this work did show that long term treatment with brusatol is safe in this KPC mouse model. Additionally, the effect of brusatol appeared highly promising *in vitro*, particularly in regard to preventing migration and colony formation. This work may therefore provide a foundation to study brusatol *in vivo* in more detail, such as in combination with other therapies, at a higher dosage, or as part of a preclinical trial with a set point of enrolment based upon tumour-bearing status.

Chemotherapy and other conventional forms of cancer intervention provide only a modest effect to PDAC patient outlook, and efforts to improve this have been met with little success. It may be that inherent limitations of these approaches render them ineffective against PDAC. As such, identification of alternative forms of therapy may be a major focus in future. One example of novel research is a recent investigation into the role of the tumour and gut microbiome in PDAC (206). The findings suggest that the microbiome may be used as a prognostic marker or manipulated to exert an effect upon the tumour, potentially therapeutically. Although the novel approach may suggest that previous difficulties to improve therapeutic response may not be as much of a problem, it is important to bear in mind that a preclinical trial to determine the effect upon survival time and quality of life has not been performed. As such, this is basic research and the approach should not be assumed to have any beneficial effect if it were to be used in humans. However, future development

of this and other novel approaches may bypass the issues that research into conventional PDAC therapy has not been able to overcome so far.

6.5 Overall Conclusions

I had hypothesised that Nrf2, an inducible component of the anti-stress response, would be induced following treatment with chemotherapy (gemcitabine and 5-FU). Instead I found that Nrf2 was depleted in response to chemotherapy, and although Nrf2 activity in cultured cells appeared to increase in response to chemotherapy this was not recapitulated in an *in vivo* Nrf2 activity reporter model. Additionally it was found that, contrary to many other types of cancers, the *NQO1* rs1800566 SNP did not correlate with either the probability of developing pancreatic or patient prognosis. As such, the role of Nrf2 in pancreatic cancer is more complex than previously anticipated and may need to be re-examined.

As discussed, brusatol is described as having potent anti-tumour properties. During the course of this work I examined the anti-cancer properties of brusatol in cultured cells and found that it inhibited viability, motility, and colony forming potential, as well as acting as a chemosensitiser for gemcitabine and 5-FU. Although brusatol is commonly used as an Nrf2 inhibitor, I found no evidence that the anti-cancer effects of brusatol upon pancreatic cancer cells were attributable to Nrf2 depletion. I also found that brusatol treatment did not improve the prognosis of KPC mice. I therefore concluded that although brusatol exhibits potent anti-cancer properties in cultured cells, these cannot be immediately applied to animal models (and therefore potentially patients). Either brusatol is not effective upon pancreatic cancer *in vivo*, or it was prevented from working through some other mechanism (such as failing to reach the tumour or being too low a dose). Further work may address these issues to devise an effective treatment plan incorporating brusatol, such as using it as a chemosensitiser rather than a single agent chemotherapy.

References

1. Strouhal E. Ancient Egyptian case of carcinoma. *Bull N Y Acad Med.* 1978;54(3):290-302.
2. Seiler R, Ohrstrom LM, Eppenberger P, Gascho D, Ruhli FJ, Galassi FM. The earliest known case of frontal sinus osteoma in man. *Clin Anat.* 2019;32(1):105-9.
3. Hajdu SI. A note from history: Landmarks in history of cancer, part 1. *Cancer.* 2011;117(5):1097-102.
4. Di Lonardo A, Nasi S, Pulciani S. Cancer: we should not forget the past. *J Cancer.* 2015;6(1):29-39.
5. Watson JD, Crick FHC. Molecular structure of nucleic acids: A structure for deoxyribose nucleic acid. *Nature.* 1953;171(4356):737-8.
6. Brookes P, Lawley PD. Evidence for the Binding of Polynuclear Aromatic Hydrocarbons to the Nucleic Acids of Mouse Skin : Relation between Carcinogenic Power of Hydrocarbons and their Binding to Deoxyribonucleic Acid. *Nature.* 1964;202(4934):781-4.
7. Brookes P, Lawley PD. The reaction of mustard gas with nucleic acids in vitro and in vivo. *The Biochemical journal.* 1960;77(3):478-84.
8. Duncum BM. An outline of the history of anaesthesia, 1846-1900. *Br Med Bull.* 1946;4(2):120-8.
9. Cancer Research: Chemotherapy and Radium Therapy. *British medical journal.* 1932;2(3746):766-8.
10. Boyland E. Experiments on the chemotherapy of cancer: The effect of certain antibacterial substances and related compounds. *The Biochemical journal.* 1938;32(7):1207-13.
11. Siegel RL, Miller KD, Jemal A. Cancer statistics, 2019. *CA Cancer J Clin.* 2019;69(1):7-34.
12. Definition of cancer - NCI Dictionary of Cancer Terms - National Cancer Institute. 2011.
13. Hanahan D, Weinberg RA. The hallmarks of cancer. *Cell.* 2000;100(1):57-70.
14. Hanahan D, Weinberg Robert A. Hallmarks of Cancer: The Next Generation. *Cell.* 2011;144(5):646-74.
15. Jemal A, Ward EM, Johnson CJ, Cronin KA, Ma J, Ryerson AB, et al. Annual Report to the Nation on the Status of Cancer, 1975–2014, Featuring Survival. *JNCI: Journal of the National Cancer Institute.* 2017;109(9).
16. Guraya SY. Pattern, Stage, and Time of Recurrent Colorectal Cancer After Curative Surgery. *Clin Colorectal Cancer.* 2019;18(2):e223-e8.
17. gov.uk. Chapter 2: trends in mortality 2018 [updated 2018 Sep 11; cited 2019 Jul 09]. Available from: <https://www.gov.uk/government/publications/health-profile-for-england-2018/chapter-2-trends-in-mortality>.
18. Schildberg FW, Meyer G, Piltz S, Koebe HG. Surgical treatment of tumor metastases: general considerations and results. *Surg Today.* 1995;25(1):1-10.
19. Dhir M, Sasson AR. Surgical Management of Liver Metastases From Colorectal Cancer. *J Oncol Pract.* 2016;12(1):33-9.
20. Zhou H, Kang X, Dai L, Yan W, Yang Y, Lin Y, et al. Efficacy of repeated surgery is superior to that of non-surgery for recurrent/second primary lung cancer after initial operation for primary lung cancer. *Thorac Cancer.* 2018;9(8):1062-8.
21. Moletta L, Serafini S, Valmasoni M, Pierobon ES, Ponzoni A, Sperti C. Surgery for Recurrent Pancreatic Cancer: Is It Effective? *Cancers (Basel).* 2019;11(7).
22. Davis W, Larionov LF. PROGRESS IN CHEMOTHERAPY OF CANCER. *Bulletin of the World Health Organization.* 1964;30:327-41.

23. Klaiber U, Leonhardt CS, Strobel O, Tjaden C, Hackert T, Neoptolemos JP. Neoadjuvant and adjuvant chemotherapy in pancreatic cancer. *Langenbecks Arch Surg.* 2018;403(8):917-32.
24. World Health Organisation. Cancer Diagnosis and Treatment [cited 2020 06 Jan]. Available from: <https://www.who.int/cancer/treatment/en/>.
25. Raufi AG, Manji GA, Chabot JA, Bates SE. Neoadjuvant Treatment for Pancreatic Cancer. *Semin Oncol.* 2019;46(1):19-27.
26. Niesen W, Hank T, Buchler M, Strobel O. Local radicality and survival outcome of pancreatic cancer surgery. *Ann Gastroenterol Surg.* 2019;3(5):464-75.
27. Cunningham D, Chau I, Stocken DD, Valle JW, Smith D, Steward W, et al. Phase III randomized comparison of gemcitabine versus gemcitabine plus capecitabine in patients with advanced pancreatic cancer. *Journal of clinical oncology : official journal of the American Society of Clinical Oncology.* 2009;27(33):5513-8.
28. Fink U, Carmichael J, Russell RCG, Spittle MF, Harris A, Spiessl G, et al. Phase II study of gemcitabine in patients with advanced pancreatic cancer. *Onkologie.* 1993;16(SUPPL. 1):15.
29. Macleod JJ. INSULIN AND DIABETES: A GENERAL STATEMENT OF THE PHYSIOLOGICAL AND THERAPEUTIC EFFECTS OF INSULIN. *British medical journal.* 1922;2(3227):833-5.
30. Rennie J, Fraser T. The Islets of Langerhans in Relation to Diabetes. *Biochemical Journal.* 1907;2(1-2):7-19.
31. Adamska A, Domenichini A, Falasca M. Pancreatic Ductal Adenocarcinoma: Current and Evolving Therapies. *International journal of molecular sciences.* 2017;18(7):1338.
32. Siegel RL, Miller KD, Jemal A. Cancer Statistics, 2017. *CA Cancer J Clin.* 2017;67(1):7-30.
33. Rahib L, Smith BD, Aizenberg R, Rosenzweig AB, Fleshman JM, Matrisian LM. Projecting Cancer Incidence and Deaths to 2030: The Unexpected Burden of Thyroid, Liver, and Pancreas Cancers in the United States. *Cancer Res.* 2014.
34. Testini M, Gurrado A, Lissidini G, Venezia P, Greco L, Piccinni G. Management of mucinous cystic neoplasms of the pancreas. *World Journal of Gastroenterology : WJG.* 2010;16(45):5682-92.
35. Thompson LDR, Becker RC, Przygodzki RM, Adair CF, Heffess CS. Mucinous cystic neoplasm (mucinous cystadenocarcinoma of low-grade malignant potential) of the pancreas: A clinicopathologic study of 130 cases. *American Journal of Surgical Pathology.* 1999;23(1):1-16.
36. Yonezawa S, Higashi M, Yamada N, Goto M. Precursor Lesions of Pancreatic Cancer. *Gut and Liver.* 2008;2(3):137-54.
37. Gourgiotis S, Ridolfini MP, Germanos S. Intraductal papillary mucinous neoplasms of the pancreas. *European journal of surgical oncology : the journal of the European Society of Surgical Oncology and the British Association of Surgical Oncology.* 2007;33(6):678-84.
38. Machado NO, al Qadhi H, al Wahibi K. Intraductal Papillary Mucinous Neoplasm of Pancreas. *North American Journal of Medical Sciences.* 2015;7(5):160-75.
39. Distler M, Aust D, Weitz J, Pilarsky C, Grutzmann R. Precursor lesions for sporadic pancreatic cancer: PanIN, IPMN, and MCN. *BioMed research international.* 2014;2014:474905.
40. Pylayeva-Gupta Y, Grabocka E, Bar-Sagi D. RAS oncogenes: weaving a tumorigenic web. *Nature reviews Cancer.* 2011;11(11):761-74.
41. Bryant KL, Mancias JD, Kimmelman AC, Der CJ. KRAS: feeding pancreatic cancer proliferation. *Trends in biochemical sciences.* 2014;39(2):91-100.
42. Kanda M, Matthaehi H, Wu J, Hong SM, Yu J, Borges M, et al. Presence of somatic mutations in most early-stage pancreatic intraepithelial neoplasia. *Gastroenterology.* 2012;142(4):730-3.e9.

43. DeNicola GM, Karreth FA, Humpton TJ, Gopinathan A, Wei C, Frese K, et al. Oncogene-induced Nrf2 transcription promotes ROS detoxification and tumorigenesis. *Nature*. 2011;475(7354):106-9.
44. Olive KP, Tuveson DA, Ruhe ZC, Yin B, Willis NA, Bronson RT, et al. Mutant p53 gain of function in two mouse models of Li-Fraumeni syndrome. *Cell*. 2004;119(6):847-60.
45. Morton JP, Timpson P, Karim SA, Ridgway RA, Athineos D, Doyle B, et al. Mutant p53 drives metastasis and overcomes growth arrest/senescence in pancreatic cancer. *Proc Natl Acad Sci U S A*. 2010;107(1):246-51.
46. Wang Z, Li Y, Zhan S, Zhang L, Zhang S, Tang Q, et al. SMAD4 Y353C promotes the progression of PDAC. *BMC cancer*. 2019;19(1):1037.
47. Wang F, Xia X, Yang C, Shen J, Mai J, Kim HC, et al. SMAD4 Gene Mutation Renders Pancreatic Cancer Resistance to Radiotherapy through Promotion of Autophagy. *Clin Cancer Res*. 2018;24(13):3176-85.
48. Ahmed S, Bradshaw AD, Gera S, Dewan MZ, Xu R. The TGF-beta/Smad4 Signaling Pathway in Pancreatic Carcinogenesis and Its Clinical Significance. *J Clin Med*. 2017;6(1).
49. Bardeesy N, Cheng KH, Berger JH, Chu GC, Pahler J, Olson P, et al. Smad4 is dispensable for normal pancreas development yet critical in progression and tumor biology of pancreas cancer. *Genes & development*. 2006;20(22):3130-46.
50. Hahn SA, Schutte M, Hoque AT, Moskaluk CA, da Costa LT, Rozenblum E, et al. DPC4, a candidate tumor suppressor gene at human chromosome 18q21.1. *Science*. 1996;271(5247):350-3.
51. Singh P, Srinivasan R, Wig JD. SMAD4 genetic alterations predict a worse prognosis in patients with pancreatic ductal adenocarcinoma. *Pancreas*. 2012;41(4):541-6.
52. Neoptolemos JP, Palmer DH, Ghaneh P, Psarelli EE, Valle JW, Halloran CM, et al. Comparison of adjuvant gemcitabine and capecitabine with gemcitabine monotherapy in patients with resected pancreatic cancer (ESPAC-4): a multicentre, open-label, randomised, phase 3 trial. *Lancet*. 2017;389(10073):1011-24.
53. Macarulla T, Fernandez T, Gallardo ME, Hernando O, Lopez AM, Hidalgo M. Adjuvant treatment for pancreatic ductal carcinoma. *Clinical & translational oncology : official publication of the Federation of Spanish Oncology Societies and of the National Cancer Institute of Mexico*. 2017;19(10):1199-204.
54. Kim R. FOLFIRINOX: a new standard treatment for advanced pancreatic cancer? *The Lancet Oncology*. 2011;12(1):8-9.
55. Conroy T, Desseigne F, Ychou M, Bouche O, Guimbaud R, Becouarn Y, et al. FOLFIRINOX versus gemcitabine for metastatic pancreatic cancer. *The New England journal of medicine*. 2011;364(19):1817-25.
56. Zimmerman SE, Smith FP, Schein PS. CHEMOTHERAPY OF PANCREATIC-CARCINOMA. *Cancer*. 1981;47(6):1724-8.
57. Reber HA. Surgical resection of lesions of the head of the pancreas UpToDate2019 [cited 2020 Jan 25]. Available from: <https://www.uptodate.com/>.
58. Reber HA. Pylorus-preserving pancreaticoduodenectomy UpToDate2019 [cited 2020 Jan 25]. Available from: <https://www.uptodate.com/>.
59. Modolell I, Guarner L, Malagelada JR. Vagaries of clinical presentation of pancreatic and biliary tract cancer. *Ann Oncol*. 1999;10 Suppl 4:82-4.
60. Timothy R Donahue OJH. Surgical resection of lesions of the body and tail of the pancreas UpToDate2019 [cited 2020 Jan 25]. Available from: <https://www.uptodate.com/>.
61. de Sousa Cavalcante L, Monteiro G. Gemcitabine: metabolism and molecular mechanisms of action, sensitivity and chemoresistance in pancreatic cancer. *Eur J Pharmacol*. 2014;741:8-16.
62. Nordh S, Ansari D, Andersson R. hENT1 expression is predictive of gemcitabine outcome in pancreatic cancer: a systematic review. *World J Gastroenterol*. 2014;20(26):8482-90.

63. Van Rompay AR, Johansson M, Karlsson A. Phosphorylation of Deoxycytidine Analog Monophosphates by UMP-CMP Kinase: Molecular Characterization of the Human Enzyme. *Molecular Pharmacology*. 1999;56(3):562.
64. Gandhi V, Legha J, Chen F, Hertel LW, Plunkett W. Excision of 2',2'-difluorodeoxycytidine (gemcitabine) monophosphate residues from DNA. *Cancer Res*. 1996;56(19):4453-9.
65. Longley DB, Harkin DP, Johnston PG. 5-Fluorouracil: mechanisms of action and clinical strategies. *Nature Reviews Cancer*. 2003;3(5):330-8.
66. Siddiqui NS, Godara A, Byrne MM, Saif MW. Capecitabine for the treatment of pancreatic cancer. *Expert Opin Pharmacother*. 2019;20(4):399-409.
67. Von Hoff DD, Ervin T, Arena FP, Chiorean EG, Infante J, Moore M, et al. Increased survival in pancreatic cancer with nab-paclitaxel plus gemcitabine. *The New England journal of medicine*. 2013;369(18):1691-703.
68. Von Hoff DD, Ramanathan RK, Borad MJ, Laheru DA, Smith LS, Wood TE, et al. Gemcitabine plus nab-paclitaxel is an active regimen in patients with advanced pancreatic cancer: a phase I/II trial. *J Clin Oncol*. 2011;29(34):4548-54.
69. Kleeff J, Korc M, Apte M, La Vecchia C, Johnson CD, Biankin AV, et al. Pancreatic cancer. *Nature reviews Disease primers*. 2016;2:16022.
70. Conroy T, Paillot B, Francois E, Bugat R, Jacob JH, Stein U, et al. Irinotecan plus oxaliplatin and leucovorin-modulated fluorouracil in advanced pancreatic cancer--a Groupe Tumeurs Digestives of the Federation Nationale des Centres de Lutte Contre le Cancer study. *Journal of clinical oncology : official journal of the American Society of Clinical Oncology*. 2005;23(6):1228-36.
71. Neoptolemos JP, Stocken DD, Bassi C, Ghaneh P, Cunningham D, Goldstein D, et al. Adjuvant chemotherapy with fluorouracil plus folinic acid vs gemcitabine following pancreatic cancer resection: A randomized controlled trial. *JAMA - Journal of the American Medical Association*. 2010;304(10):1073-81.
72. Van den Broeck A, Sergeant G, Ectors N, Van Steenberghe W, Aerts R, Topal B. Patterns of recurrence after curative resection of pancreatic ductal adenocarcinoma. *European journal of surgical oncology : the journal of the European Society of Surgical Oncology and the British Association of Surgical Oncology*. 2009;35(6):600-4.
73. Kang Y, Zhang R, Suzuki R, Li S, Roife D, Truty MJ, et al. Two-dimensional culture of human pancreatic adenocarcinoma cells results in an irreversible transition from epithelial to mesenchymal phenotype. *Lab Invest*. 2015;95(2):207-22.
74. Kim YE, Jeon HJ, Kim D, Lee SY, Kim KY, Hong J, et al. Quantitative Proteomic Analysis of 2D and 3D Cultured Colorectal Cancer Cells: Profiling of Tankyrase Inhibitor XAV939-Induced Proteome. *Scientific Reports*. 2018;8(1):1-12.
75. Tölle RC, Gaggioli C, Dengjel J. Three-Dimensional Cell Culture Conditions Affect the Proteome of Cancer-Associated Fibroblasts. *Journal of proteome research*. 2018;17(8).
76. Rasheena E, Jenkins BJ, Adcock A, Liju Y. Three-dimensional Cell Culture Systems and Their Applications in Drug Discovery and Cell-Based Biosensors. *Assay and drug development technologies*. 2014;12(4).
77. Huang L, Holtzinger A, Jagan I, BeGora M, Lohse I, Ngai N, et al. Ductal pancreatic cancer modeling and drug screening using human pluripotent stem cell- and patient-derived tumor organoids. *Nat Med*. 2015;advance online publication.
78. Longati P, Jia X, Eimer J, Wagman A, Witt M-R, Rehnmark S, et al. 3D pancreatic carcinoma spheroids induce a matrix-rich, chemoresistant phenotype offering a better model for drug testing. *BMC Cancer*. 2013;13(1):1-13.
79. Ware MJ, Keshishian V, Law JJ, Ho JC, Favela CA, Rees P, et al. Generation of an in vitro 3D PDAC stroma rich spheroid model. *Biomaterials*. 2016;108:129-42.
80. Drost J, Clevers H. Organoids in cancer research. *Nat Rev Cancer*. 2018.

81. Erstad D, Sojoodi M, Taylor M, Ghoshal S, Razavi A, Graham-O'Regan K, et al. Orthotopic and Heterotopic Murine Models of Pancreatic Cancer and Their Different Responses to FOLFIRINOX Chemotherapy. *Disease models & mechanisms*. 2018;11(7).
82. DJ E, M S, MS T, S G, AA R, KA G-OR, et al. Orthotopic and Heterotopic Murine Models of Pancreatic Cancer and Their Different Responses to FOLFIRINOX Chemotherapy. *Disease models & mechanisms*. 2018;11(7).
83. Lee JW, Komar CA, Bengsch F, Graham K, Beatty GL. Genetically Engineered Mouse Models of Pancreatic Cancer: The KPC Model (LSL-Kras(G12D/+);LSL-Trp53(R172H/+);Pdx-1-Cre), Its Variants, and Their Application in Immuno-oncology Drug Discovery. *Current protocols in pharmacology*. 2016;73:14.39.1-14.39.20.
84. Garcia PL, Miller AL, Yoon KJ. Patient-Derived Xenograft Models of Pancreatic Cancer: Overview and Comparison with Other Types of Models. *Cancers*. 2020;12(5):1327.
85. Jonsson J, Carlsson L, Edlund T, Edlund H. Insulin-promoter-factor 1 is required for pancreas development in mice. *Nature*. 1994;371(6498):606-9.
86. Madsen OD, Jensen J, Petersen HV, Pedersen EE, Oster A, Andersen FG, et al. Transcription factors contributing to the pancreatic beta-cell phenotype. *Hormone and metabolic research = Hormon- und Stoffwechselforschung = Hormones et métabolisme*. 1997;29(6):265-70.
87. Jiang H, Hegde S, Knolhoff BL, Zhu Y, Herndon JM, Meyer MA, et al. Targeting focal adhesion kinase renders pancreatic cancers responsive to checkpoint immunotherapy. *Nat Med*. 2016;22(8):851-60.
88. Hingorani SR, Wang L, Multani AS, Combs C, Deramaudt TB, Hruban RH, et al. Trp53R172H and KrasG12D cooperate to promote chromosomal instability and widely metastatic pancreatic ductal adenocarcinoma in mice. *Cancer cell*. 2005;7(5):469-83.
89. Muller PA, Caswell PT, Doyle B, Iwanicki MP, Tan EH, Karim S, et al. Mutant p53 drives invasion by promoting integrin recycling. *Cell*. 2009;139(7):1327-41.
90. Zhu Y, Herndon JM, Sojka DK, Kim KW, Knolhoff BL, Zuo C, et al. Tissue-Resident Macrophages in Pancreatic Ductal Adenocarcinoma Originate from Embryonic Hematopoiesis and Promote Tumor Progression. *Immunity*. 2017;47(2):323-38.e6.
91. Hingorani SR, Petricoin EF, Maitra A, Rajapakse V, King C, Jacobetz MA, et al. Preinvasive and invasive ductal pancreatic cancer and its early detection in the mouse. *Cancer cell*. 2003;4(6):437-50.
92. Morton JP, Karim SA, Graham K, Timpson P, Jamieson N, Athineos D, et al. Dasatinib inhibits the development of metastases in a mouse model of pancreatic ductal adenocarcinoma. *Gastroenterology*. 2010;139(1):292-303.
93. Bai H, Li H, Zhang W, Matkowskyj KA, Liao J, Srivastava SK, et al. Inhibition of chronic pancreatitis and pancreatic intraepithelial neoplasia (PanIN) by capsaicin in LSL-KrasG12D/Pdx1-Cre mice. *Carcinogenesis*. 2011;32(11):1689-96.
94. Husain K, Centeno BA, Chen DT, Fulp WJ, Perez M, Zhang Lee G, et al. Prolonged survival and delayed progression of pancreatic intraepithelial neoplasia in LSL-KrasG12D/+;Pdx-1-Cre mice by vitamin E delta-tocotrienol. *Carcinogenesis*. 2013;34(4):858-63.
95. Lampson BL, Kendall SD, Ancrile BB, Morrison MM, Shealy MJ, Barrientos KS, et al. Targeting eNOS in pancreatic cancer. *Cancer Res*. 2012;72(17):4472-82.
96. Liou GY, Storz P. Reactive oxygen species in cancer. *Free Radic Res*. 2010;44(5).
97. Ghanbari M, Rastegari-Pouyani M, Mohammadi M, Mansouri K. Cancer cells change their glucose metabolism to overcome increased ROS: One step from cancer cell to cancer stem cell? *Biomedicine & pharmacotherapy = Biomedecine & pharmacotherapie*. 2019;112.
98. Wang M, Topalovski M, Toombs JE, Wright CM, Moore ZR, Boothman DA, et al. Fibulin-5 Blocks Microenvironmental ROS in Pancreatic Cancer. *Cancer Research*. 2015;75(23):5058-69.

99. Abdul-Aziz A, MacEwan DJ, Bowles KM, Rushworth SA. Oxidative stress responses and NRF2 in human leukaemia. *Oxidative Med Cell Longev*. 2015;2015:454659-.
100. Jeong SM, Hwang S, Seong RH. Transferrin receptor regulates pancreatic cancer growth by modulating mitochondrial respiration and ROS generation. *Biochemical and Biophysical Research Communications*. 2016;471(3):373-9.
101. Sun X, Wang Q, Wang Y, Du L, Xu C, Liu Q. Brusatol Enhances the Radiosensitivity of A549 Cells by Promoting ROS Production and Enhancing DNA Damage. *International Journal Of Molecular Sciences*. 2016;17(7).
102. Ju HQ, Gocho T, Aguilar M, Wu M, Zhuang ZN, Fu J, et al. Mechanisms of Overcoming Intrinsic Resistance to Gemcitabine in Pancreatic Ductal Adenocarcinoma through the Redox Modulation. *Molecular Cancer Therapeutics*. 2015;14(3):788-98.
103. Rofstad E, Mathiesen B, Kindem K, Galappathi K. Acidic extracellular pH promotes experimental metastasis of human melanoma cells in athymic nude mice. *Cancer research*. 2006;66(13).
104. Moi P, Chan K, Asunis I, Cao A, Kan YW. Isolation of NF-E2-related factor 2 (Nrf2), a NF-E2-like basic leucine zipper transcriptional activator that binds to the tandem NF-E2/AP1 repeat of the beta-globin locus control region. *Proc Natl Acad Sci U S A*. 1994;91(21):9926-30.
105. Hayes JD, Dinkova-Kostova AT. The Nrf2 regulatory network provides an interface between redox and intermediary metabolism. *Trends in biochemical sciences*. 2014;39(4):199-218.
106. Lau A, Villeneuve NF, Sun Z, Wong PK, Zhang DD. Dual roles of Nrf2 in cancer. *Pharmacol Res*. 2008;58(5-6):262-70.
107. Hamada S, Shimosegawa T, Taguchi K, Nabeshima T, Yamamoto M, Masamune A. Simultaneous K-ras activation and Keap1 deletion cause atrophy of pancreatic parenchyma. *American journal of physiology Gastrointestinal and liver physiology*. 2017:ajpgi.00228.2017.
108. Kwak MK, Itoh K, Yamamoto M, Kensler TW. Enhanced expression of the transcription factor Nrf2 by cancer chemopreventive agents: role of antioxidant response element-like sequences in the nrf2 promoter. *Molecular and cellular biology*. 2002;22(9):2883-92.
109. Wang XJ, Sun Z, Villeneuve NF, Zhang S, Zhao F, Li Y, et al. Nrf2 enhances resistance of cancer cells to chemotherapeutic drugs, the dark side of Nrf2. *Carcinogenesis*. 2008;29(6):1235-43.
110. Itoh K, Chiba T, Takahashi S, Ishii T, Igarashi K, Katoh Y, et al. An Nrf2/small Maf heterodimer mediates the induction of phase II detoxifying enzyme genes through antioxidant response elements. *Biochem Biophys Res Commun*. 1997;236(2):313-22.
111. Milkovic L, Zarkovic N, Saso L. Controversy about pharmacological modulation of Nrf2 for cancer therapy. *Redox Biol*. 2017;12:727-32.
112. Tao S, Rojo de la Vega M, Chapman E, Ooi A, Zhang DD. The effects of NRF2 modulation on the initiation and progression of chemically and genetically induced lung cancer. *Molecular carcinogenesis*. 2017.
113. Lister A, Nedjadi T, Kitteringham NR, Campbell F, Costello E, Lloyd B, et al. Nrf2 is overexpressed in pancreatic cancer: implications for cell proliferation and therapy. *Mol Cancer*. 2011;10:37.
114. Marchan R, Bolt HM. The cytoprotective and the dark side of Nrf2. *Archives of toxicology*. 2013;87(12):2047-50.
115. Soini Y, Eskelinen M, Juvonen P, Karja V, Haapasaari KM, Saarela A, et al. Nuclear Nrf2 expression is related to a poor survival in pancreatic adenocarcinoma. *Pathology, research and practice*. 2014;210(1):35-9.

116. Chio, II, Jafarnejad SM, Ponz-Sarvisé M, Park Y, Rivera K, Palm W, et al. NRF2 Promotes Tumor Maintenance by Modulating mRNA Translation in Pancreatic Cancer. *Cell*. 2016;166(4):963-76.
117. Duong HQ, You KS, Oh S, Kwak SJ, Seong YS. Silencing of NRF2 Reduces the Expression of ALDH1A1 and ALDH3A1 and Sensitizes to 5-FU in Pancreatic Cancer Cells. *Antioxidants (Basel, Switzerland)*. 2017;6(3).
118. Wu KC, Cui JY, Klaassen CD. Beneficial role of Nrf2 in regulating NADPH generation and consumption. *Toxicological sciences : an official journal of the Society of Toxicology*. 2011;123(2):590-600.
119. Sekhar KR, Soltaninassab SR, Borrelli MJ, Xu ZQ, Meredith MJ, Domann FE, et al. Inhibition of the 26S proteasome induces expression of GLCLC, the catalytic subunit for gamma-glutamylcysteine synthetase. *Biochem Biophys Res Commun*. 2000;270(1):311-7.
120. Wild AC, Moinova HR, Mulcahy RT. Regulation of gamma-glutamylcysteine synthetase subunit gene expression by the transcription factor Nrf2. *The Journal of biological chemistry*. 1999;274(47):33627-36.
121. Chan JY, Kwong M. Impaired expression of glutathione synthetic enzyme genes in mice with targeted deletion of the Nrf2 basic-leucine zipper protein. *Biochimica et biophysica acta*. 2000;1517(1):19-26.
122. Snoke JE, Bloch K. Formation and utilization of gamma-glutamylcysteine in glutathione synthesis. *The Journal of biological chemistry*. 1952;199(1):407-14.
123. Snoke JE. Isolation and properties of yeast glutathione synthetase. *The Journal of biological chemistry*. 1955;213(2):813-24.
124. Chan K, Han XD, Kan YW. An important function of Nrf2 in combating oxidative stress: detoxification of acetaminophen. *Proc Natl Acad Sci U S A*. 2001;98(8):4611-6.
125. Lee TD, Yang H, Whang J, Lu SC. Cloning and characterization of the human glutathione synthetase 5'-flanking region. *The Biochemical journal*. 2005;390(Pt 2):521-8.
126. Rall TW, Lehninger AL. Glutathione reductase of animal tissues. *The Journal of biological chemistry*. 1952;194(1):119-30.
127. Harvey CJ, Thimmulappa RK, Singh A, Blake DJ, Ling G, Wakabayashi N, et al. Nrf2-regulated glutathione recycling independent of biosynthesis is critical for cell survival during oxidative stress. *Free Radic Biol Med*. 2009;46(4):443-53.
128. McMahon M, Thomas N, Itoh K, Yamamoto M, Hayes JD. Dimerization of substrate adaptors can facilitate cullin-mediated ubiquitylation of proteins by a "tethering" mechanism: a two-site interaction model for the Nrf2-Keap1 complex. *The Journal of biological chemistry*. 2006;281(34):24756-68.
129. Itoh K, Wakabayashi N, Katoh Y, Ishii T, O'Connor T, Yamamoto M. Keap1 regulates both cytoplasmic-nuclear shuttling and degradation of Nrf2 in response to electrophiles. *Genes to Cells*. 2003;8(4):379-91.
130. Furfaro AL, Traverso N, Domenicotti C, Piras S, Moretta L, Marinari UM, et al. The Nrf2/HO-1 Axis in Cancer Cell Growth and Chemoresistance. *Oxidative Med Cell Longev*. 2016:14.
131. Guan L, Zhang L, Gong ZC, Hou XN, Xu YX, Feng XH, et al. FoxO3 Inactivation Promotes Human Cholangiocarcinoma Tumorigenesis and Chemoresistance Through Keap1-Nrf2 Signaling. *Hepatology*. 2016;63(6):1914-27.
132. Tao S, Wang S, Moghaddam SJ, Ooi A, Chapman E, Wong PK, et al. Oncogenic KRAS confers chemoresistance by upregulating NRF2. *Cancer Res*. 2014;74(24):7430-41.
133. Wang Y, Wang Y, Zhang Z, Park J-Y, Guo D, Liao H, et al. Mechanism of progesterin resistance in endometrial precancer/cancer through Nrf2-AKR1C1 pathway. *Oncotarget*. 2016;7(9):10363-72.
134. Palam LR, Gore J, Craven KE, Wilson JL, Korc M. Integrated stress response is critical for gemcitabine resistance in pancreatic ductal adenocarcinoma. *Cell Death Dis*. 2015;6:e1913.

135. Choi EJ, Jung BJ, Lee SH, Yoo HS, Shin EA, Ko HJ, et al. A clinical drug library screen identifies clobetasol propionate as an NRF2 inhibitor with potential therapeutic efficacy in KEAP1 mutant lung cancer. *Oncogene*. 2017;36(37):5285-95.
136. Martinez VD, Vucic EA, Thu KL, Pikor LA, Lam S, Lam WL. Disruption of KEAP1/CUL3/RBX1 E3-ubiquitin ligase complex components by multiple genetic mechanisms: Association with poor prognosis in head and neck cancer. *Head & neck*. 2015;37(5):727-34.
137. Abu-Alainin W, Gana T, Liloglou T, Olayanju A, Barrera LN, Ferguson R, et al. UHRF1 regulation of the Keap1-Nrf2 pathway in pancreatic cancer contributes to oncogenesis. *The Journal of pathology*. 2016;238(3):423-33.
138. Barbano R, Muscarella LA, Pasculli B, Valori VM, Fontana A, Coco M, et al. Aberrant Keap1 methylation in breast cancer and association with clinicopathological features. *Epigenetics*. 2013;8(1):105-12.
139. Hanada N, Takahata T, Zhou Q, Ye X, Sun R, Itoh J, et al. Methylation of the KEAP1 gene promoter region in human colorectal cancer. *BMC cancer*. 2012;12:66.
140. Muscarella LA, Barbano R, D'Angelo V, Copetti M, Coco M, Balsamo T, et al. Regulation of KEAP1 expression by promoter methylation in malignant gliomas and association with patient's outcome. *Epigenetics*. 2011;6(3):317-25.
141. Lau A, Tian W, Whitman SA, Zhang DND. The Predicted Molecular Weight of Nrf2: It Is What It Is Not. *Antioxid Redox Signal*. 2013;18(1):91-3.
142. Gana T. Evaluation of UHRF1 and the antioxidant response pathway in pancreatic cancer and the prediction of response to treatment: University of Liverpool; 2017.
143. Nebert DW, Roe AL, Vandale SE, Bingham E, Oakley GG. NAD(P)H:quinone oxidoreductase (NQO1) polymorphism, exposure to benzene, and predisposition to disease: A HuGE review. *Genetics in Medicine*. 2002;4(2):62-70.
144. Zhang H, Wen X, Lu X, Zhang H. Association between NAD(P)H:quinone oxidoreductase 1 rs1800566 polymorphism and risk of bladder cancer. *Tumour Biol*. 2013;34(6):3377-81.
145. Ding R, Lin S, Chen D. Association of NQO1 rs1800566 polymorphism and the risk of colorectal cancer: a meta-analysis. *Int J Colorectal Dis*. 2012;27(7):885-92.
146. Yadav U, Kumar P, Rai V. "NQO1 Gene C609T Polymorphism (dbSNP: rs1800566) and Digestive Tract Cancer Risk: A Meta-Analysis.". *Nutrition and cancer*. 2018;70(4):557-68.
147. Yin J, Wang L, Wang X, Zheng L, Shi Y, Shao A, et al. NQO1 rs1800566 C>T polymorphism was associated with a decreased risk of esophageal cancer in a Chinese population. *Scand J Gastroenterol*. 2014;49(3):317-22.
148. Mohelnikova-Duchonova B, Marsakova L, Vrana D, Holcatova I, Ryska M, Smerhovsky Z, et al. Superoxide dismutase and nicotinamide adenine dinucleotide phosphate: quinone oxidoreductase polymorphisms and pancreatic cancer risk. *Pancreas*. 2011;40(1):72-8.
149. Gjyshi O, Roy A, Dutta S, Veettil MV, Dutta D, Chandran B. Activated Nrf2 Interacts with Kaposi's Sarcoma-Associated Herpesvirus Latency Protein LANA-1 and Host Protein KAP1 To Mediate Global Lytic Gene Repression. *Journal Of Virology*. 2015;89(15):7874-92.
150. Turpaev K, Welsh N. Aromatic malononitriles stimulate the resistance of insulin-producing beta-cells to oxidants and inflammatory cytokines. *European Journal Of Pharmacology*. 2016;784:69-80.
151. Ren DM, Villeneuve NF, Jiang T, Wu TD, Lau A, Toppin HA, et al. Brusatol enhances the efficacy of chemotherapy by inhibiting the Nrf2-mediated defense mechanism. *Proc Natl Acad Sci U S A*. 2011;108(4):1433-8.
152. Olayanju A, Copple IM, Bryan HK, Edge GT, Sison RL, Wong MW, et al. Brusatol provokes a rapid and transient inhibition of Nrf2 signaling and sensitizes mammalian cells

- to chemical toxicity-implications for therapeutic targeting of Nrf2. *Free Radic Biol Med*. 2015;78:202-12.
153. Cai SJ, Liu Y, Han S, Yang C. Brusatol, an NRF2 inhibitor for future cancer therapeutic. *Cell & bioscience*. 2019;9:45.
154. Evans JP, Winiarski BK, Sutton PA, Jones RP, Ressel L, Duckworth CA, et al. The Nrf2 inhibitor brusatol is a potent antitumour agent in an orthotopic mouse model of colorectal cancer. *Oncotarget*. 2018;9(43):27104-16.
155. Liu Y, Lu Y, Celiku O, Li A, Wu Q, Zhou Y, et al. Targeting IDH1-Mutated Malignancies with NRF2 Blockade. *Journal of the National Cancer Institute*. 2019.
156. Lee KH, Tani S, Imakura Y. Antimalarial agents, 4. Synthesis of a brusatol analog and biological activity of brusatol-related compounds. *Journal of natural products*. 1987;50(5):847-51.
157. Lu Z, Lai ZQ, Leung AWN, Leung PS, Li ZS, Lin ZX. Exploring brusatol as a new anti-pancreatic cancer adjuvant: biological evaluation and mechanistic studies. *Oncotarget*. 2017;8(49):84974-85.
158. Wang D, Qu X, Zhuang X, Geng G, Hou J, Xu N, et al. Seed Oil of *Brucea javanica* Induces Cell Cycle Arrest and Apoptosis via Reactive Oxygen Species-Mediated Mitochondrial Dysfunction in Human Lung Cancer Cells. *Nutrition and cancer*. 2016;68(8):1394-403.
159. Harder B, Tian W, La Clair JJ, Tan AC, Ooi A, Chapman E, et al. Brusatol overcomes chemoresistance through inhibition of protein translation. *Molecular carcinogenesis*. 2016.
160. Tang X, Fu X, Liu Y, Yu D, Cai SJ, Yang C. Blockade of glutathione metabolism in IDH1-mutated glioma. *Mol Cancer Ther*. 2019.
161. Li J, Wang Q, Yang Y, Lei C, Yang F, Liang L, et al. GSTZ1 deficiency promotes hepatocellular carcinoma proliferation via activation of the KEAP1/NRF2 pathway. *J Exp Clin Cancer Res*. 2019;38(1):438.
162. Tao S, Rojo de la Vega M, Chapman E, Ooi A, Zhang DD. The effects of NRF2 modulation on the initiation and progression of chemically and genetically induced lung cancer. *Molecular carcinogenesis*. 2018;57(2):182-92.
163. Vartanian S, Ma TP, Lee J, Haverty PM, Kirkpatrick DS, Yu K, et al. Application of mass spectrometry profiling to establish brusatol as an inhibitor of global protein synthesis. *Mol Cell Proteomics*. 2015.
164. Willingham W, Jr., Stafford EA, Reynolds SH, Chaney SG, Lee KH, Okano M, et al. Mechanism of eukaryotic protein synthesis inhibition by brusatol. *Biochimica et biophysica acta*. 1981;654(2):169-74.
165. Fresno M, Gonzales A, Vazquez D, Jimenez A. Bruceantin, a novel inhibitor of peptide bond formation. *Biochimica et biophysica acta*. 1978;518(1):104-12.
166. Singh A, Venkannagari S, Oh KH, Zhang YQ, Rohde JM, Liu L, et al. Small Molecule Inhibitor of NRF2 Selectively Intervenes Therapeutic Resistance in KEAP1-Deficient NSCLC Tumors. *ACS chemical biology*. 2016;11(11):3214-25.
167. MRI Wound Healing Tool [Available from: http://dev.mri.cnrs.fr/projects/imagej-macros/wiki/Wound_Healing_Tool].
168. Karczewski KJ, Francioli LC, Tiao G, Cummings BB, Alföldi J, Wang Q, et al. Variation across 141,456 human exomes and genomes reveals the spectrum of loss-of-function intolerance across human protein-coding genes. *bioRxiv*. 2019:531210.
169. Forootan SS, Mutter FE, Kipar A, Iwawaki T, Francis B, Goldring CE, et al. Real-time in vivo imaging reveals localised Nrf2 stress responses associated with direct and metabolism-dependent drug toxicity. *Scientific reports*. 2017;7(1):16084.
170. Oikawa D, Akai R, Tokuda M, Iwawaki T. A transgenic mouse model for monitoring oxidative stress. *Scientific reports*. 2012;2:229.

171. Venugopal R, Jaiswal AK. Nrf1 and Nrf2 positively and c-Fos and Fra1 negatively regulate the human antioxidant response element-mediated expression of NAD(P)H:quinone oxidoreductase1 gene. *Proc Natl Acad Sci U S A*. 1996;93(25):14960-5.
172. Samatiwat P, Prawan A, Senggunprai L, Kukongviriyapan V. Repression of Nrf2 enhances antitumor effect of 5-fluorouracil and gemcitabine on cholangiocarcinoma cells. *Naunyn-Schmiedeberg's Archives of Pharmacology*. 2015;388(6):601-12.
173. Hajatdoost L, Sedaghat K, Walker EJ, Thomas J, Kosari S. Chemotherapy in Pancreatic Cancer: A Systematic Review. *Medicina (Kaunas)*. 2018;54(3):48.
174. Tsuchida K, Tsujita T, Hayashi M, Ojima A, Keleku-Lukwete N, Katsuoka F, et al. Halofuginone enhances the chemo-sensitivity of cancer cells by suppressing NRF2 accumulation. *Free Radic Biol Med*. 2016;103:236-47.
175. Chen F, Wang H, Zhu J, Zhao R, Xue P, Zhang Q, et al. Camptothecin suppresses NRF2-ARE activity and sensitises hepatocellular carcinoma cells to anticancer drugs. *Br J Cancer*. 2017.
176. Oh ET, Kim CW, Kim HG, Lee JS, Park HJ. Brusatol-Mediated Inhibition of c-Myc Increases HIF-1 α Degradation and Causes Cell Death in Colorectal Cancer under Hypoxia. *Theranostics*. 2017;7(14):3415-31.
177. Razin A, Cedar H. DNA methylation and gene expression. *Microbiological reviews*. 1991;55(3):451-8.
178. Irvine RA, Lin IG, Hsieh C-L. DNA Methylation Has a Local Effect on Transcription and Histone Acetylation. *Molecular and cellular biology*. 2002;22(19):6689-96.
179. Kemmerer ZA, Mulroy S, Ader NR, Egger AL. Comparison of Human Nrf2 Antibodies: All Is Not as It Seems. *Free Radic Biol Med*. 2014;76:S70-S.
180. Menegon S, Columbano A, Giordano S. Review: The Dual Roles of NRF2 in Cancer. *Trends in Molecular Medicine*. 2016;22:578-93.
181. Wang Y-Y, Yang Y-X, Zhe H, He Z-X, Zhou S-F. Bardoxolone methyl (CDDO-Me) as a therapeutic agent: an update on its pharmacokinetic and pharmacodynamic properties. *Drug Design, Development and Therapy*. 2014;8:2075-88.
182. Walsh J, Jenkins RE, Wong M, Olayanju A, Powell H, Copple I, et al. Identification and quantification of the basal and inducible Nrf2-dependent proteomes in mouse liver: biochemical, pharmacological and toxicological implications. *Journal of proteomics*. 2014;108:171-87.
183. Tang Z, Zhao L, Yang Z, Liu Z, Gu J, Bai B, et al. Mechanisms of oxidative stress, apoptosis, and autophagy involved in graphene oxide nanomaterial anti-osteosarcoma effect. *Int J Nanomedicine*. 2018;13:2907-19.
184. Li M, Yu H, Pan H, Zhou X, Ruan Q, Kong D, et al. Nrf2 Suppression Delays Diabetic Wound Healing Through Sustained Oxidative Stress and Inflammation. *Front Pharmacol*. 2019;10:1099.
185. He Y, Jiang K, Zhao X. Taraxasterol protects hippocampal neurons from oxygen-glucose deprivation-induced injury through activation of Nrf2 signalling pathway. *Artif Cells Nanomed Biotechnol*. 2020;48(1):252-8.
186. Samatiwat P, Prawan A, Senggunprai L, Kukongviriyapan V. Repression of Nrf2 enhances antitumor effect of 5-fluorouracil and gemcitabine on cholangiocarcinoma cells. *Naunyn-Schmiedeberg's Arch Pharmacol*. 2015;388(6):601-12.
187. Liu HY, Tuckett AZ, Fennell M, Garippa R, Zakrzewski JL. Repurposing of the CDK inhibitor PHA-767491 as a NRF2 inhibitor drug candidate for cancer therapy via redox modulation. *Invest New Drugs*. 2018.
188. Miller KD, Nogueira L, Mariotto AB, Rowland JH, Yabroff KR, Alfano CM, et al. Cancer treatment and survivorship statistics, 2019. *CA Cancer J Clin*. 2019;69(5):363-85.
189. Neoptolemos JP, Palmer DH, Ghaneh P, Psarelli EE, Valle JW, Halloran CM, et al. Comparison of adjuvant gemcitabine and capecitabine with gemcitabine monotherapy in

patients with resected pancreatic cancer (ESPA-4): a multicentre, open-label, randomised, phase 3 trial. *Lancet*. 2017;389(10073):1011-24.

190. Ren D, Villeneuve NF, Jiang T, Wu T, Lau A, Toppin HA, et al. Brusatol enhances the efficacy of chemotherapy by inhibiting the Nrf2-mediated defense mechanism. *Proc Natl Acad Sci U S A*. 2011;108(4):1433-8.
191. Guo N, Zhang X, Bu F, Wang L, Cao Z, Geng C, et al. Determination of brusatol in plasma and tissues by LC-MS method and its application to a pharmacokinetic and distribution study in mice. *Journal of chromatography B, Analytical technologies in the biomedical and life sciences*. 2017;1053:20-6.
192. Yadav B, Wennerberg K, Aittokallio T, Tang J. Searching for Drug Synergy in Complex Dose-Response Landscapes Using an Interaction Potency Model. *Comput Struct Biotechnol J*. 2015;13:504-13.
193. He L, Kuleskiy E, Saarela J, Turunen L, Wennerberg K, Aittokallio T, et al. Methods for High-throughput Drug Combination Screening and Synergy Scoring. *Methods Mol Biol*. 2018;1711:351-98.
194. Franken NA, Rodermond HM, Stap J, Haveman J, van Bree C. Clonogenic assay of cells in vitro. *Nat Protoc*. 2006;1(5):2315-9.
195. Whatcott CJ, Ng S, Barrett MT, Hostetter G, Von Hoff DD, Han H. Inhibition of ROCK1 kinase modulates both tumor cells and stromal fibroblasts in pancreatic cancer. *PLoS one*. 2017;12(8):e0183871-e.
196. Jacobetz MA, Chan DS, Neesse A, Bapiro TE, Cook N, Frese KK, et al. Hyaluronan impairs vascular function and drug delivery in a mouse model of pancreatic cancer. *Gut*. 2013;62(1):112.
197. D'Costa Z, Jones K, Azad A, van Stiphout R, Lim SY, Gomes AL, et al. Gemcitabine-Induced TIMP1 Attenuates Therapy Response and Promotes Tumor Growth and Liver Metastasis in Pancreatic Cancer. *Cancer Res*. 2017;77(21):5952-62.
198. Zimta AA, Cenariu D, Irimie A, Magdo L, Nabavi SM, Atanasov AG, et al. The Role of Nrf2 Activity in Cancer Development and Progression. *Cancers (Basel)*. 2019;11(11).
199. YS W, CY L, KS S, A M, I C. Soluble factors from stellate cells induce pancreatic cancer cell proliferation via Nrf2-activated metabolic reprogramming and ROS detoxification. *Oncotarget*. 2016;7(24):36719-32.
200. Jamieson D, Cresti N, Bray J, Sludden J, Griffin MJ, Hawsawi NM, et al. Two minor NQO1 and NQO2 alleles predict poor response of breast cancer patients to adjuvant doxorubicin and cyclophosphamide therapy. *Pharmacogenet Genomics*. 2011;21(12):808-19.
201. Tian G, Wang M, Xu X. The role of NQO1 polymorphisms in the susceptibility and chemotherapy response of Chinese NSCLC patients. *Cell Biochem Biophys*. 2014;69(3):475-9.
202. Awadallah NS, Shah RJ, Chen YK, Dehn D, Ross D, Russell Nash S, et al. NQO1 expression in pancreatic cancer and its potential use as a biomarker. *Applied Immunohistochemistry and Molecular Morphology*. 2008;16(1):24-31.
203. Gopinathan A, Morton JP, Jodrell DI, Sansom OJ. GEMMs as preclinical models for testing pancreatic cancer therapies. *Disease models & mechanisms*. 2015;8(10):1185-200.
204. Westphalen CB, Olive KP. Genetically engineered mouse models of pancreatic cancer. *Cancer journal (Sudbury, Mass)*. 2012;18(6):502-10.
205. Gonneaud A, Asselin C, Boudreau F, Boisvert F. Phenotypic Analysis of Organoids by Proteomics. *Proteomics*. 2017;17(20).
206. Riquelme E, Zhang Y, Zhang L, Montiel M, Zoltan M, Dong W, et al. Tumor Microbiome Diversity and Composition Influence Pancreatic Cancer Outcomes. *Cell*. 2019;178(4):795-806.e12.